INTERIM REPORT ON THE
USE OF SM-2 ELEMENTS
IN SM-1, SM-1A AND
PM-2A CORES

ALCO   **ALCO PRODUCTS, INC.**

NUCLEAR POWER ENGINEERING DEPARTMENT
P. O. BOX 414, SCHENECTADY 1, N.Y.

DISCLAIMER

This report was prepared as an account of work sponsored by an agency of the United States Government. Neither the United States Government nor any agency Thereof, nor any of their employees, makes any warranty, express or implied, or assumes any legal liability or responsibility for the accuracy, completeness, or usefulness of any information, apparatus, product, or process disclosed, or represents that its use would not infringe privately owned rights. Reference herein to any specific commercial product, process, or service by trade name, trademark, manufacturer, or otherwise does not necessarily constitute or imply its endorsement, recommendation, or favoring by the United States Government or any agency thereof. The views and opinions of authors expressed herein do not necessarily state or reflect those of the United States Government or any agency thereof.

DISCLAIMER

Portions of this document may be illegible in electronic image products. Images are produced from the best available original document.

INTERIM REPORT ON THE USE OF SM-2 ELEMENTS IN SM-1, SM-1A AND PM-2A CORES

By:

S. L. Davidson

J. P. Oggerino

Approved By:

J. G. Gallagher - Head, Nuclear Technology Unit

Issued: June 20, 1961

ALCO PRODUCTS, INC.
Nuclear Power Engineering Department
Post Office Box 414
Schenectady 1, N. Y.

THIS PAGE

WAS INTENTIONALLY

LEFT BLANK

DISTRIBUTION

External
Copies

1 - 2	New York Operations Office U. S. Atomic Energy Commission 376 Hudson Street New York, 14, New York Attention: Chief, Army Reactors Staff Reactor Division
3 - 5	U. S. Atomic Energy Commission Washington 25, D. C. Attention: Chief, Water Systems Project Branch (Army Reactors) Division of Reactor Development Mail Station F-311
6	U. S. Atomic Energy Commission Washington 25, D. C. Attention: Chief, Evaluation and Planning Branch Civilian Reactors, Division of Reactor Development
7	U. S. Atomic Energy Commission Chief, New York Patent Group Brookhaven National Laboratory Upton, New York Attention: Harman Potter
8	U. S. Atomic Energy Commission Idaho Operations Office P. O. Box 2108 Idaho Falls, Idaho Attention: Director, Division of Military Reactors

9   U. S. Atomic Energy Commission
     Reports and Statistic Branch
     Division of Reactor Development
     Washington, 25, D. C.

10 - 11   Office of the Chief of Engineers
          Department of the Army
          Building T-7
          Washington, 25, D. C.

          Attention: Chief, Projects Branch
                     Nuclear Power Division

12 - 14   Nuclear Power Field Office
          U. S. Army Engineer Reactors Group
          Fort Belvoir, Virginia

          Attention: Chief, Nuclear Power Field Office

15   Nuclear Power Field Office
          U. S. Army Engineer Reactors Group
          Fort Belvoir, Virginia

          Attention: O. I. C. SM-1

16   Chief, U. S. Army Reactors Group
          Fort Greeley, Alaska
          APO 733
          Seattle, Washington

          Attention: O. I. C. SM-1A

17   Chief, USAPR&DC
          Thule, Greenland
          APO 23
          New York, New York

          Attention: O. I. C. PM-2A

18 - 20   Office of Technical Information Extension
        P. O. Box 62
        Oak Ridge, Tennessee

21   Union Carbide Nuclear Corporation
        Oak Ridge National Laboratory
        Y-12 Building 9704-1
        P. O. Box "Y"
        Oak Ridge, Tennessee

        Attention: A. L. Boch

22   The Martin Company
        P. O. Box 5042
        Middle River, Maryland

        Attention: AEC Contract Document Custodian

23   Combustion Engineering, Incorporated
        Nuclear Division
        Windsor, Connecticut

        Attention: Director, Nuclear Division

24 - 25   Alco Products, Inc.
        P. O. Box 145
        Fort Belvoir, Va.

        Attention: W. K. Stromquist

Internal
Copies

26	K. Kasschau	38		S. L. Davidson
27	J. Gronan	39		P. L. Bradley
28	E. B. Gunyou	40		R. H. Beam
29	J. G. Gallagher	41		S. H. Weiss
30	H. L. Hoover	42		B. E. Fried
31	W. S. Brown	43		J. P. Oggerino
32	P. E. Bobe	44		S. Paluszkiewicz
33	W. T. Williams	45		E. F. Clancy
34	W. J. McCool	46		M. A. Alford
35	I. Segalman	47 - 48		Core Analysis File
36	D. H. Lee	49		Thermal and Hydraulic File
37	F. T. Matthews	50 - 54		NPED File

THIS PAGE

WAS INTENTIONALLY

LEFT BLANK

ABSTRACT

Interim results of an analytical investigation of nuclear and thermal characteristics of SM-2 type fuel elements in SM-1, SM-1A and PM-2A reactor cores are reported. Utilizing modified two group diffusion theory, predictions of power distribution, and core and rod reactivity were performed. The calculations performed to date indicate that use of SM-2 fuel elements in SM-1, SM-1A and PM-2A is feasible from the nuclear standpoint. Critical experiments and further analysis are expected to verify results of the initial investigation.

A steady state thermal analysis of each plant utilizing SM-2 elements was carried out. This analysis showed that the minimum DNBR's (departure from nuclear boiling ratios) were considerably above the minimum value from the design criteria standpoint at both the operating and scram power levels. The investigation at this point indicated that SM-2 elements can successfully be employed in SM-1, SM-1A, and PM-2A as replacement core elements. The final thermal analysis based on more accurate estimates of power distribution and internal element flow distribution is expected to verify results of the initial investigation.

THIS PAGE

WAS INTENTIONALLY

LEFT BLANK

TABLE OF CONTENTS

x

LIST OF FIGURES

LIST OF FIGURES (CONT'D)

LIST OF FIGURES (CONT'D)

LIST OF TABLES

SUMMARY

This is an interim report covering nuclear and thermal analysis of
the use of SM-2 elements in SM-1, SM-1A and PM-2A reactor cores. Critical
experiments and further analysis are expected to verify the results of this
initial investigation. This investigation is part of Task 3 - Replacement Core
Development Program, of the AEC-Army Pressurized Water Support and
Development Program.

The major effort in the core analysis area was the prediction of most
adverse power distribution. These predictions were performed utilizing
one - and two-dimensional diffusion theory calculations. The deviations
between calculated power distributions of this task and measured distributions
determined in the SM-2 flexible critical experiments program were employed
to modify the analytical predictions in this report. Calculations performed
to date indicate that the higher fuel loaded SM-2 elements are feasible for
use as replacement cores in SM-1, SM-1A and PM-2A.

A detailed steady state thermal analysis of SM-2 elements in SM-1,
SM-1A and PM-2A plants was performed. This analysis utilized the IBM-704
code, STDY-3. The flow distributions were based on the full scale air flow
test of the reactor vessels. Results to date of the steady state thermal
analysis indicate that the cores employing SM-2 elements will operate in
SM-1, SM-1A and PM-2A with adequate thermal safety.

THIS PAGE

WAS INTENTIONALLY

LEFT BLANK

1.0 INTRODUCTION

Replacement core development for the SM-1, SM-1A and PM-2A is a major part of the AEC-Army PWR Research and Development Program. The principal effort in the replacement core development program at this time is devoted to utilization of SM-2 fuel elements in SM-1, SM-1A and PM-2A. The SM-2 fuel elements with their increased fuel content relative to the fuel content of the initial cores for these fuel plants offer significant improvements in core life.

This is an interim report on the nuclear and thermal analysis performance to date, as part of the Replacement Core Development Program. The overall Replacement Core Development Program includes nuclear analysis and critical experiments, thermal analysis, laboratory single element flow test, and miniature fuel plate and full size fuel element irradiation. The end product of this work will be procurement specifications for SM-2 fuel elements for use in the three plants. The work in this report is preliminary due to the following limitations:

1. The analytical predictions of power distribution have not been checked against exact critical experiment mockups of SM-2 elements in SM-1, SM-1A, and PM-2A arrays.

2. The velocity variation within the SM-2 fuel elements in the various core structures has been estimated and not as yet compared with experiment.

3. The loss of pump problem has been treated only as a quasi - steady state problem.

Critical experiments are now being performed using SM-2 fuel elements in the exact SM-1, SM-1A, and PM-2A core arrays. The results of these measurements will be utilized to check and correct the analytical predictions of power distribution and reactivity. This will permit the power distribution to be developed with improved accuracy necessary for final thermal analysis. Results of this work will be contained in a final report, which will also contain core burnup studies.

Laboratory tests are now under way in which the velocity variation between the plates within an element will be measured for SM-2 fuel plate bundles in the various end box and core support configurations. The final thermal analysis will utilize the most accurate power distribution, experimentally measured plate-to-plate velocity variations, and final estimates of hot channel factors. The final report of this work will be issued in late 1961.

THIS PAGE

WAS INTENTIONALLY

LEFT BLANK

2.0 NUCLEAR ANALYSIS

This section contains the preliminary nuclear analysis of the use of SM-2 type fuel elements in the SM-1, SM-1A and PM-2A. Table 2.1 lists the loadings of the SM-2 fuel elements compared to those of the original cores.

It is seen that the boron and uranium loadings for the SM-2 elements are significantly higher than the loading of the original cores; this will result in a more adverse power distribution.

In the SM-1 Core I and SM-1A Core I, five of the seven control rods are operated as a bank with the two remaining rods nearly fully withdrawn. However, for preliminary studies with SM-2 elements, it was decided to utilize a seven rod bank for the SM-1 and SM-1A with SM-2 elements. Therefore, both the critical experiments and the analyses presented in this report are based upon seven rod bank operation in the SM-1 and SM-1A. The decision for utilization of a seven rod bank was based upon stuck rod considerations. For five rod bank operation there is a possibility that one or both of the remaining rods could stick in the full out position; however, for seven rod bank operation, if one or more rods should stick, the rods would stick at the operating position. This would be less hazardous than for one or more rods to be stuck full out. The relative merits of five vs. seven rod bank operation will be studied further and presented in the final report.

A brief description of the calculational models employed is given, followed by a summary of the calculations performed.

TABLE 2.1
TABLE OF CORE LOADINGS

Fixed Element Loadings	SM-1 Core I *	SM-2 Elements
U-235 (gm/element)	611.88	833.4
B-10 (gm/element)	0.42813	1.3055

Control Rod Fuel Element Loadings		
U-235 (gm/element)	417.14	655.68
B-10 (gm/element)	0.29286	1.027

* Similar loadings are used in SM-1A and PM-2A.

2.1 CALCULATIONAL APPROACH

The nuclear analyses in this report were performed by utilizing various IBM-650 and IBM-704 codes to solve the two-group diffusion equations. The IBM-650 codes used were the Program 50 (PROMPT-1), Plate Type P_3, MUFT-III, VALPROD, and the WINDOWSHADE. These codes are described in reference (1). The IBM-704 code used was the PDQ-3.[3]

2.1.1 Nuclear Parameters

2.1.1.1 Thermal Constants

For most of the core regions, thermal constants were obtained by the Program 50 and Plate Type P_3, IBM-650 codes. In regions that did not require this code, homogenized properties were used. In addition, the absorber region constants, $(\sum a)_e$ and D_e (where e means effective), were calculated by methods described in reference (3).

2.1.1.2 Fast Constants

The fast constants were obtained by calculating the number densities of the material in each region and using them as input to the MUFT III, IBM-650 code.

2.1.1.3 Nomenclature

Parameter	Definition	Units
D^f	Fast Diffusion coefficient	cm
D	Thermal diffusion coefficient	cm
K^f	Fast multiplication factor	
K^{th}	Thermal multiplication factor	
$\sum_a^f$	Fast macroscopic absorption cross section	cm^{-1}
$\sum_a$	Thermal macroscopic absorption corss section	cm^{-1}
τ	Age	cm^2
L^2	Diffusion length	cm^2
P	Resonance escape probability	

Parameter	Definition	Units
$\sum_{sl}$	Slowing down cross section	
$\nu\sum_f^f$	Fast macroscopic fission cross section	cm^{-1}
$\nu\sum_f$	Thermal macroscopic fission cross section	cm^{-1}
$\sum_R$	Regional cross section (i.e., fixed element dead retion)	cm^{-1}
$\sum_P$	Calculated thermal poison macroscopic cross section	cm^{-1}
σ	Miscroscopic cross section	cm^2
$\overline{\overline{\sum}}$	Flux weighted cross section	cm^{-1}
N_H	Number density of hydrogen oxygen	$atoms/cm^3$
N_O	Number density of oxygen	$atoms/cm^3$
N_{SS}	Number density of stainless steel	$atoms/cm^3$
N_{B-10}	Number density of B-10	$atoms/cm^3$
N_{U-235}	Number density of U-235	$atoms/cm^3$
H	Symbol for hydrogen	
O	Symbol for oxygen	
SS	Symbol for stainless steel	
U-235	Symbol for Uranium-235	
X	Elemental subscript (i.e., H, O, etc.)	
N_X	Number density of some element x	$atoms/cm^3$
ρ_X	Density of element X	gms/cm^3
A	Atomic weight	$gms/gm\text{-}atom$
N_A	Avogadro's numbers	$atoms/gm\text{-}atom$
V_f	Volume fraction	
V_{TOT}	Total volume	cm^3
V_X	Volume of element X	cm^3

7

2.1.2 Power Distributions and Reactivity

2.1.2.1 Radial Power Distributions

All radial flux and power distributions were calculated using PDQ-3, an IBM-704 code. One problem in using this code was mesh point limitations. It was impossible to mockup a core with 7 rods full in. Thus, it was necessary to use a 5 rod full in PDQ calculation and devise a method to obtain 7 rod bank parameters for use in the axial power distribution calculation. This method will be discussed in the next section.

2.1.2.2 Axial Power Distribution

The axial power distribution for the PM-2A was calculated using an axial VALPROD, an IBM-650 Code. The input nuclear parameters for the VALPROD were obtained by flux weighting both the rods-in and the rods-out nuclear constants of the PDQ-3 input by the integrated regional fluxes of the PDQ output. [3] This method has been found to agree much better with experimental results than the WINDOWSHADE code. In the WINDOWSHADE code, a calculated thermal poison cross section, Σ_p is added to the core group constants in the rodded region.

The axial power distribution with no xenon for the SM-1 and the SM-1A was calculated by the following technique.

1. A 5 rod flux weighted axial VALPROD was run to obtain a K_{eff} (as close to 1 as possible) and a rod bank position.

2. A WINDOWSHADE (using SM-2 fixed element homogenized constants) was run searching for a 5 control rod Σ_p to be used with the rod bank position and K_{eff} obtained from the axial VALPROD.

3. When a Σ_p for 5 rods was obtained in this fashion, a Σ_p for 7 rods was obtained using the Jo^2 method described in reference (1).

4. After obtaining Σ_p for 7 rods, another WINDOWSHADE using the 7 rod Σ_p (with a K_{eff} of 1.00) was run to obtain the proper 7 rod bank position and corresponding axial power distribution.

2.1.2.3 Reactivity Calculations

Reactivity values for all three cases were obtained from the PDQ-3 output by the following:

$$\rho = \frac{K_{eff} - 1}{K_{eff}}$$

8

From previous studies employing the same analytical models,[11] it was found that the predicted reactivities underestimated the measured values by approximately 2% ρ . Therefore a model correction of 2% ρ was added to all calculated reactivities.

Also evaluated by use of PDQ-3 were the rod bank worths in each of the cores. This was calculated by performing PDQ-3's for rods full-in and rods full-out cases. The value of the control rod bank worth was then obtained by:

$$\rho_{rods} = \frac{(K_{eff})_{out} - (K_{eff})_{in}}{(K_{eff})_{out}}$$

2.2 POWER DISTRIBUTION CALCULATIONS

2.2.1 SM-1 Core

This section contains a preliminary analysis of the power distribution and radial power factors for the SM-1 core (Fig. 2.1) at 68°F and 440°F, using SM-2 fuel elements. The power generation within the core must be known in order to perform a thermal analysis. To perform this thermal analysis, certain nuclear factors must be available; these include:

$F_n (\Delta T)$ = nuclear hot spot factor to allow for uncertainty in the calculated power distribution used in the calculation of bulk coolant temperature rise.

$F_n (\Delta \theta)$ = nuclear hot spot factor to allow for uncertainty in the calculated power distribution used in the calculation of the film temperature rise.

$Q (\Delta T)$ = power generation rate for worst channel in each element, normalized to an average radial power of one over the whole core.

$\overline{Q (\Delta T)}$ = average power generation rate in each element, normalized to an average radial power of one over the whole core.

$Q (\Delta \theta)$ = power generation rate at the hottest spot in each element normalized to an average radial power of one over the whole core.

$\psi (\Delta T)$ = fraction of total reactor power generated in the core.

9

$\psi \, (\triangle \, \theta)$ = fraction of total reactor power generated in the fuel plates

L = active core height

N = total number of space increments within the core, as used in the WINDOWSHADE calculations.

To obtain the radial power peaking factors, four PDQ-3 cases were performed:

1. Rods Out, T = 440°F

2. Rods In, T = 440°F (5 rod bank)

3. Rods Out, T = 68°F

4. Rods In, T = 68°F (5 rod bank)

Figures 2.2 through 2.9 show graphically the calculated radial power distributions along the central radial plane both parallel and perpendicular to the fuel plates, for the hot and cold cores, rods in and rods out, for the SM-1 core with SM-2 elements.

Figures 2.10 through 2.13 show the radial values obtained from the SM-1 Core I PDQ's. [4] In comparing Fig. 2.3 with Fig. 2.11 it is noticed that the intercell power peaking is greater in the SM-1 core with SM-2 elements due to the higher absorption in the SM-2 elements. The wider meat region in the SM-2 elements decreases the relative value of the power peaks, but the relatively high SM-2 loading (Table 2.1) tends to override this effect and increases the peaking.

Table 2.2 lists the radial (x, y) maximum-to-average power ratio for various elements in the core. Central element values are essentially the same for both cases, but the ratio in the outer elements is substantially higher for the SM-2 element core. This is due once again to the higher loading in the SM-2 elements.

TABLE 2.2
MAXIMUM-TO-AVERAGE RADIAL POWER PEAKING VALUES
FOR SM-1 CORE I AND SM-1 CORE WITH SM-2 ELEMENTS, 440°F

Perpendicular To Fuel Plates

Element No.	SM-1 Core I	SM-1 Core (SM-2 Elements)
44 (Control Rod C)	1.039	1.085
45	1.100	1.157
46 (Control Rod 2)	1.175	1.181
47	1.464	2.100

Parallel To Fuel Plates

Element No.	SM-1 Core I	SM-1 Core (SM-2 Elements)
44 (Control Rod C)	1.124	1.158
34	1.150	1.233
24 (Control Rod 1)	1.243	1.215
14	1.318	1.800

The axial power distributions were calculated by the WINDOWSHADE and VALPROD codes. As mentioned in Section 2.1.2.2, flux weighted values for axial VALPROD inputs are calculated from the PDQ output.

Five rod bank axial VALPRODS were run with and without Eu_2O_3 flux suppressors at the bottom of the fixed fuel elements. Figures 2.14 and 2.15 show graphically the axial power distribution for each case. The use of flux suppressors effectively eliminates the power spike but increases the power peak within the core.

Five rod bank calculations were converted to 7 rod bank calculations by the method described in Section 2.1.2.2. Figure 2.16 shows the axial power distribution obtained from both the 5 and 7 rod WINDOWSHADE. The WINDOW-SHADE calculation gave a rod bank change of 1/2-in. with a change from 5 to 7 rods. Based on Fig. 10 in reference (6), a value closer to one inch is predicted. The effect of this difference on power distribution is negligible.

A comparison was made between the axial power distribution in the SM-1 Core I and SM-1 with SM-2 elements. Figures 2.16 and 2.17 show that except for an axial shift due to rod bank position, the relative values for the 5 rod SM-1 Core I and the 7 rod SM-1 with SM-2 elements are very similar for the initial case. Figures 2.14 and 2.15 show that a flux suppressor causes a higher power peak inside the core, while effectively eliminating the power spike at the bottom of the core; therefore, if flux suppressors were used in the calculations presented in Fig. 2.17, the power distributions would be in better agreement with the 7 rod bank curve in Fig. 2.16.

When the analyses of the radial and axial power distributions were completed, calculation of the power peaking factors was possible.

F_n ($\triangle T$) and F_n ($\triangle \theta$) were assigned values of 1.05 and 1.10 respectively.[8]

The factor Q ($\triangle \theta$) is calculated by the following equations:

$$Q \ (\triangle \theta) = \left[P(x, y,)_{\substack{max. \\ element}} \right] \left[F_{rods} \right] \left[F_{\substack{local \\ correction}} \right]$$

Where $P(x, y,)_{max; \ element}$ is the hottest spot in each element as calculated by the PDQ-3 code, and F_{rods} and $F_{local \ correction}$ are correction factors which will be discussed in another section.

The factor Q ($\triangle T$) is calculated with the following equation:

$$Q \ (\triangle T) = \left[P_{hot \ plate} \right] \left[F_T \right]$$

where $F_T = \left[F_{rods} \right] \left[F_{local \ correction} \right]$

The value of $\overline{Q \ (\triangle T)}$ is obtained from the equation:

$$\overline{Q \ (\triangle T)} = \left[P_{element} \right] \quad F_T$$

Correction factors, F_{rods} and $F_{local \ correction}$, were incorporated to bring calculated radial power values more into agreement with measured values. F_{rods} is used to make the calculated value of the power at the center of each element agree with the experimental values of the power at the center of each element. The equation for F_{rods} for a given element is:

$$F_{rods} = \frac{\left[\dfrac{P\,(x, y, z) \text{ measured at the center of the element}}{P \text{ (measured with a core average of 1.0)}} \right]}{\left[\dfrac{P\,(x, y)\ P\,(z) \text{ calculated at the center of the element}}{P \text{ (calculated with a core average of 1.0)}} \right]}$$

where

$P\,(x, y, z)$ = the power measured by a foil count

$P\,(x, y)$ = radial power from a PDQ calculation

$P\,(z)$ = the maximum calculated axial power

$F_{local\ correction}$ is a correction factor used to make the calculated power values at the edge of each element agree with the experimental power value at the edge of each element. The equation for $F_{local\ correction}$ for a given element is:

$$F_{local\ correction} = \frac{\left[\dfrac{P(x, y, x) \text{ measured at the edge of the element}}{P(x, y, x) \text{ measured at the center of the element}} \right]}{\left[\dfrac{P(x, y)\ P(z) \text{ calculated at the edge of the element}}{P(x, y)\ P(z) \text{ calculated at the center of the element}} \right]}$$

In this report a value F_T was used. This is the product of the above two correction factors.

Table 2.3 lists the values of $Q\,(\triangle \theta)_0$, $Q\,(\triangle T)_0$, and $\overline{Q\,(\triangle T)_0}$ for the SM-1 at $440^O F$ and 0 MWYRS. These values will not be the most severe encountered due to the mode of burnup of SM-2 elements. Table 2.3 also lists the values of $Q\,(\triangle \theta)_B$, $Q\,(\triangle T)_B$ $Q\,(\triangle T)_B$ estimated to be their maximum value using SM-2 data. These values were used in the thermal analysis together with the axial power distribution calculated at 0 MWRY.

The heat release factors are:

$$\psi\,(\triangle T) = 1.00$$

$$\psi\,(\triangle \theta) = 0.95$$

These values are reported in reference (8). The value of L is 55.88 cm or 22 in. The value of N is 44 calculational points, or a point at every 1/2 in. in the WINDOWSHADE calculations.

Figure 2.16 shows the relative axial power values used in the thermal calculation. These results were obtained from a WINDOWSHADE calculation.

TABLE 2.3
RADIAL POWER FACTORS FOR SM-1 CORE
WITH SM-2 ELEMENTS, T = 440°F

Element No.	0 MWYR			Estimated Maximum		
	$Q(\triangle\theta)_o$	$Q(\triangle T)_o$	$\overline{Q(\triangle T)}_o$	$Q(\triangle\theta)_B$	$Q(\triangle T)_B$	$\overline{Q(\triangle T)}_B$
44	1.959	1.761	1.614	2.177	1.957	1.793
55	1.928	1.660	1.432	2.142	1.844	1.591
34	1.862	1.575	1.372	2.069	1.750	1.525
53	1.721	1.660	1.288	1.912	1.844	1.431
32	1.761	1.470	.892	1.957	1.633	.991
66	1.336	1.046	.862	1.484	1.162	.957
61	2.042	1.601	.758	2.269	1.779	.842
75	1.721	.998	.880	1.912	1.109	.978
41	2.059	1.973	.936	2.287	2.192	1.040

$$(\triangle T) = 0.95 \qquad F_n(\triangle\theta) = 1.10$$

$$(\triangle\theta) = 1.00 \qquad F_n(\triangle T) = 1.05$$

$$P(z)_{max} = 1.911$$

2.2.2 SM-1A Core

The SM-1A core is essentially the same as the SM-1. It has 38 fixed fuel elements and seven control rod fuel elements in a closed array (Fig. 2.18). The fuel loadings are the same. The SM-1A differs from the SM-1 in that all the fuel plates in the outer rows of elements in the SM-1A are perpendicular to the water reflector. This modification was incorporated to decrease the power peaking in the outer row of fuel elements.
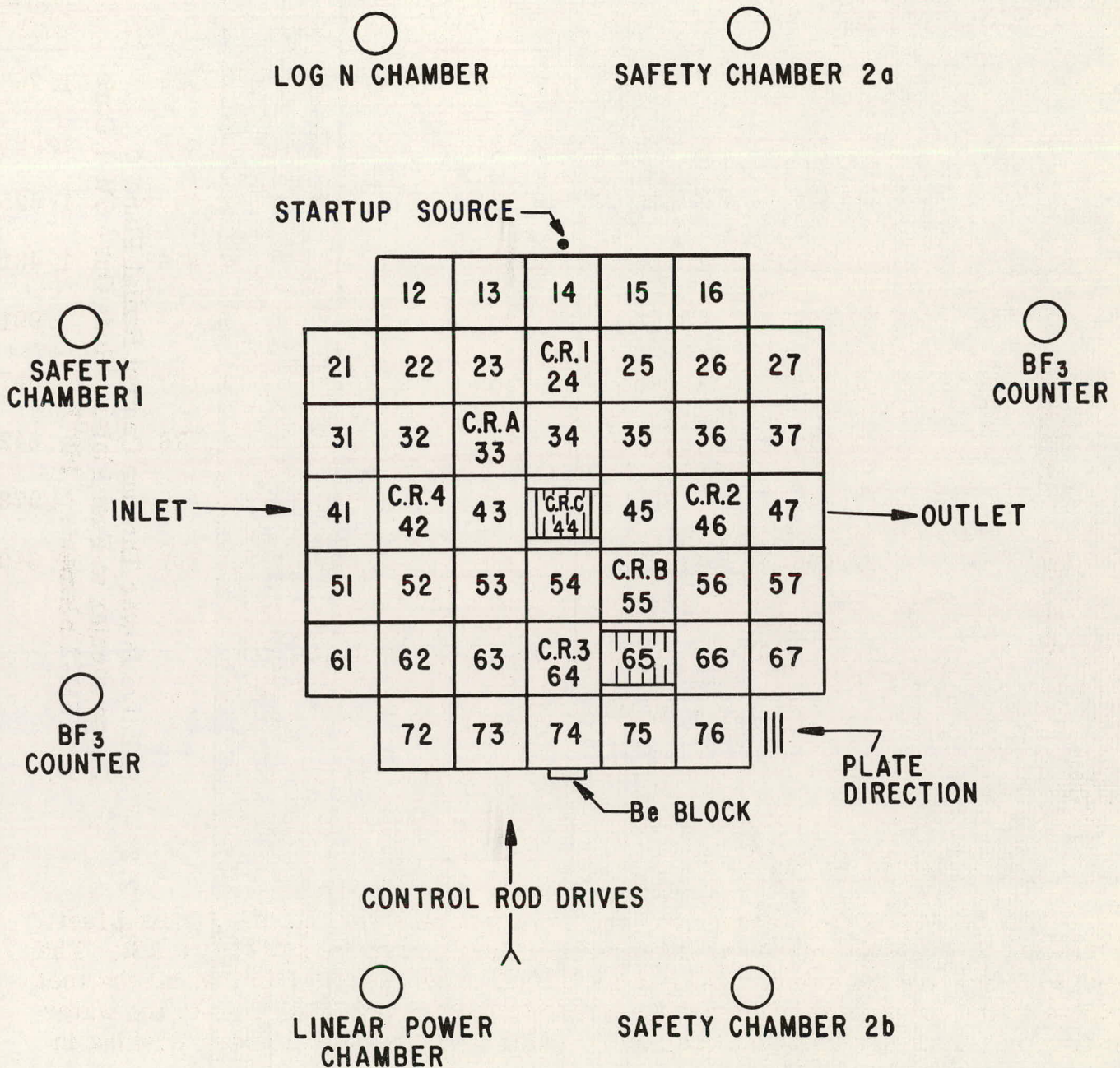
Fig. 2.1 - SM-1 Core Layout

Fig. 2.2 - Relative Power Through Central Radial Plane
Perpendicular to Fuel Plates - Rods Out - SM-1 Core
With SM-2 Elements - 440°F

Fig. 2.3 - Relative Power Through Central Radial Plane
Parallel to Fuel Plates - Rods Out - SM-1 Core
With SM-2 Elements - 440°F

Fig. 2.4 - Relative Power Through Central Radial Plane
Perpendicular to Fuel Plates - 5 Rods in - SM-1 Core
With SM-2 Elements - 440°F

RELATIVE POWER THROUGH CENTRAL RADIAL PLANE
PARALLEL TO FUEL PLATES – 5 RODS IN
SM-1 CORE WITH SM-2 ELEMENTS – 440°F

Fig. 2.5 –

Fig. 2.6 - Relative Power Through Radial Plane Perpendicular To Fuel Plates - Rods Out - SM-1 Core With SM-2 Elements - 68°F

RELATIVE POWER THROUGH CENTRAL RADIAL PLANE
PARALLEL TO FUEL PLATES - RODS OUT - 68°F
SM-1 CORE WITH SM-2 ELEMENTS

DISTANCE FROM CORE CENTER (INCHES)

Fig. 2.7 -

RELATIVE POWER THROUGH CENTRAL RADIAL PLANE
PERPENDICULAR TO FUEL PLATES - 5 RODS IN
SM-1 CORE WITH SM-2 ELEMENTS - 68°F

RELATIVE POWER

DISTANCE FROM CORE CENTER (INCHES)

Fig. 2.8 -

Fig. 2.9 - Relative Power Through Central Radial Plane Parallel To Fuel Plates - 5 Rods In - SM-1 Core With SM-2 Elements - 68°F
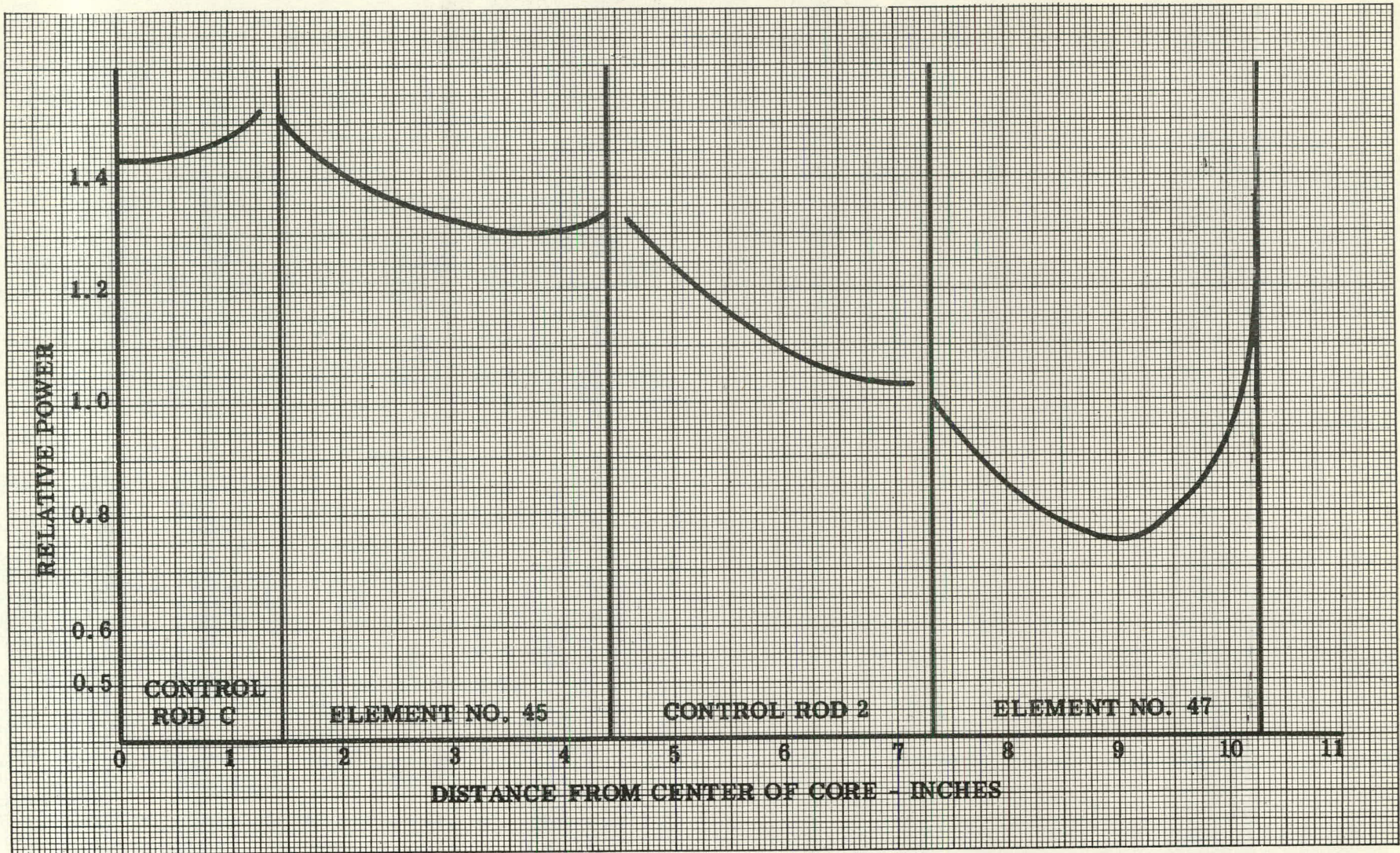
Fig. 2.10 - Relative Power Through Central Radial Plane Perpendicular To Fuel Plates - SM-1 Core I - 440°F
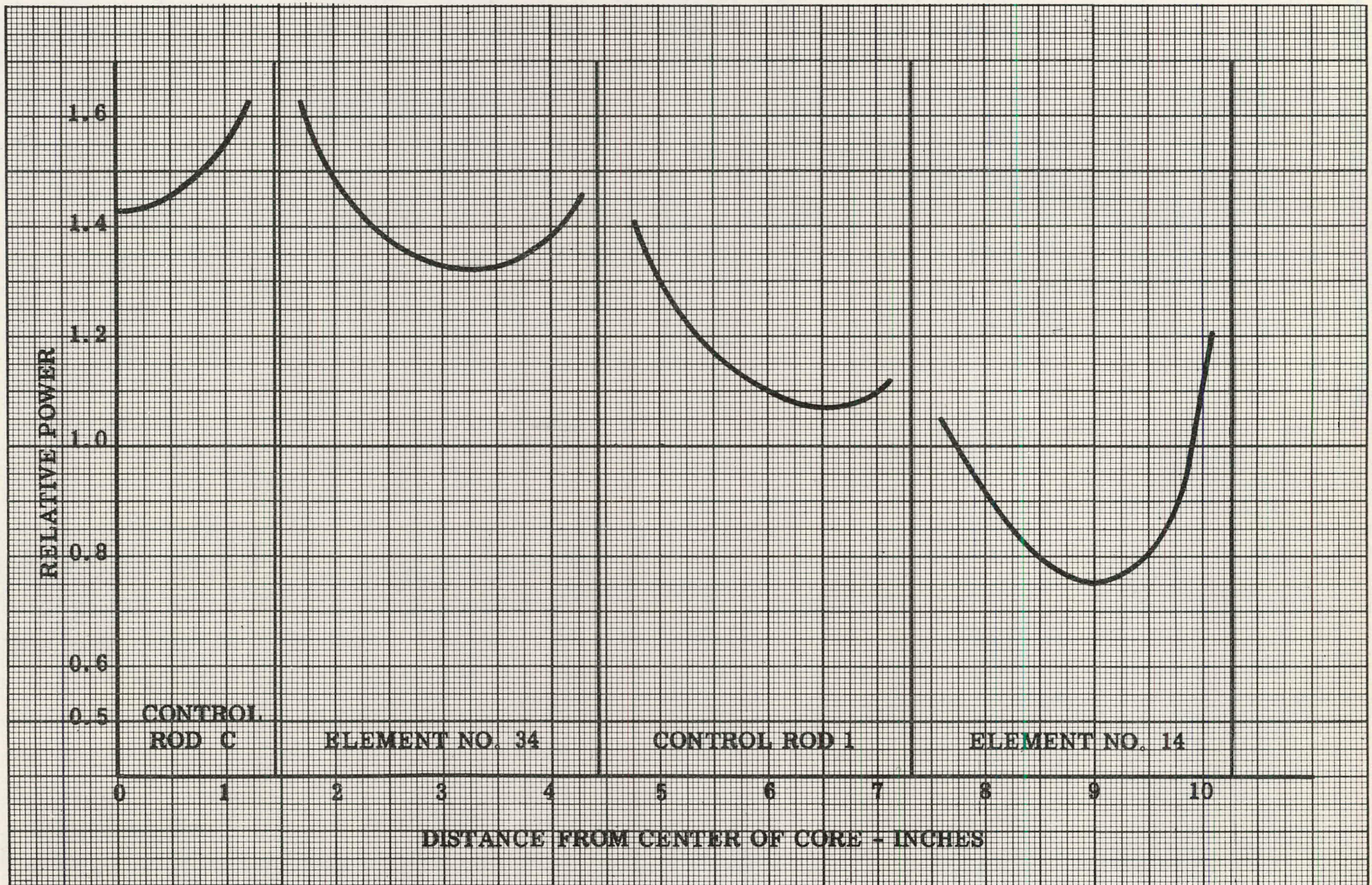
Fig. 2.11 - Relative Power Through Central Radial Plane Parallel to
Fuel Plates - SM-1 Core I - 440°F
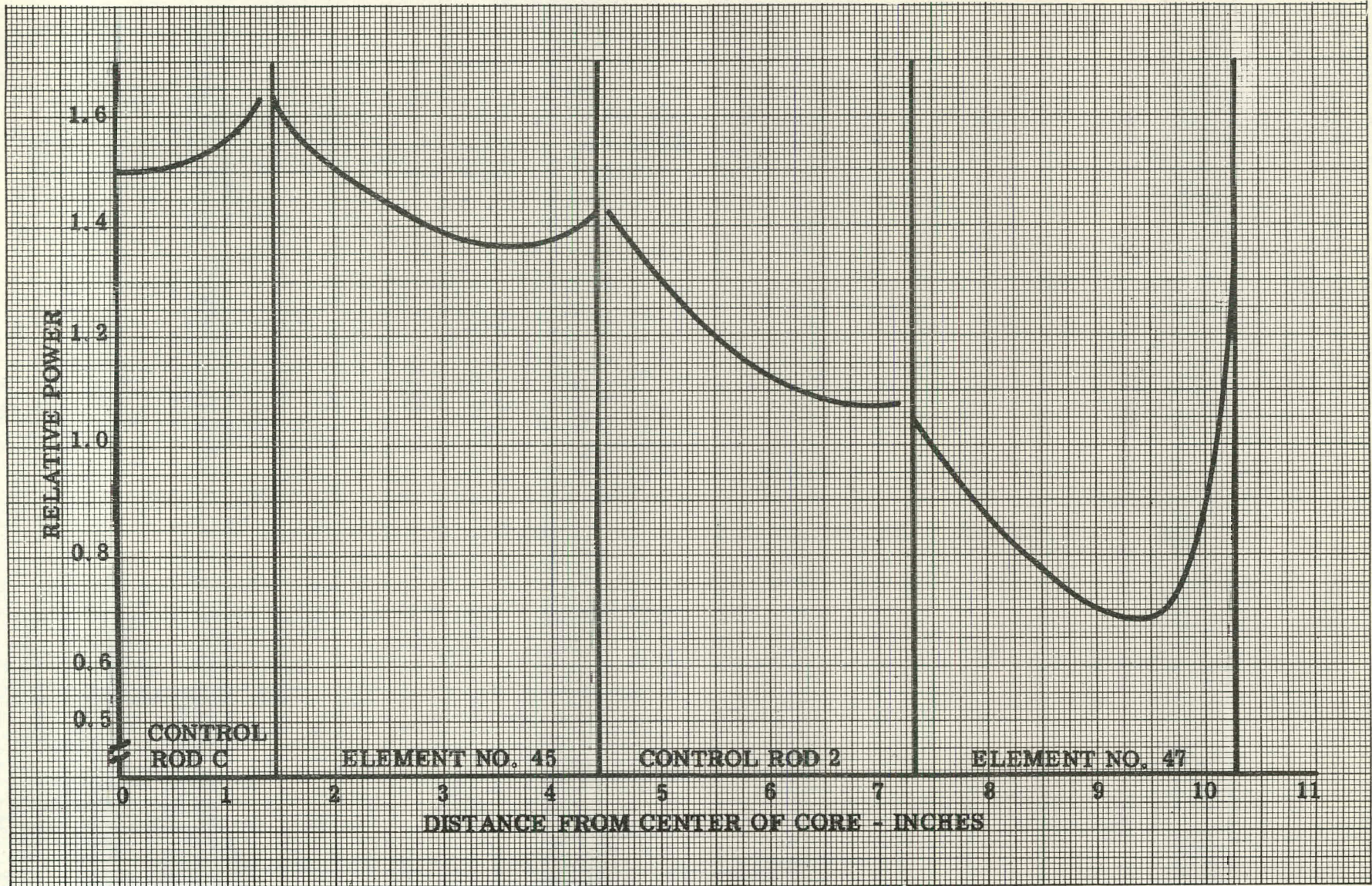
Fig. 2.12 - Relative Power Through Central Radial Plane
Perpendicular To Fuel Plates - SM-1 Core I -
68°F
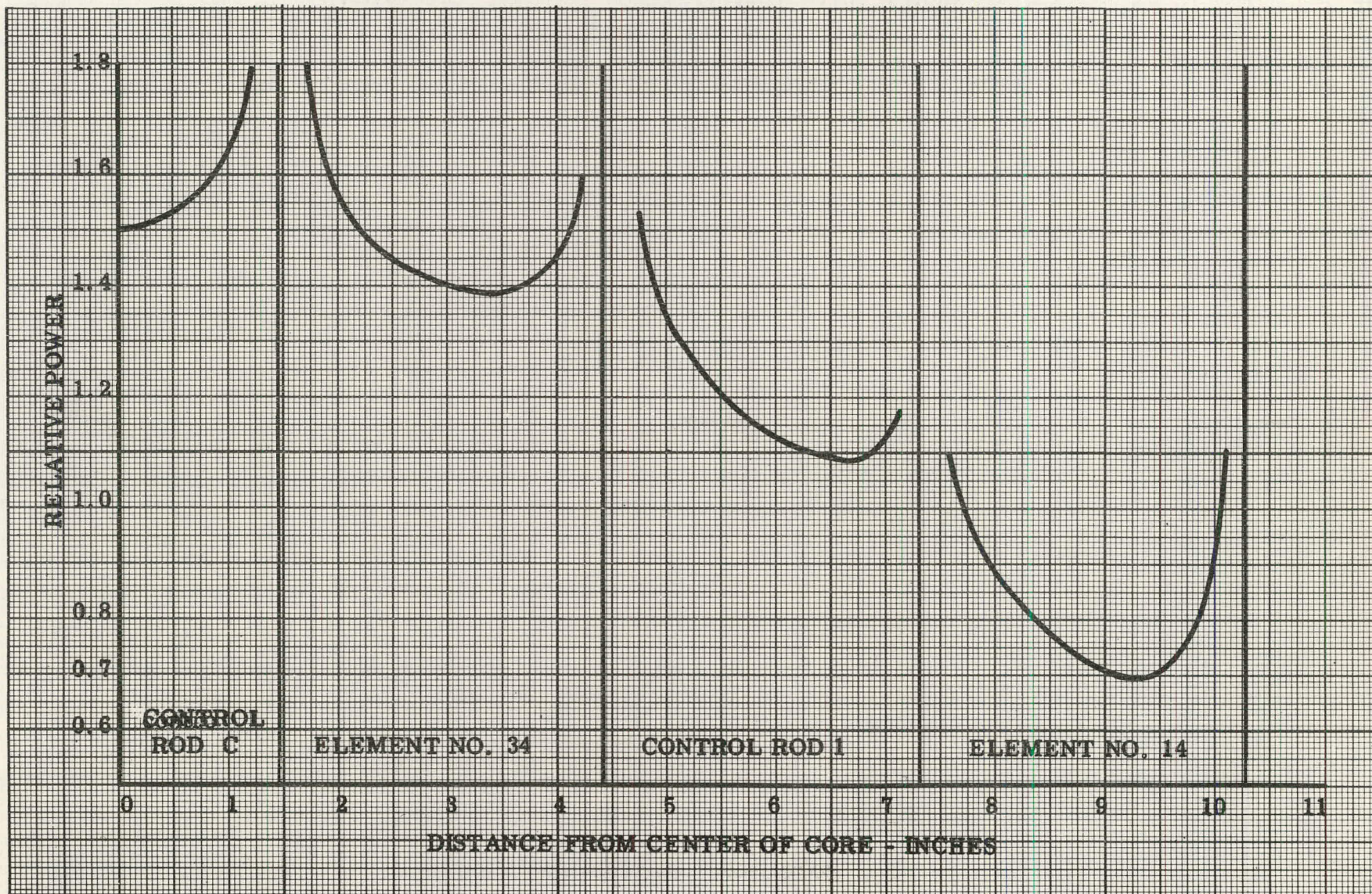
Fig. 2.13 - Relative Power Through Central Radial Plane
Parallel To Fuel Plates - SM-1 Core I - 68°F

27

RELATIVE AXIAL POWER DISTRIBUTION (VALPROD)
SM-1 CORE WITH SM-2 ELEMENTS WITHOUT FLUX SUPPRESSORS - 440°F
(BASED ON FLUX WEIGHTED GROUP CONSTANTS)

Fig. 2.14 -

RELATIVE AXIAL POWER DISTRIBUTION
SM-1 CORE - SM-2 ELEMENTS - 440°F - WITH FLUX SUPPRESSOR
(BASED ON FLUX WEIGHTED GROUP CONSTANTS)

POWER NORMALIZED TO CORE
AVERAGE OF ONE

5 ROD BANK POSITION →

RELATIVE POWER

DISTANCE FROM BOTTOM OF CORE (INCHES)
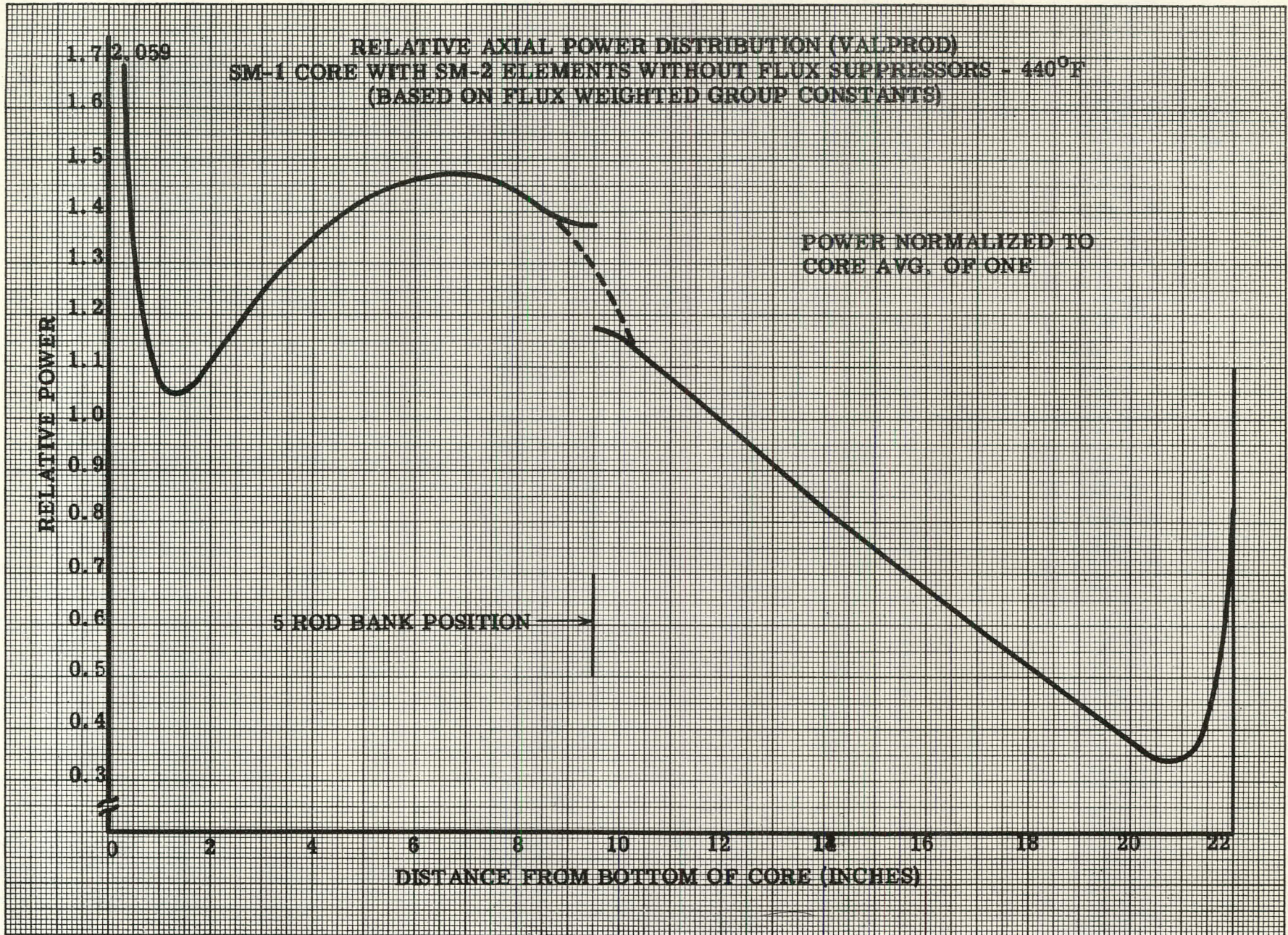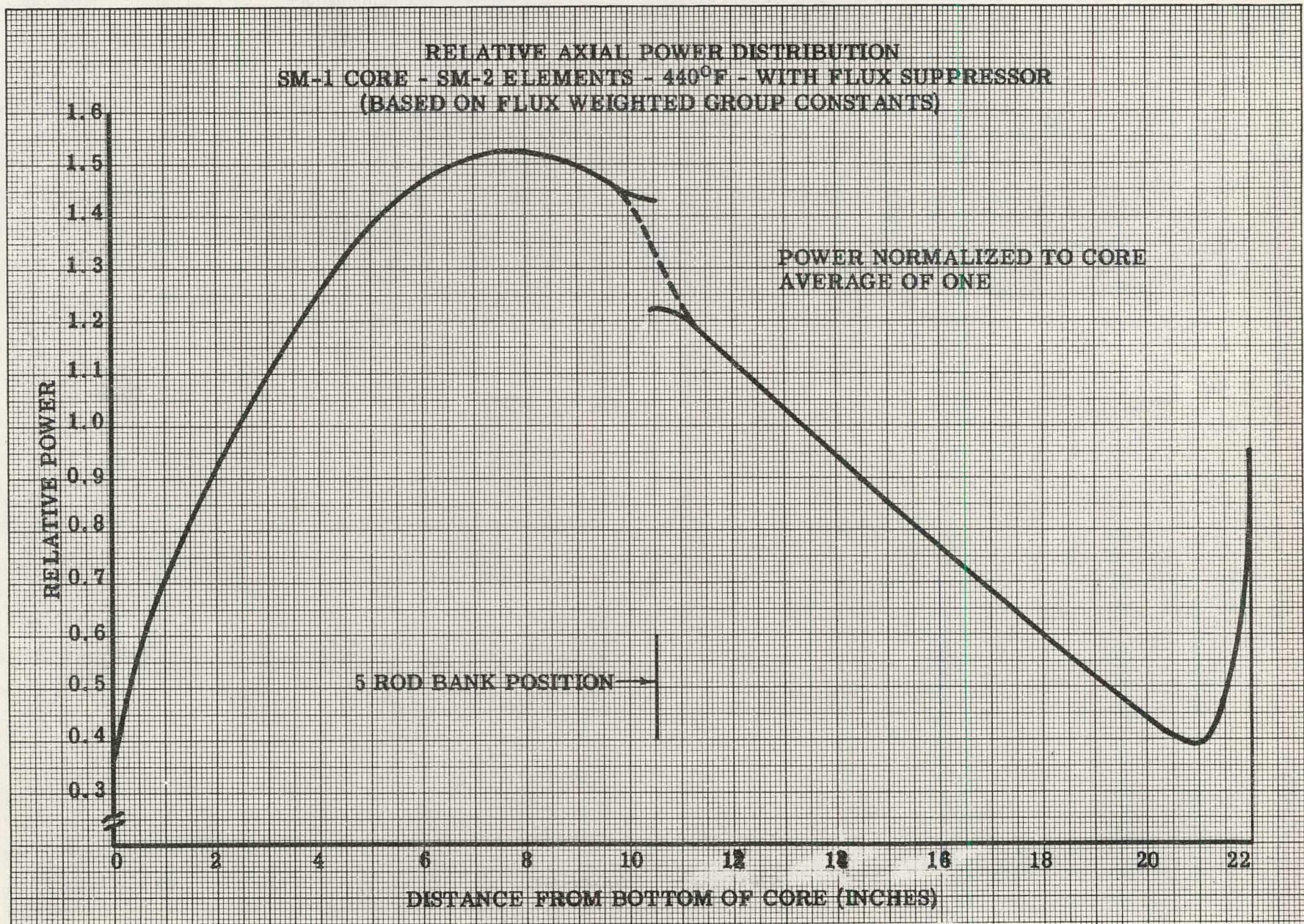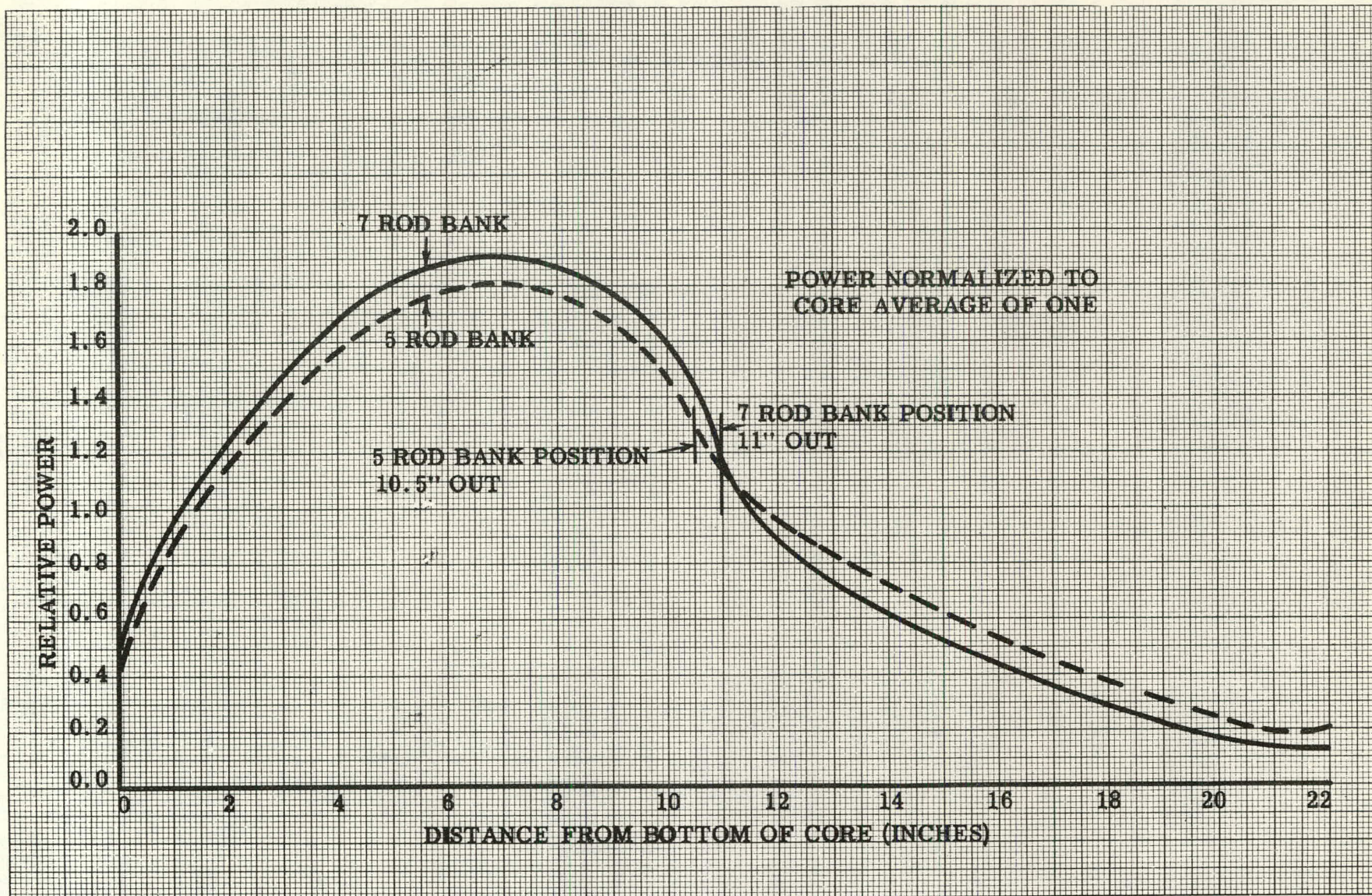
Fig. 2.15 -

Fig. 2.16 - Relative Axial Power (Windowshade) - SM-1 Core
SM-2 Elements - 440°F - With Flux Suppressor
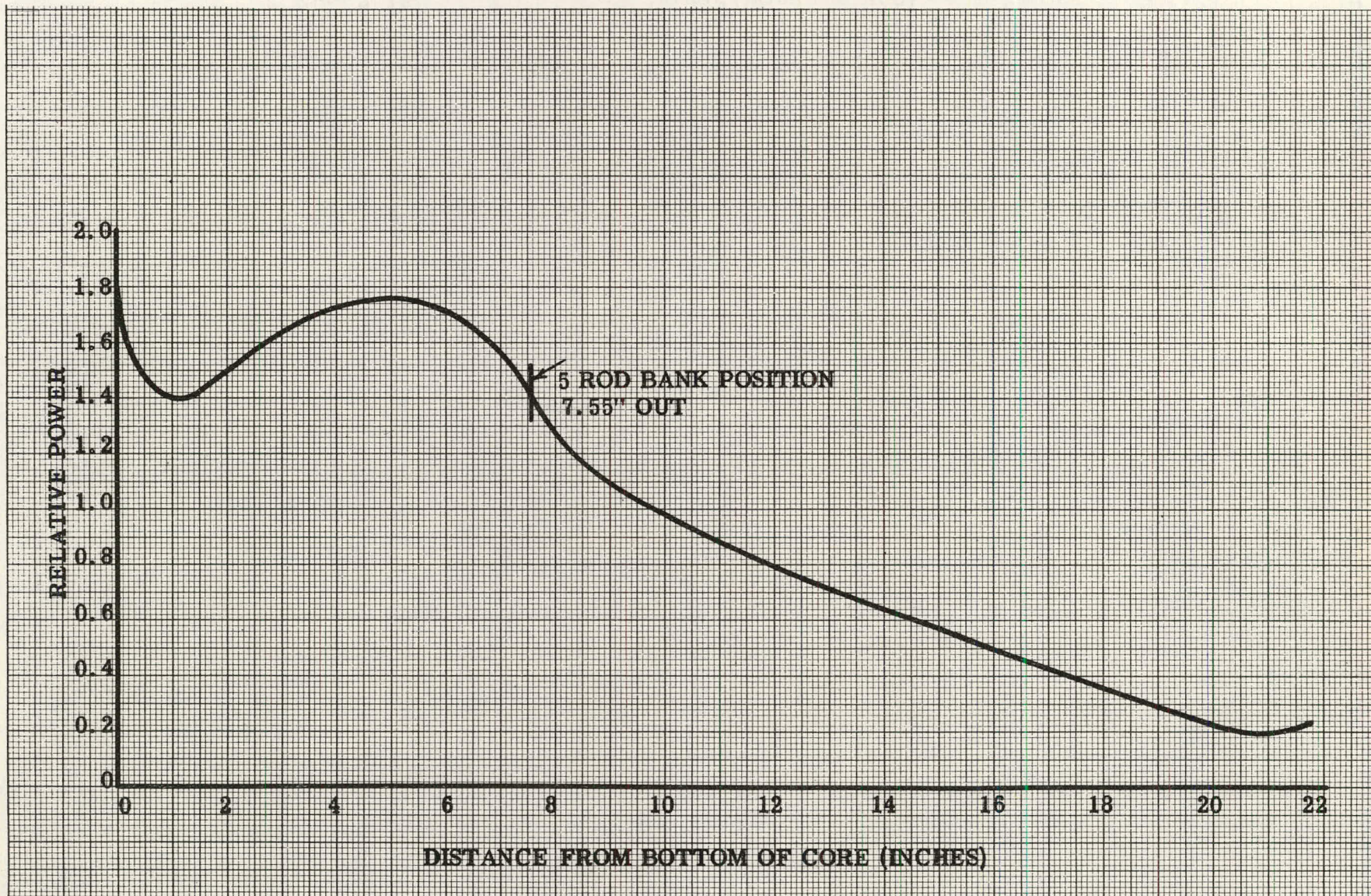
Fig. 2.17 - Relative Axial Power (Windowshade) - Sm-1 Core I - 440°F - No Flux Suppressor

THIS PAGE

WAS INTENTIONALLY

LEFT BLANK

The method of analysis for the SM-1A was the same as that for the SM-1. Figures 2.19 to 2.24 show graphically the radial power distribution along the central radial plane of the SM-1A. These distributions were obtained, using the IBM-704, PDQ-3 code. The input used was the same as that for the SM-1, except for the geometrical difference of turning the two outside rows of elements.

The PDQ output yielded the results expected along the outer row of fuel elements. Figure 2.19 shows the radial power in the outer element in the SM-1A to be less than that shown in Fig. 2.2 for the SM-1, with the fuel plates 90° out of phase, while the power distribution in the direction common to both cores is the same. There is a 16% reduction in the value of the reflector power peaks in the SM-1A compared to SM-1.

The axial power distribution with no xenon in the SM-1A was assumed to be the same as that in the SM-1.

The parameters F_n ($\triangle$ T) and F_n ($\triangle$ θ) were kept the same as the SM-1: 1.05 and 1.10, respectively.

Table 2.4 lists the values obtained for Q ($\triangle$ θ)$_o$, Q ($\triangle$ T)$_o$ and $\overline{Q (\triangle T)}_o$ at 0 MWYR in the SM-1A. The estimated maximum power for the SM-1A is the same as the SM-1. Table 2.4 also lists the values of Q ($\triangle\theta$)$_B$, Q ($\triangle$ T)$_B$ and $\overline{Q (\triangle T)}_B$ which were the values used to calculate reactor conditions in the most severe cases.

The heat release factors are:

$$\psi (\triangle T) = 1.00$$

$$\psi (\triangle\theta) = 0.95$$

The value of L is 55.88 cm or 22 in.

The value of N is 44 as in the SM-1; no WINDOWSHADES were run for this case since SM-1 axial data was used.

TABLE 2.4
RADIAL POWER FACTORS FOR SM-1A CORE WITH SM-2 ELEMENTS, $T = 440^{O}F$

Element No.	0 MWYR			Estimated Maximum		
	$Q(\Delta\theta)_O$	$Q(\Delta T)_O$	$\overline{Q(\Delta T)}_O$	$Q(\Delta\theta)_B$	$Q(\Delta T)_B$	$\overline{Q(\Delta T)}_B$
44	1.963	1.765	1.617	2.181	1.961	1.797
46	1.698	1.523	1.136	1.887	1.692	1.262
67	2.196	1.550	.503	2.440	1.720	.892
54	1.962	1.654	1.452	2.180	1.838	1.613
43	1.876	1.662	1.390	2.084	1.847	1.545
32	1.776	1.494	1.147	1.973	1.660	1.275
63	1.689	1.395	1.136	1.877	1.550	1.262
36	1.516	1.242	1.069	1.684	1.380	1.188
66	1.331	1.050	.866	1.479	1.167	.963

$$\psi(\Delta\theta) \quad 0.95 \qquad F_n(\Delta\theta) - 1.10$$

$$\psi(\Delta T) \quad 1.00 \qquad F_n(\Delta T) - 1.05$$

$$P(z)_{max} - 1.911$$

2.2.3 PM-2A Core

The analysis for the PM-2A Core (Fig. 2.25) is almost an exact duplicate, in outline, as the SM-1 and SM-1A core analysis. Figures 2.26 to 2.33 show graphically the radial power distributions obtained in each case. The axial power distribution and rod bank positions were calculated using the axial VALPROD code. Figure 2.34 shows the axial power distribution used for the thermal analysis.

Values of $Q(\Delta\theta)_O$ $Q(\Delta T)_O$ and $Q(\overline{\Delta T})_O$ are tabulated in Table 2.5. Table 2.5 also lists the values of $Q(\Delta\theta)_B$, $Q(\overline{\Delta T})_B$ and $Q(\Delta T)_B$ at their estimated maximum. The other values used for thermal information were the same as the SM-1 and SM-1A.
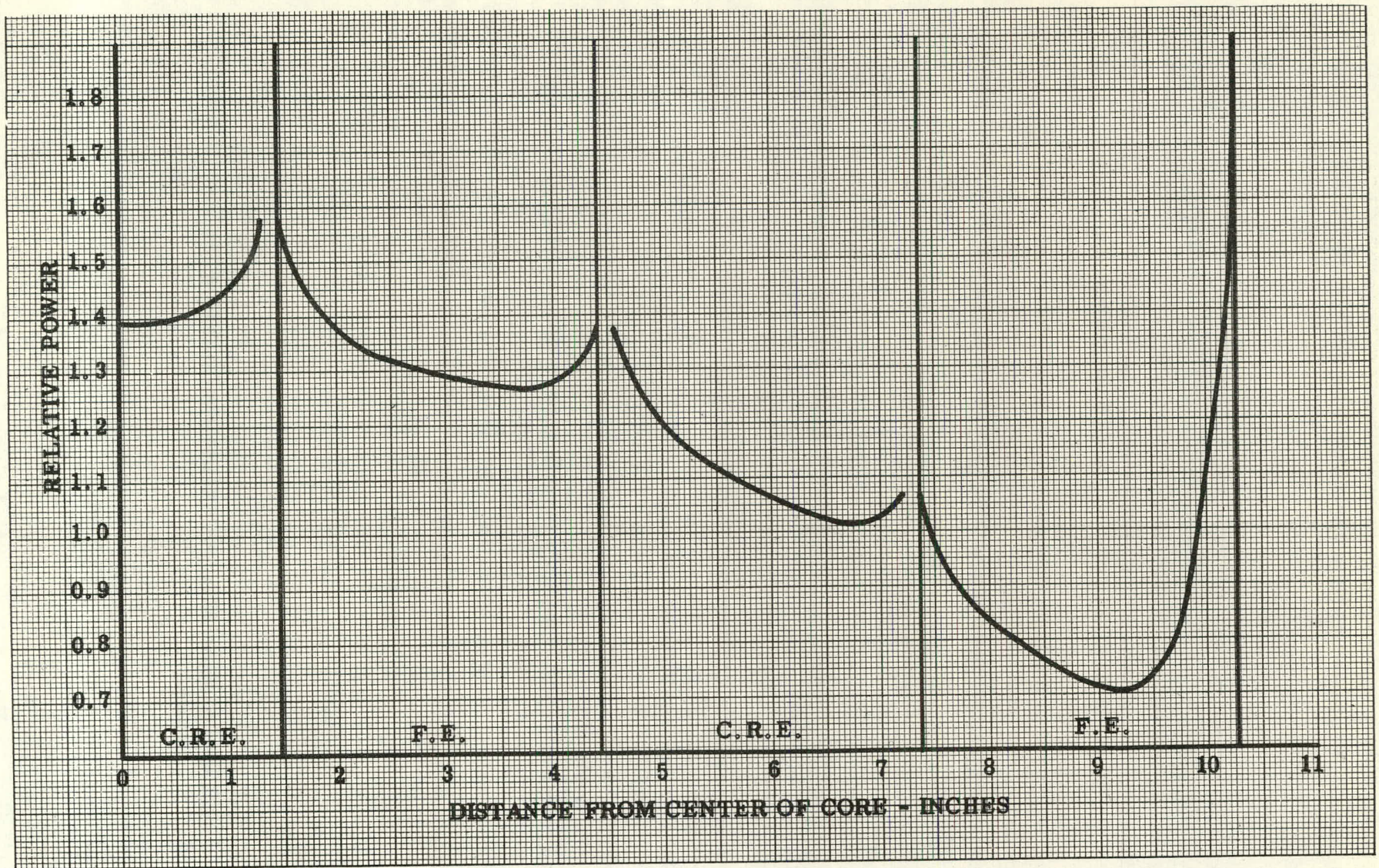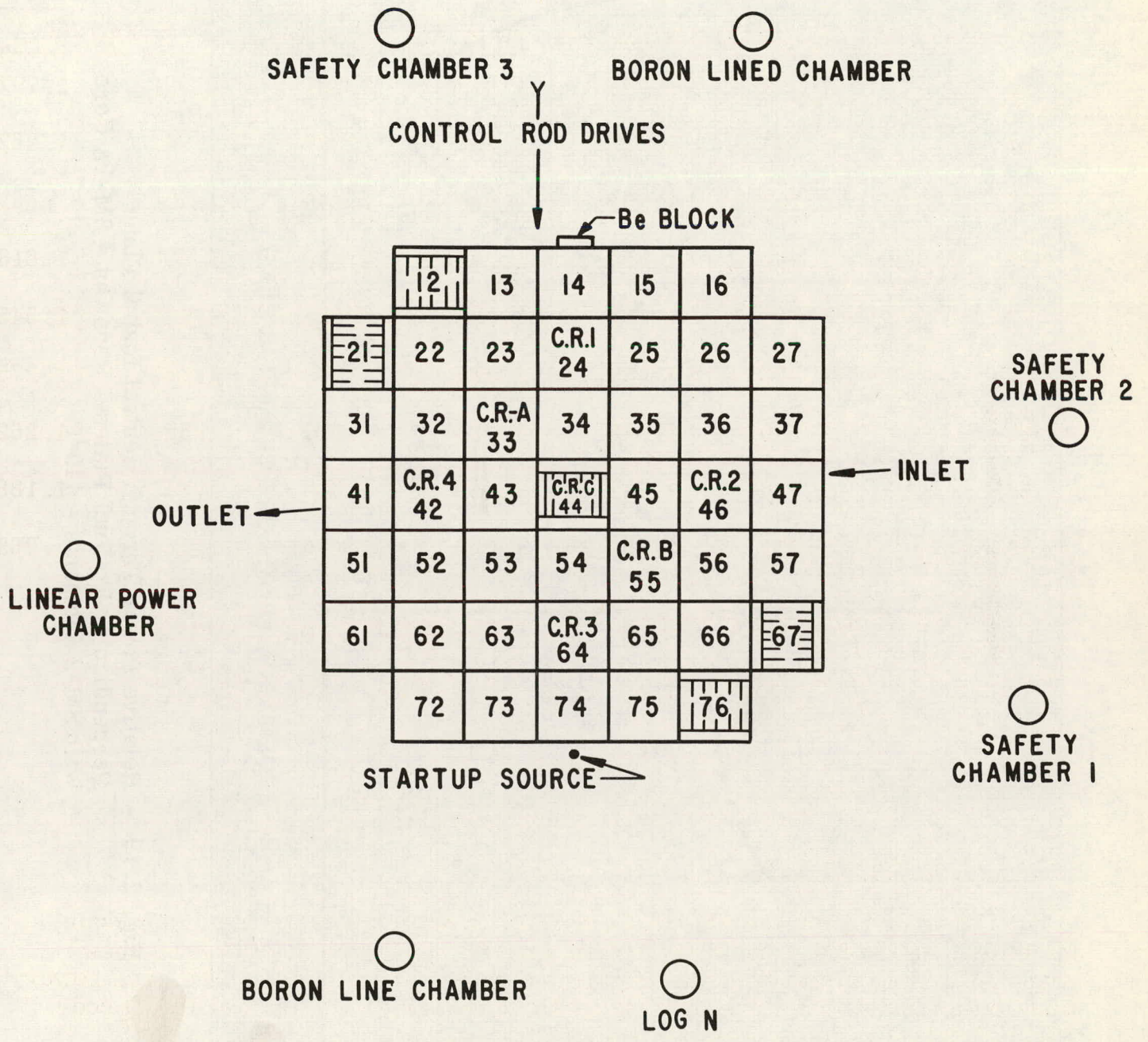
Fig. 2.18 - SM-1A Core Layout
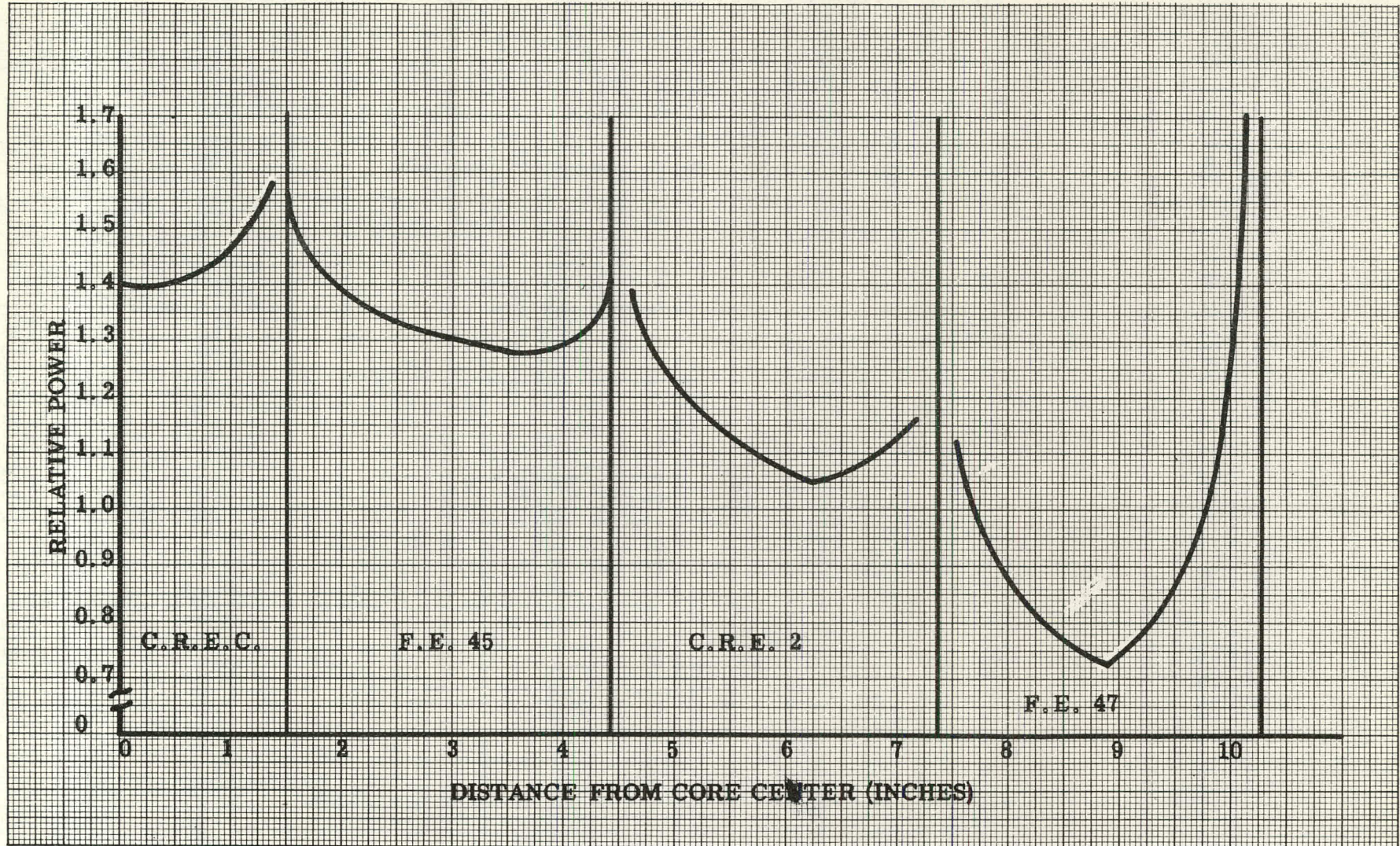
Fig. 2.19 - Relative Power Through Central Radial Plane
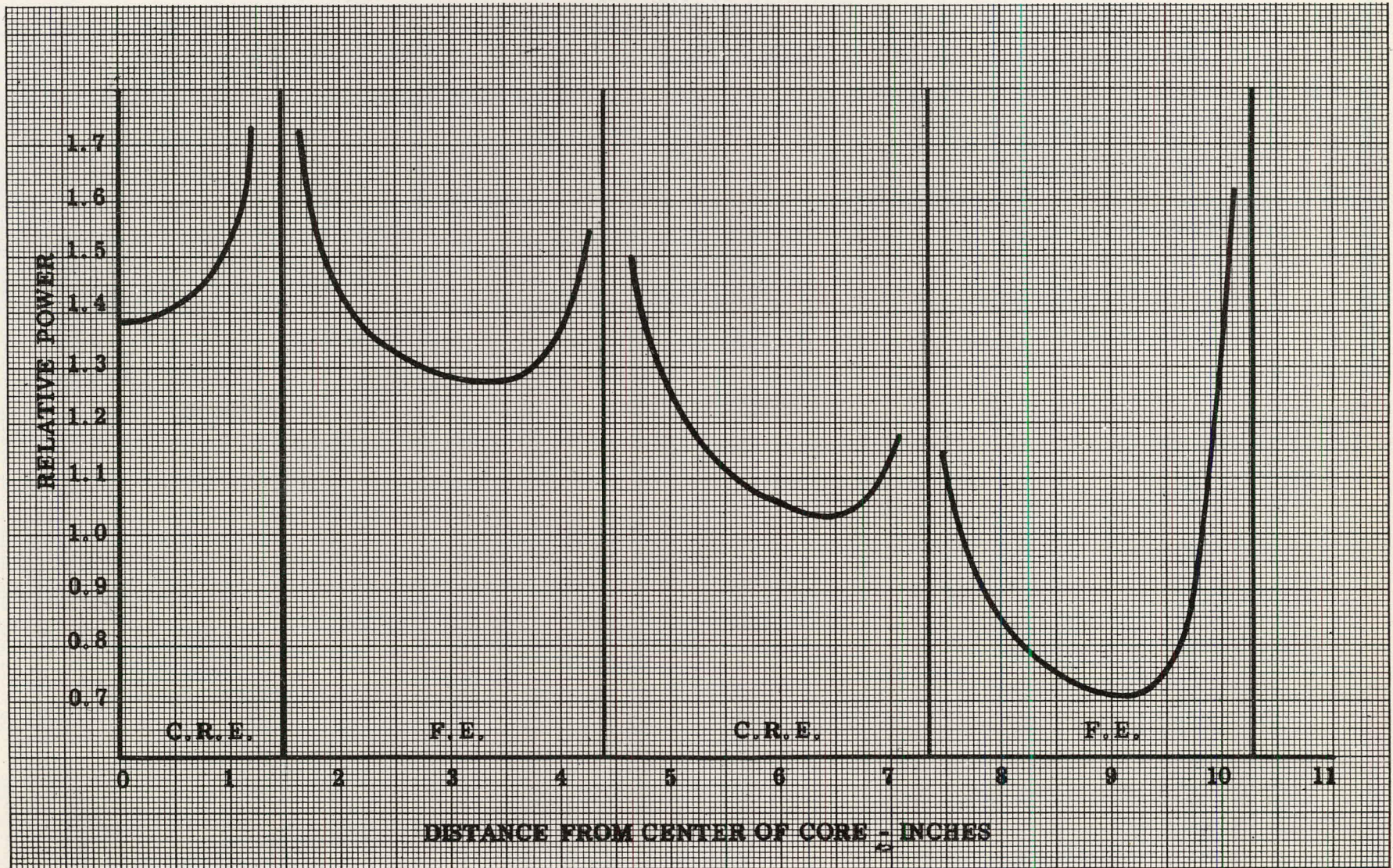Perpendicular To Fuel Plates - Rods Out - SM-1A Core
With SM-2 Elements - 440°F
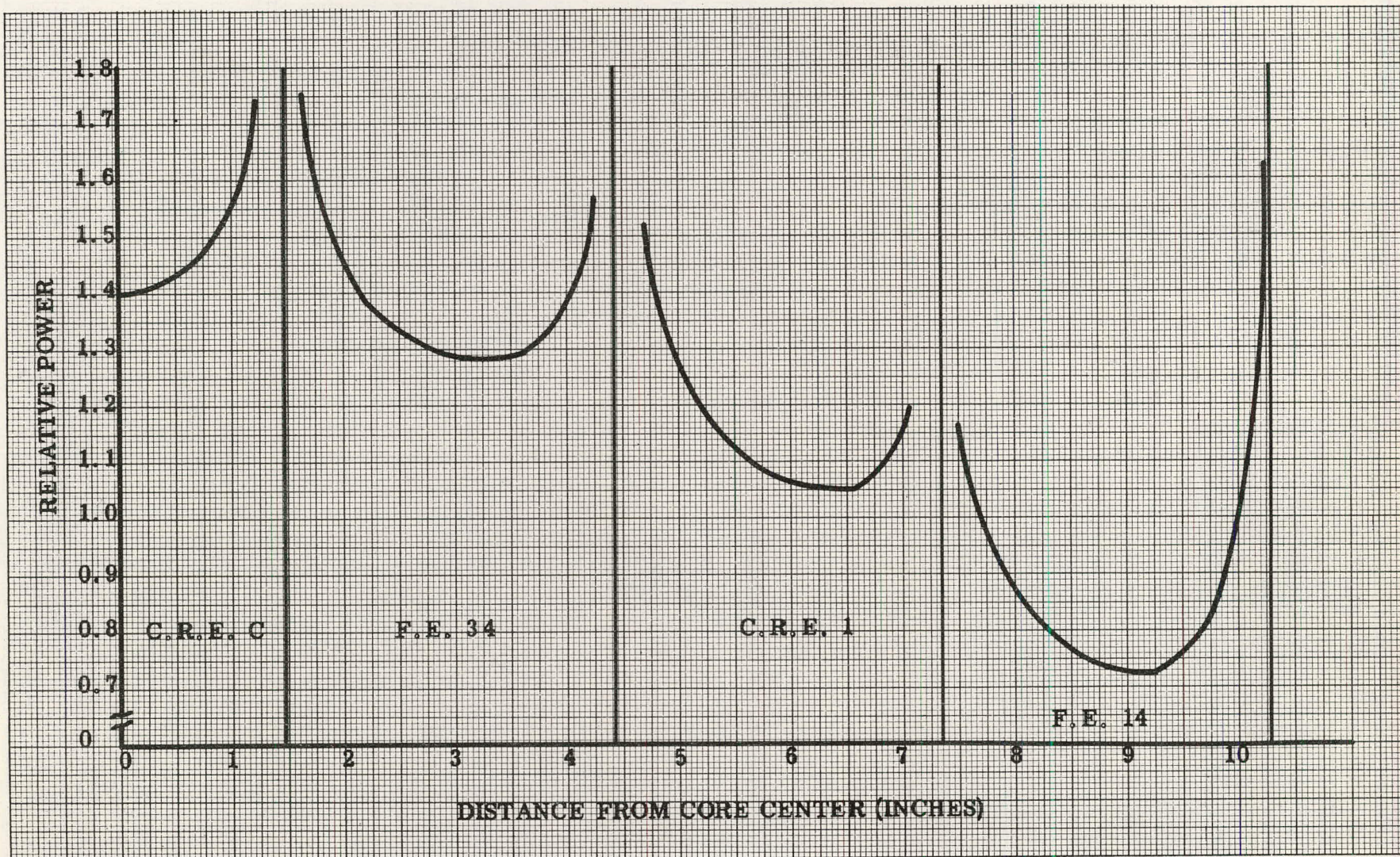
Fig. 2.20 - Relative Power Through Central Radial Plane Parallel
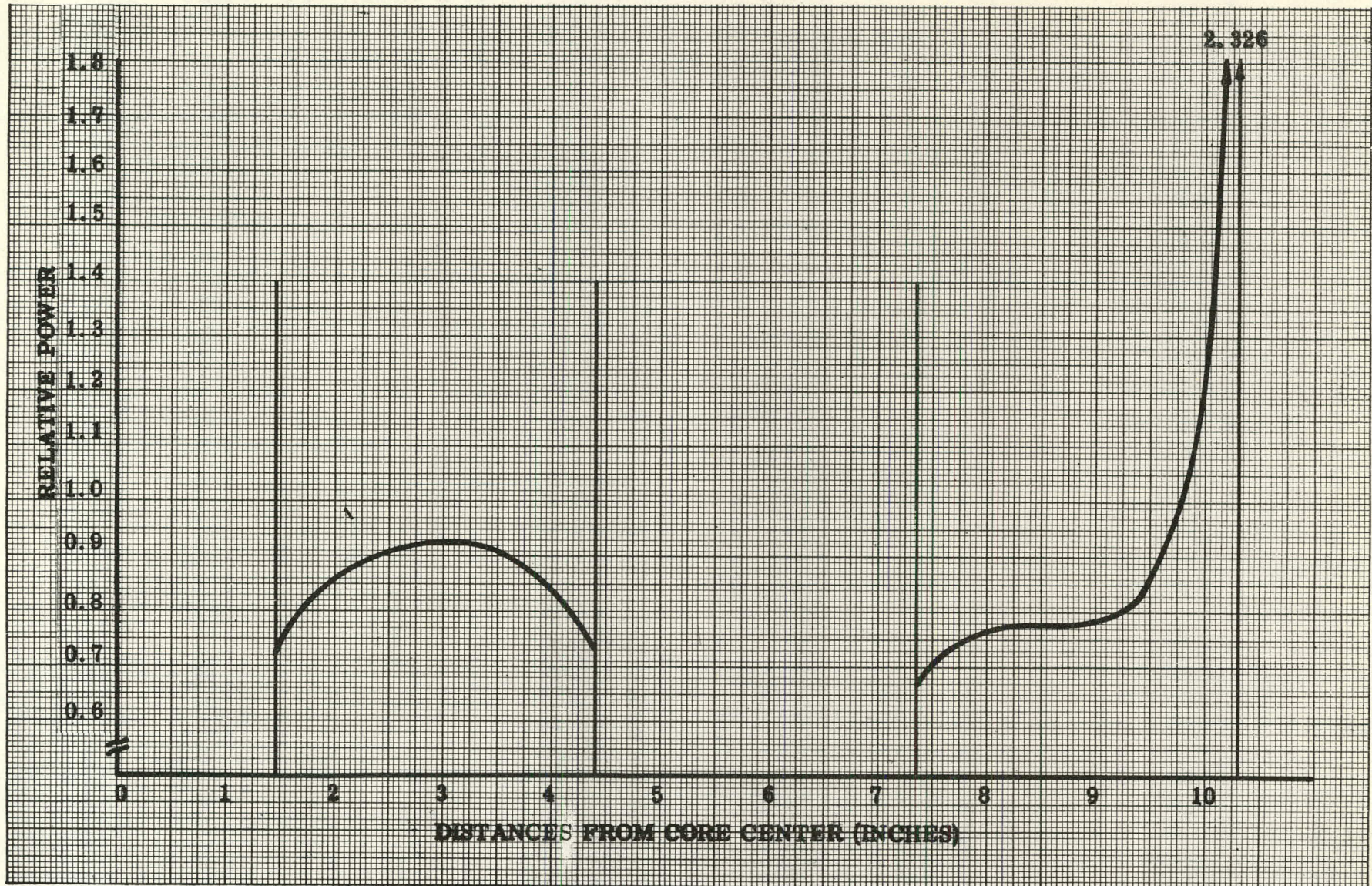To Fuel Plates - Rods Out - SM-1A Core With SM-2
Elements - 440°F

RELATIVE POWER THROUGH CENTRAL RADIAL PLANE
PERPENDICULAR TO FUEL PLATES - RODS IN
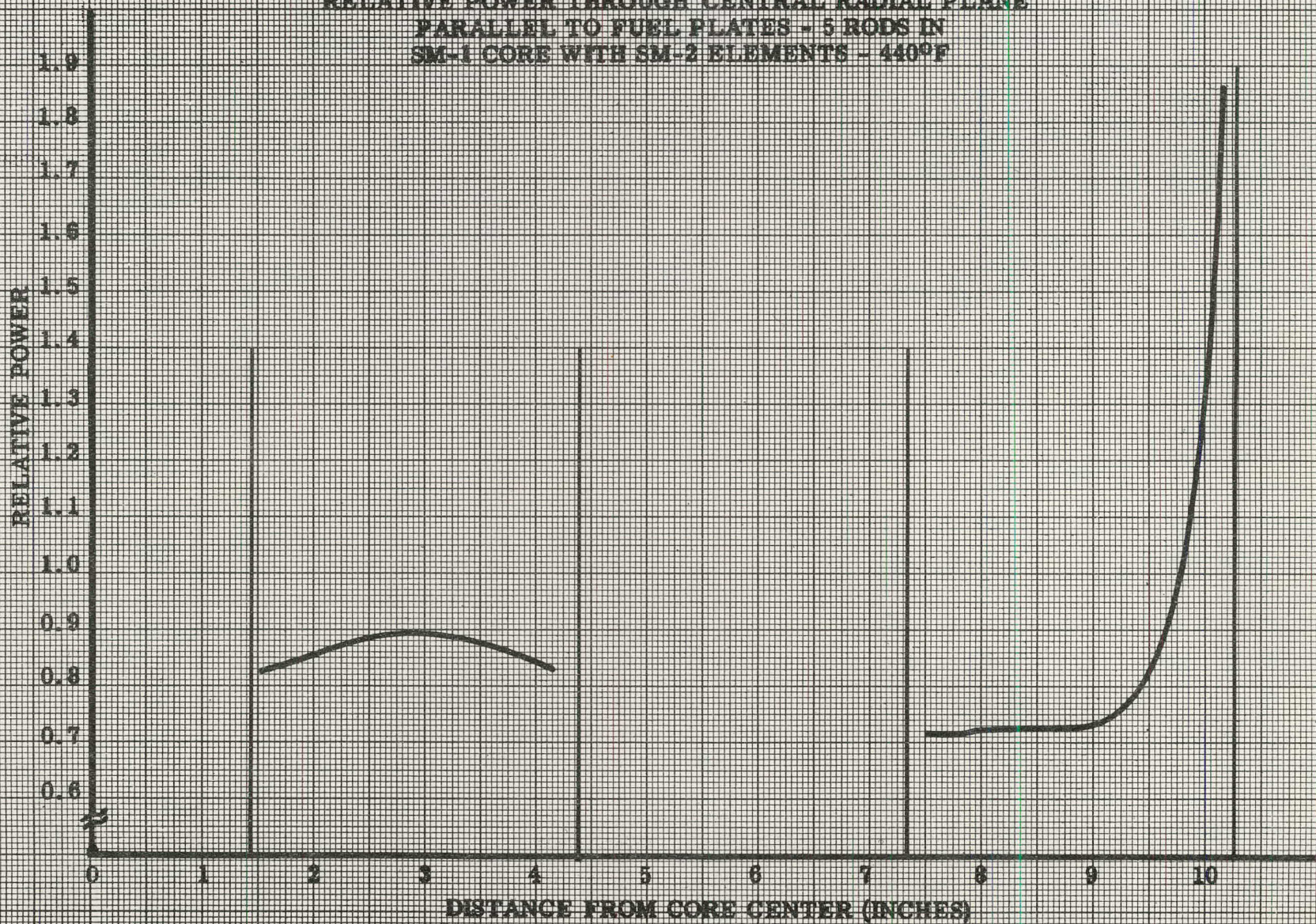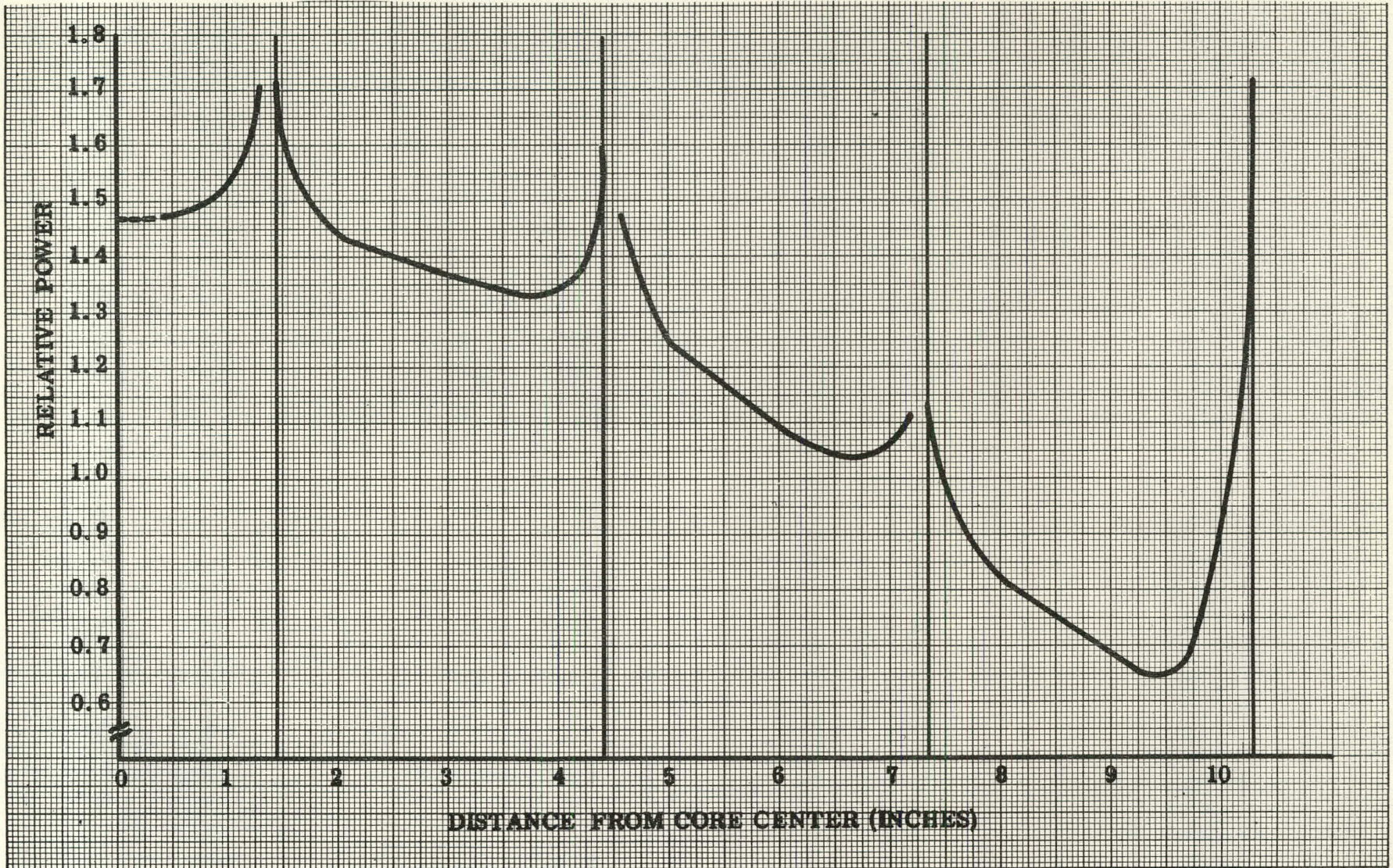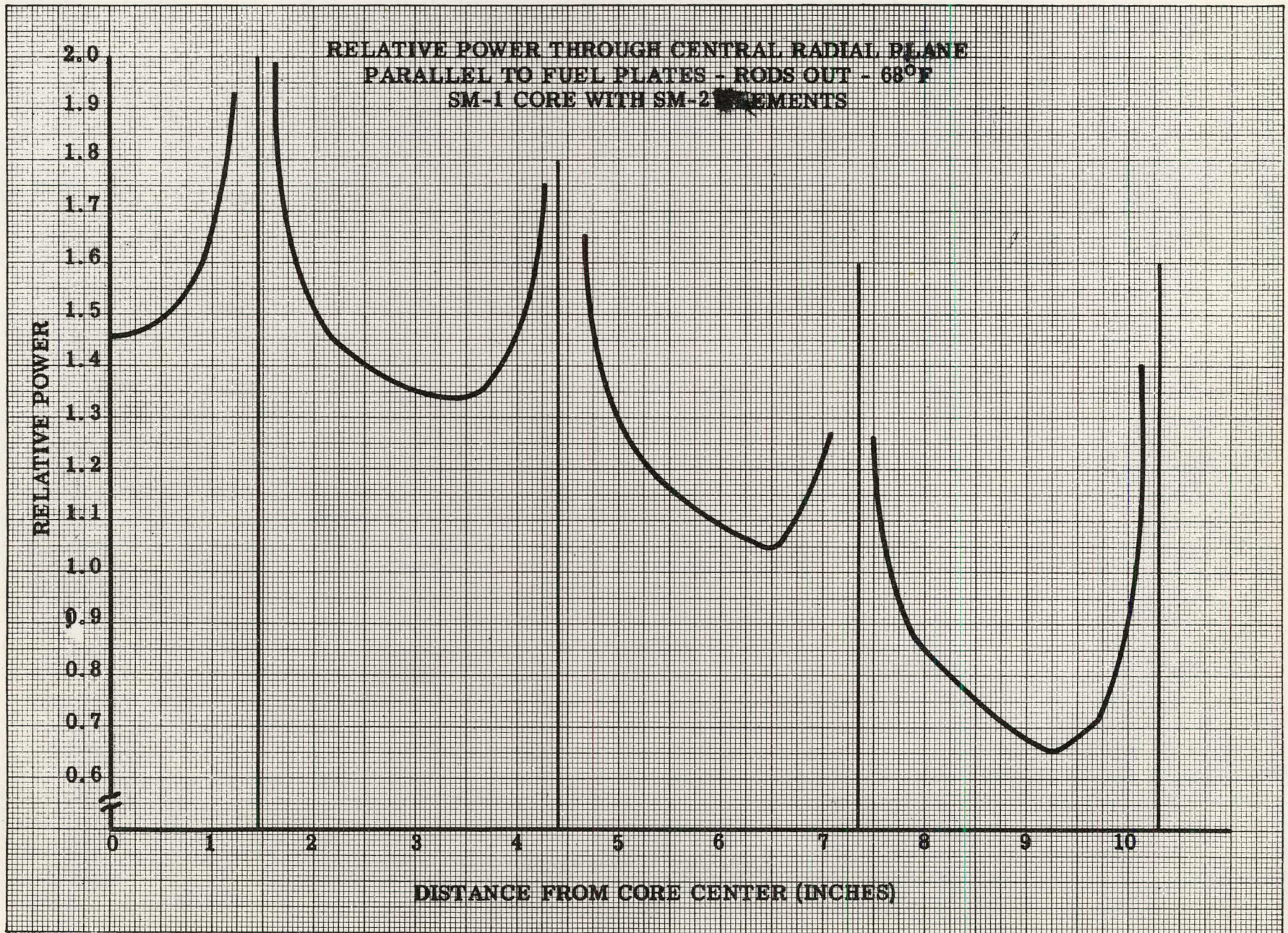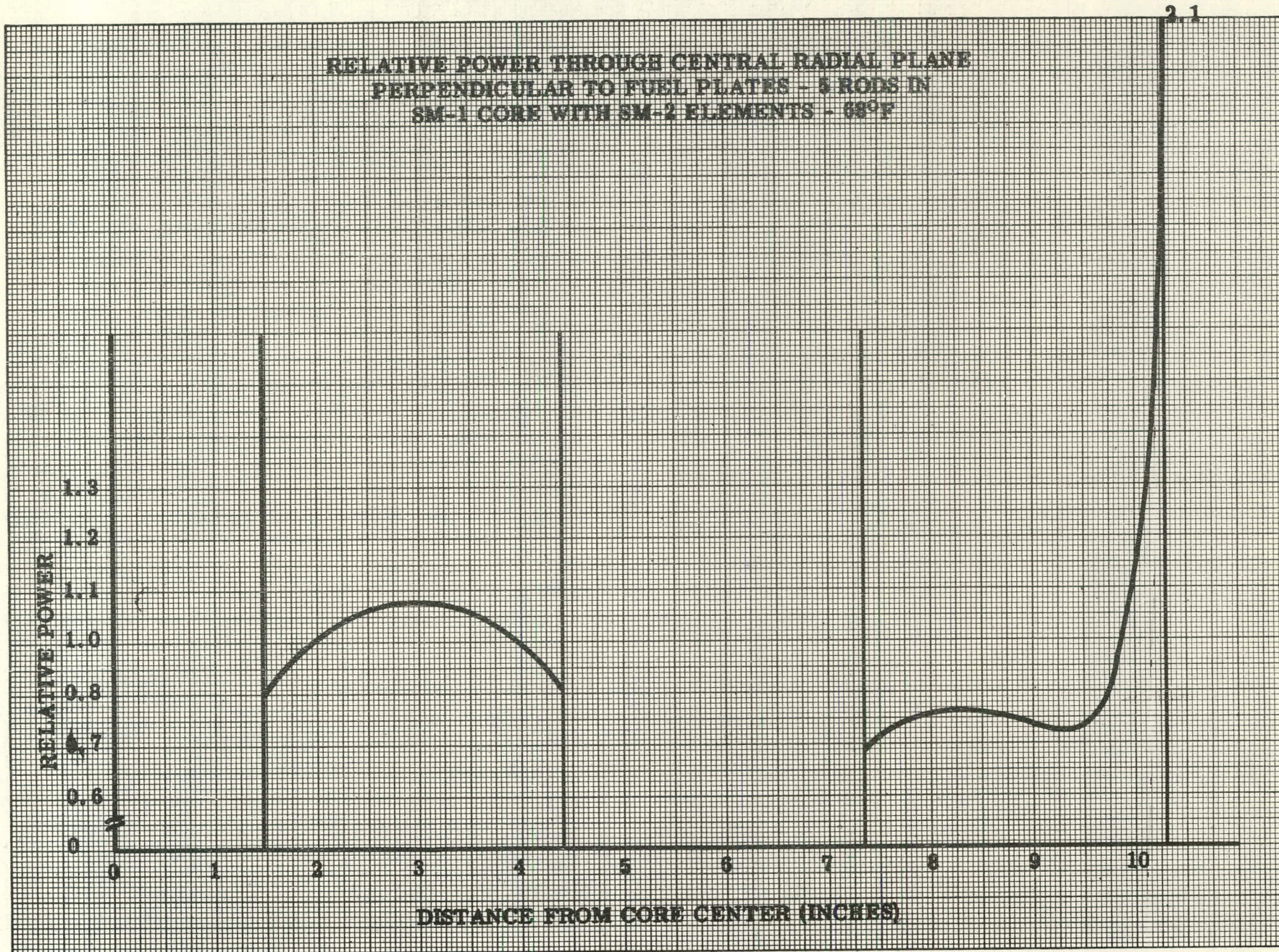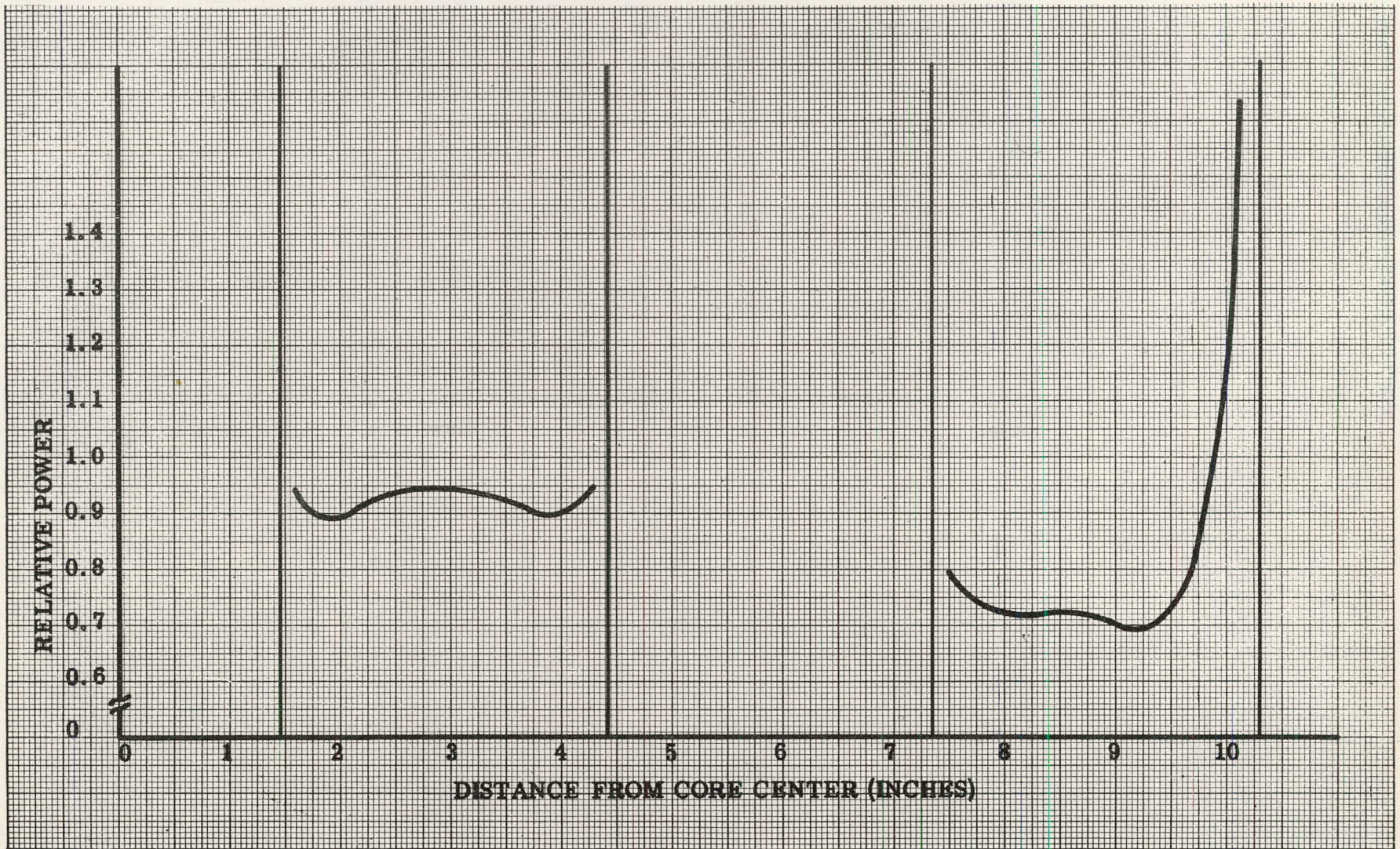SM-1A CORE WITH SM-2 ELEMENTS - 440°F

Fig. 2.21 -

RELATIVE POWER THROUGH CENTRAL RADIAL PLANE
PARALLEL TO FUEL PLATES - RODS IN
SM-1A CORE WITH SM-2 ELEMENTS - 440°F

RELATIVE POWER

DISTANCE FROM CORE CENTER (INCHES)

Fig. 2.22 -

Fig. 2.23 - Relative Power Distribution Through Central Radial Plane
Perpendicular To Fuel Plates - SM-1A With SM-2
Elements - Rods Out - 68°F

RELATIVE POWER DISTRIBUTION THROUGH CENTRAL RADIAL PLANE
PARALLEL TO FUEL PLATES - SM-1A WITH SM-2 ELEMENTS
RODS OUT - 68°F

DISTANCE FROM CENTER OF CORE - INCHES
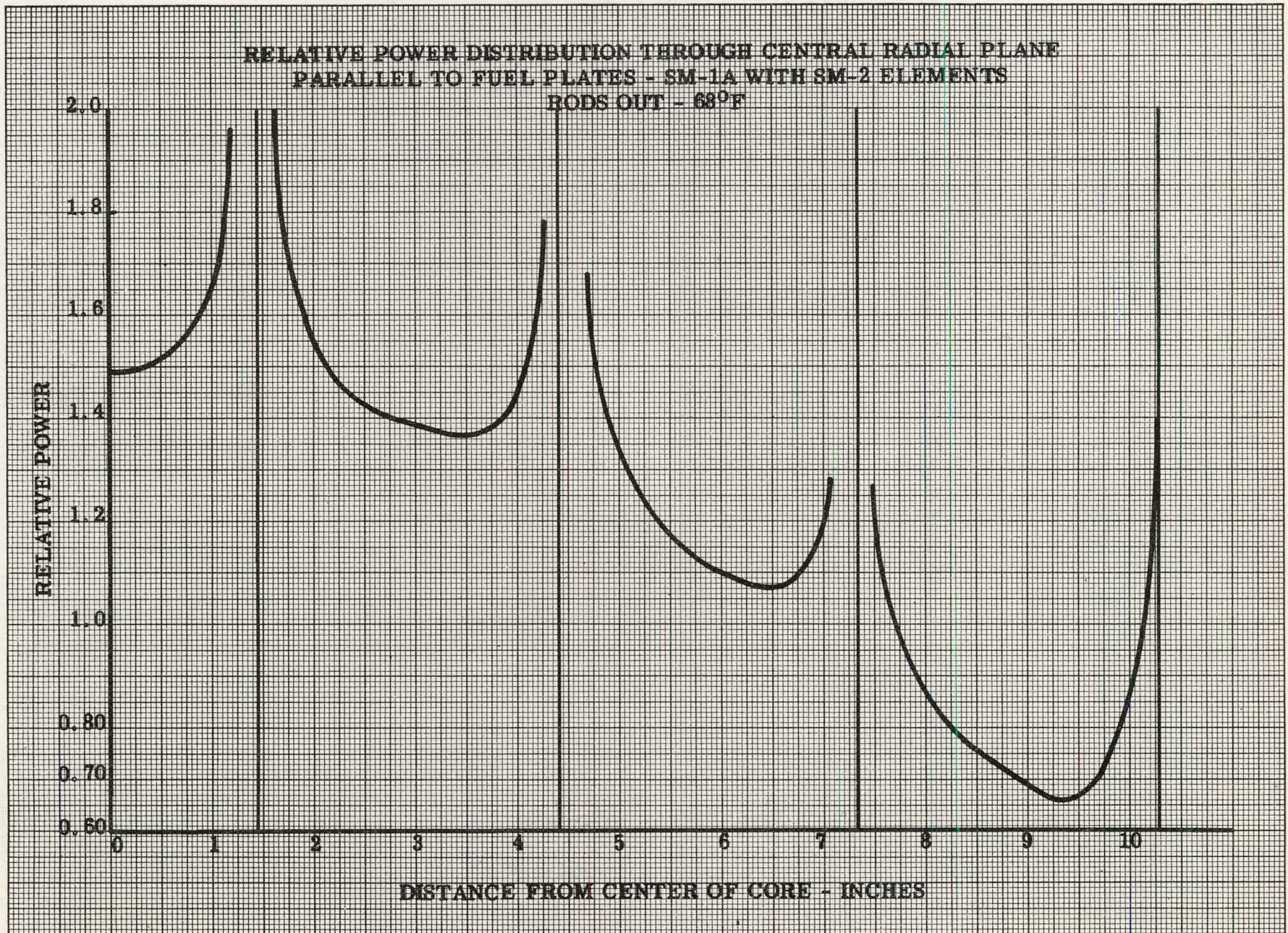
Fig. 2.24 -

THIS PAGE

WAS INTENTIONALLY

LEFT BLANK

2.3 ROD WORTH, REACTIVITY AND ROD BANK POSITION, SM-1, SM-1A, PM-2A

The total control rod bank worth was obtained using the following equation:

$$\rho_{rods} = \frac{(K_{eff}) \text{ rods out} - (K_{eff}) \text{ rods in}}{(K_{eff}) \text{ rods out}}$$

where:

ρ_{rods} = the rod bank worth

(K_{eff}) rods out = the eigenvalue with the rods fully withdrawn

(K_{eff}) rods in = the eigenvalue with the rods fully inserted

The values of K_{eff} were obtained from PDQ-3 cases run for the various cores with SM-2 elements. A 2% model correction was applied to all the calculated K_{eff}'s.

The core reactivity was calculated using the following equation:

$$\rho = \frac{K_{eff} - 1}{K_{eff}}$$

The results of the calculations for SM-1, SM-1A, and PM-2A are listed in Tables 2.6, 2.7, and 2.8 respectively.

TABLE 2.5
RADIAL POWER FACTORS FOR PM-2A
WITH SM-2 ELEMENTS, $T = 510^\circ F$

Element No.	0 MWYR			Estimated Maximum		
	$Q(\Delta\theta)_o$	$Q(\Delta T)_o$	$\overline{Q(\Delta T)}_o$	$Q(\Delta\theta)_B$	$Q(\Delta T)_B$	$\overline{Q(\Delta T)}_B$
44	1.871	1.744	1.581	2.079	1.938	1.757
34	1.721	1.377	1.380	1.912	1.530	1.534
55	1.666	1.333	1.226	1.851	1.481	1.362
23	2.016	1.628	1.346	2.240	1.809	1.496
56	1.515	1.203	1.042	1.683	1.337	1.158
22	2.016	1.674	.934	2.240	1.860	1.038
37	1.322	1.118	.844	1.469	1.242	.938
14	1.095	.757	.750	1.217	.841	.834
73	1.582	1.497	.795	1.758	1.663	.883

$$\psi(\Delta\theta) \quad 0.95 \qquad F_n(\Delta\theta) = 1.10$$

$$\psi(\Delta T) \quad 1.00 \qquad F_n(\Delta T) = 1.05$$

$$P(z)_{max} = 1.439$$

TABLE 2.6
MISCELLANEOUS SM-1 CORE CALCULATIONS

ROD BANK WORTH - ρ_{rods} (%)

Temp.	SM-1 Core I		SM-1 With SM-2 Elements	
	5 rods	7 rods	5 rods	7 rods
68°	19.0	24.13	17.38	21.52
440°	19.2	24.38	18.40	22.77

INITIAL CORE REACTIVITY (% ρ)

Temp	SM-1 Core I	SM-1 With SM-2 Elements	
		PDQ	Model corrected
68°	15.4	9.39	11.39
440° (No xenon)	10.4	6.05	8.05
440° (Equilibrium xenon)	8.2	–	6.33

ROD BANK POSITION (INCHES FROM BOTTOM OF CORE)

Temp	SM-1 Core I	SM-1 With SM-2 Elements	
	5 Rods	5 rods	7 rods
68°	3.7	6.0	–
440° (No xenon)	6.7	10.5	11.0
440° (Equilibrium xenon)	8.3	–	–

MAXIMUM CORE REACTIVITY (ESTIMATED)

68^OF, No Xe, Midlife   15.1 % ρ

TABLE 2.7
MISCELLANEOUS SM-1A CORE CALCULATIONS

ROD BANK WORTH - ρ_{rods} (%)

Temp	SM-1 Core I		SM-1 With SM-2 Elements	
	5 rods	7 rods	5 rods	7 rods
68°	16.60	20.62	17.13	21.23
440°			18.13	22.47

INITIAL CORE REACTIVITY (% ρ)

Temp	SM-1A Core I	SM-1A With SM-2 Elements	
		PDQ	Model corrected
68°	15.62	9.33	11.33
440° (No xenon)	10.3	5.76	7.76
440° (Equilibrium xenon)	7.5	-	5.30

ROD BANK POSITION (INCHES FROM BOTTOM OF CORE)

Temp	SM-1A Core I	SM-1A With SM-2 Elements	
	5 Rod Bank	5 Rod Bank	7 Rod Bank
68°	3.6	-	-
440° (No Xenon)	6.9	10.5	11.0
440° (Equilibrium xenon)	8.9	-	-

MAXIMUM CORE REACTIVITY (ESTIMATED)

68°F, No Xe, Midlife   15.0% ρ

TABLE 2.8
MISCELLANEOUS PM-2A CORE CALCULATIONS

ROD BANK WORTH - (5 rods) - ρ_{rods} (%)

Temp	PM-2A Core I	PM-2A With SM-2 Elements
68°	21.6	19.93
510°	-	20.49

INITIAL CORE REACTIVITY (% ρ)

Temp	PM-2A Core I	PDQ	Model corrected
		PM-2A With SM-2 Elements	
68°	14.30	8.45	10.45
510° (no xenon)	7.48	2.53	4.53
510° (eq. xenon)	5.34	-	2.57

ROD BANK POSITION (INCHES FROM BOTTOM OF CORE)

Temp	PM-2A Core I	PM-2A With SM-2 Elements
68°	6.45	-
510° (no xenon)	10.45	17.5
510° (eq. xenon)	12.50	-

MAXIMUM CORE REACTIVITY (ESTIMATED)

68°F, No Xe, Midlife   14.4% ρ

THIS PAGE

WAS INTENTIONALLY

LEFT BLANK

LINEAR POWER CHAMBER

LOG N

BF₃

		13	14	15		
	22	23	C.R.-1C 24	25	26	
31	32	33	34	35	36	37
41	C.R.-3C 42	43	C.R.-4C 44	45	C.R.5C 46	47
51	52	53	54	55	56	57
	62	63	C.R.-2C 64	65	66	
		73	74	75		

Be BLOCK → ← INLET

STARTUP SOURCE →

CONTROL ROD DRIVES

PLATE DIRECTION

OUTLET

SAFETY CHAMBER-1

SAFETY CHAMBER-2
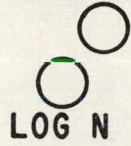
Fig. 2.25 - PM-2A Core Layout
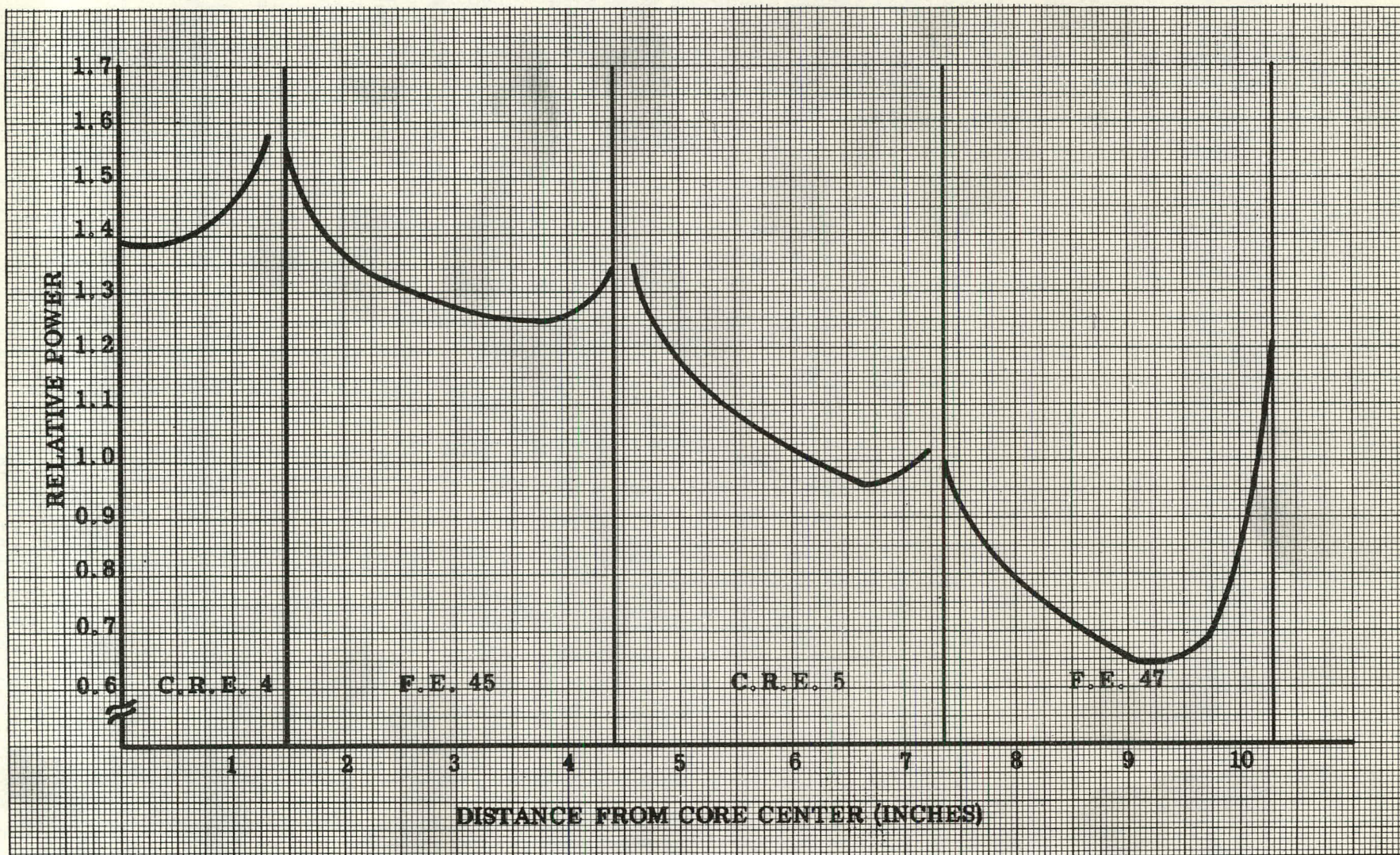
Fig. 2.26 - Relative Power Through Central Radial Plane
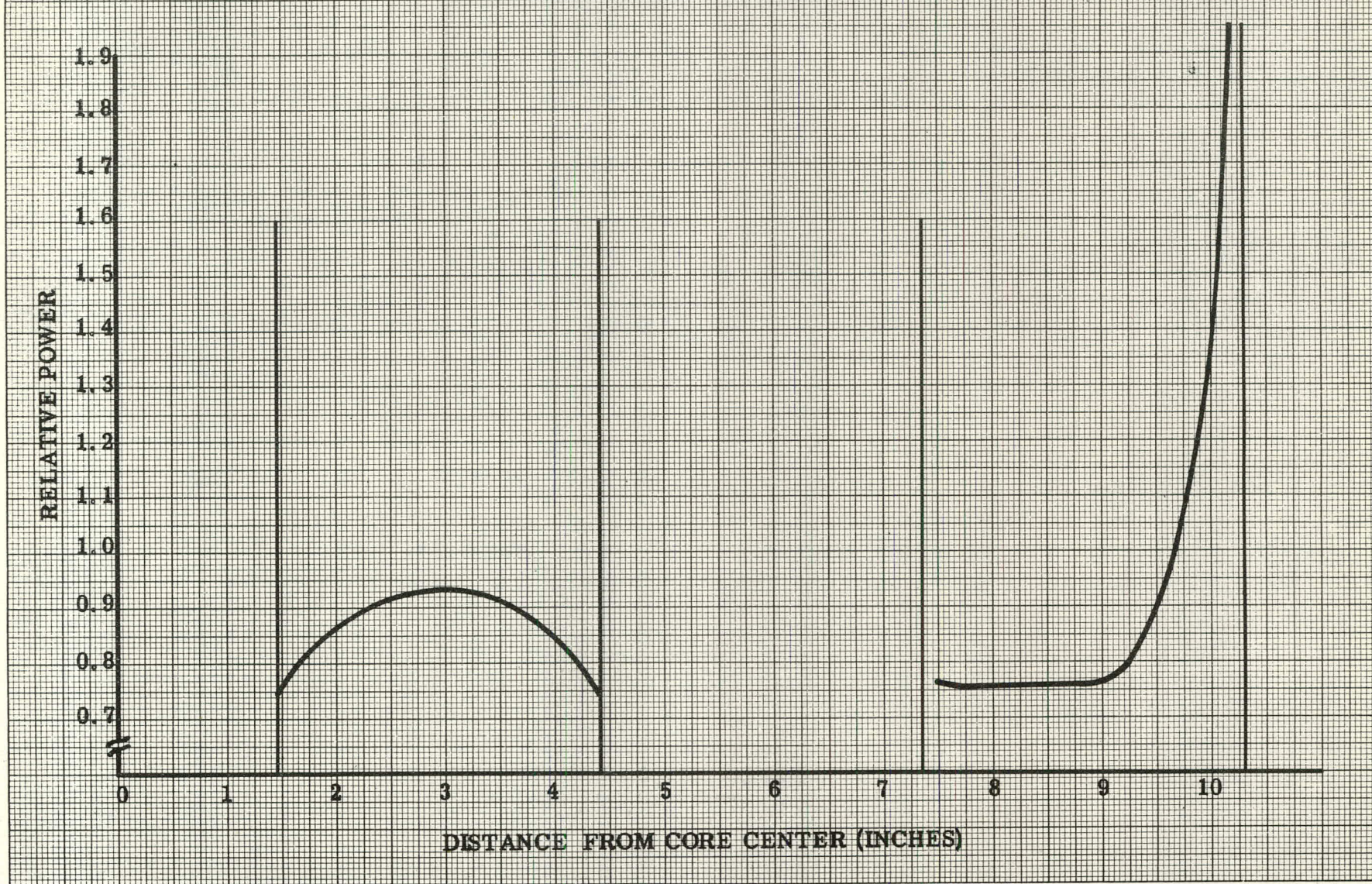Perpendicular To Fuel Plates - Rods Out - PM-2A
Core With SM-2 Elements - 510°F
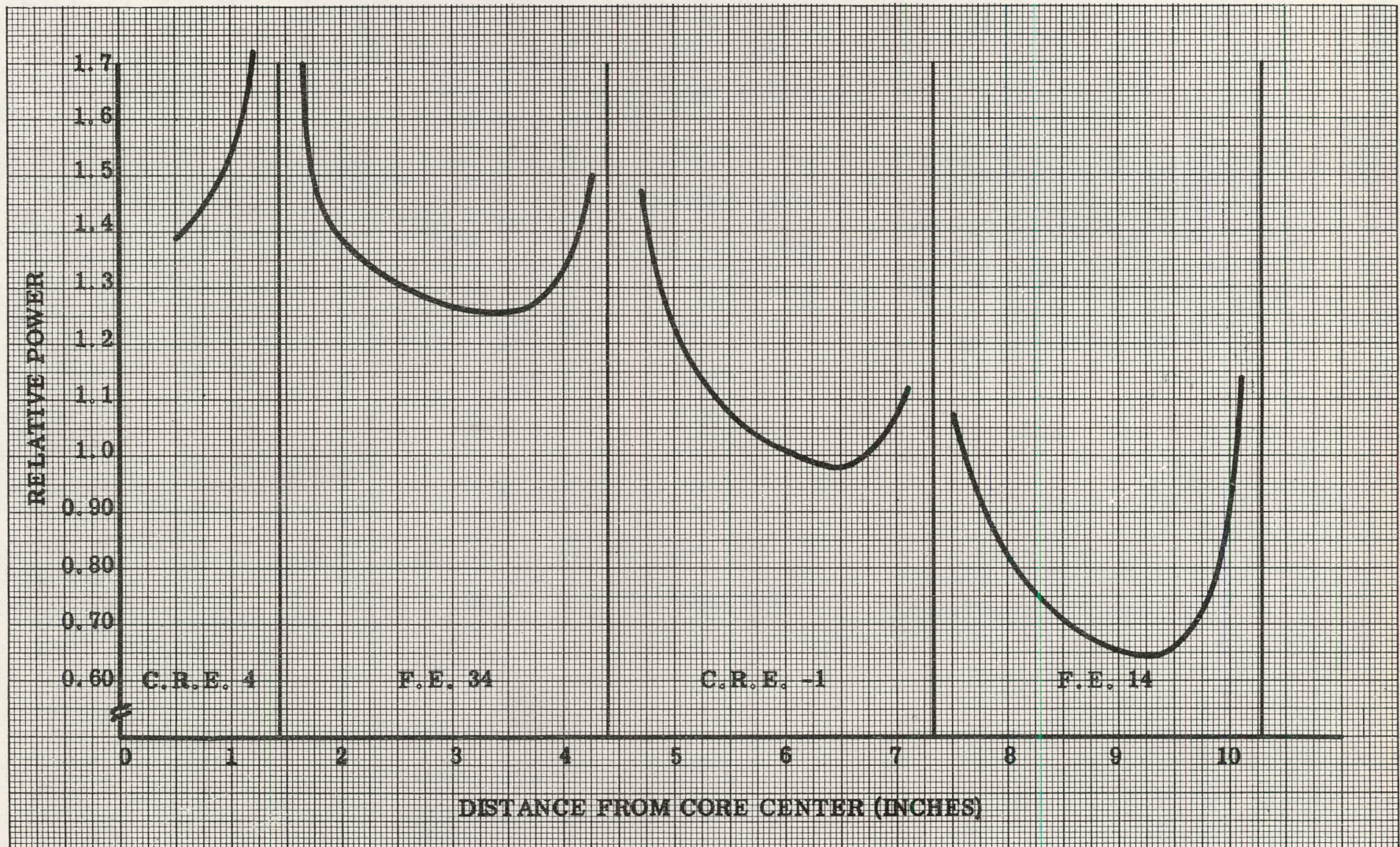
Fig. 2.27 - Relative Power Through Central Radial Plane Parallel
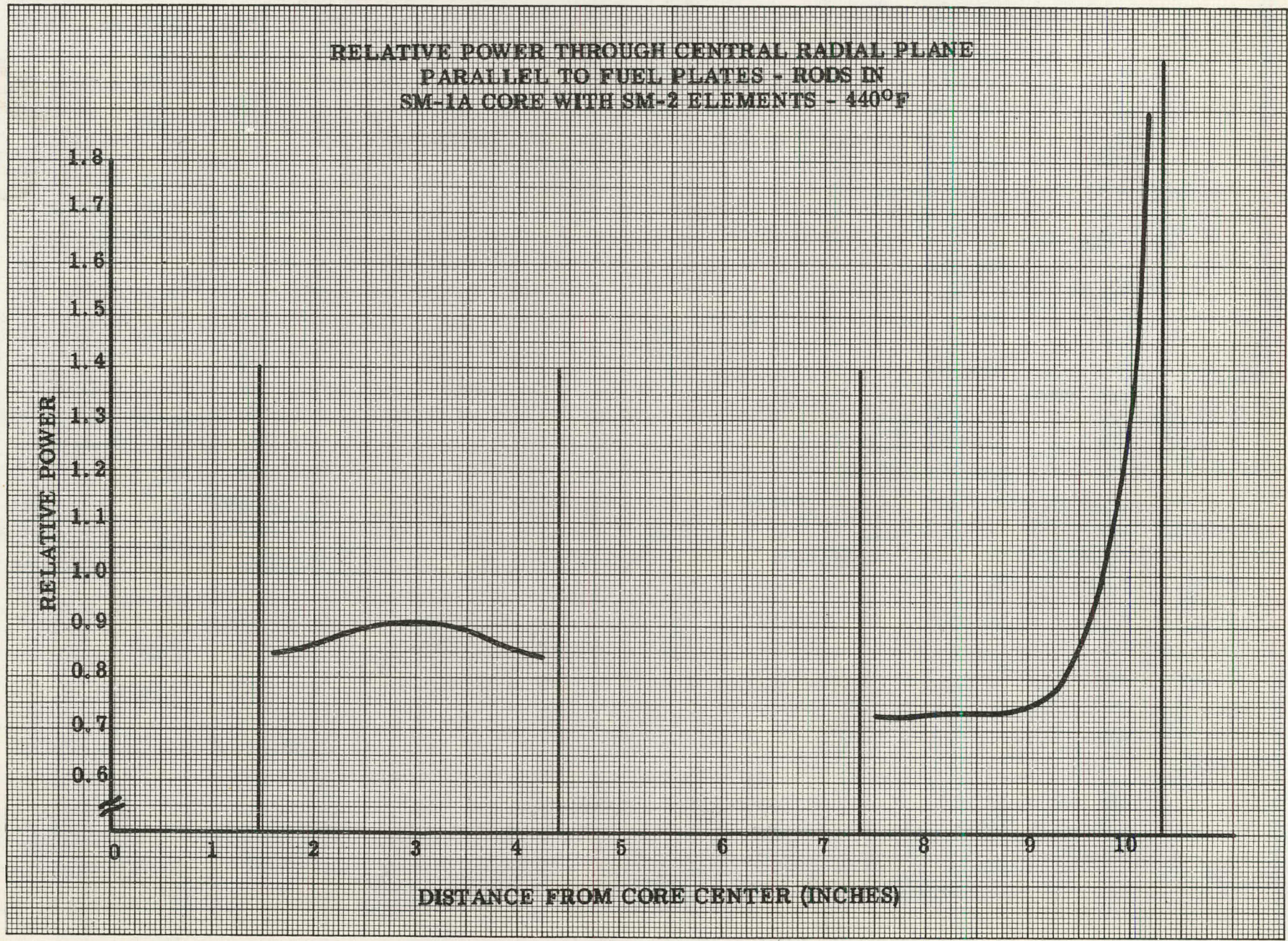To Fuel Plates - Rods Out - PM-2A Core With SM-2
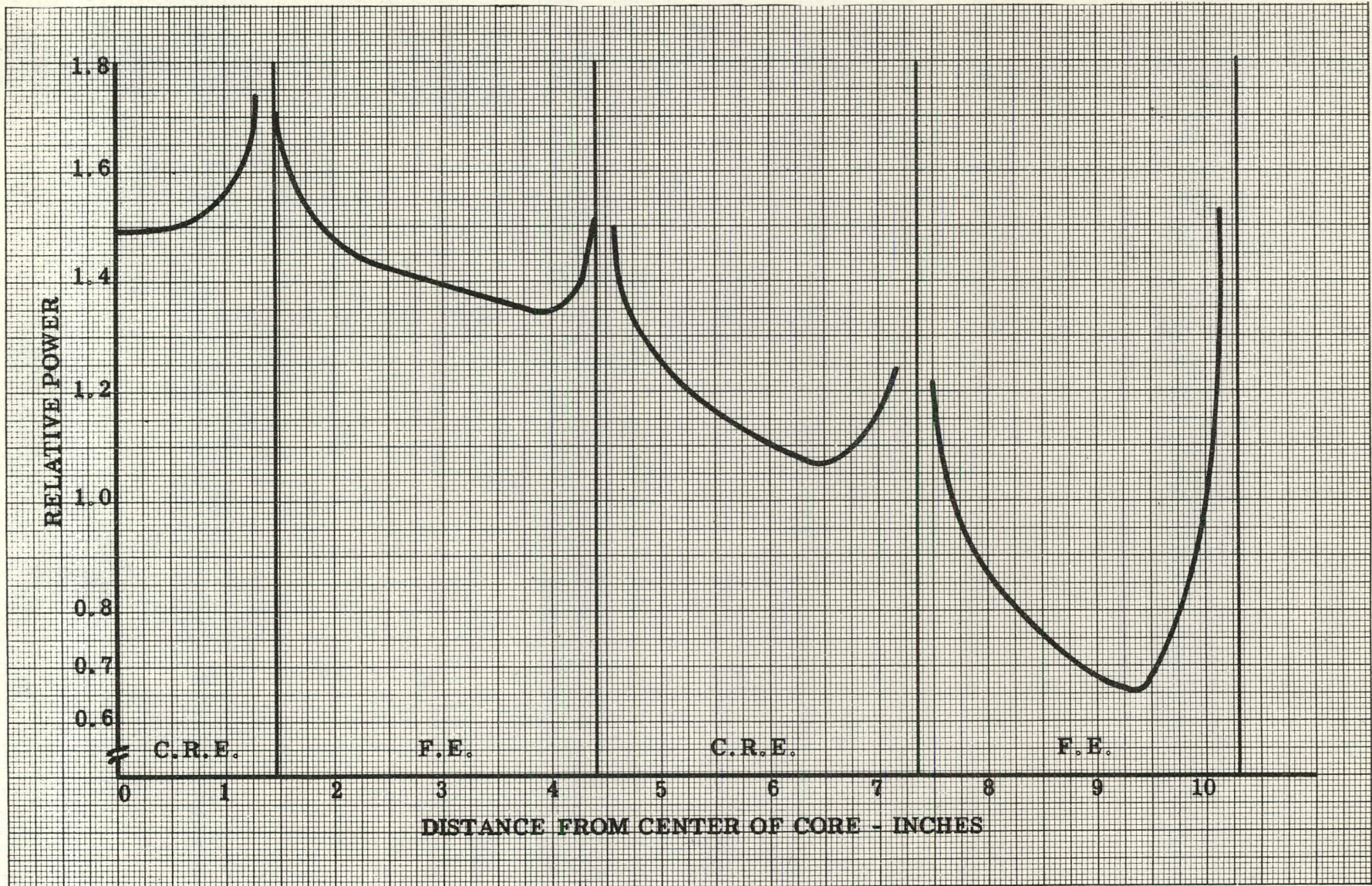Elements - 510°F
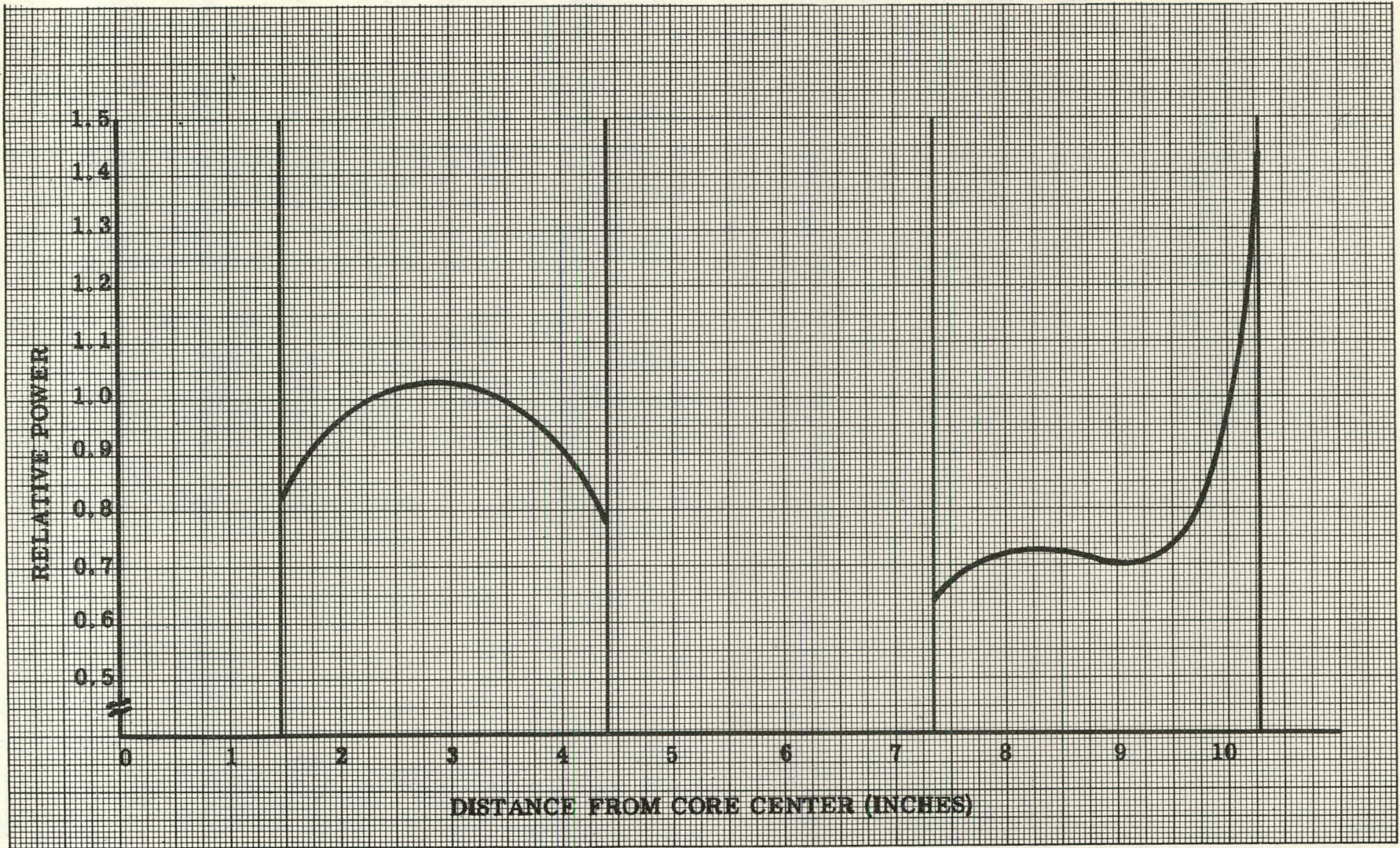
Fig. 2.28 - Relative Power Through Central Radial Plane
Perpendicular to Fuel Plates - Rods In - PM-2A Core
With SM-2 Elements - 510°F

Fig. 2.29 - Relative Power Through Central Radial Plane
Parallel To Fuel Plates - Rods In - PM-2A Core
With SM-2 Elements - 510°F

RELATIVE POWER THROUGH CENTRAL RADIAL PLANE
PERPENDICULAR TO FUEL PLATES - RODS OUT
PM-2A CORE WITH SM-2 ELEMENTS - 68°F

Fig. 2.30 -

RELATIVE POWER THROUGH CENTRAL RADIAL PLANE
PARALLEL TO FUEL PLATES - RODS OUT
PM-2A CORE WITH SM-2 ELEMENTS @ 68°F

RELATIVE POWER

DISTANCE FROM CORE CENTER (INCHES)

C.R.E. 4   F.E. 34   C.R.E. -1   F.E. 14

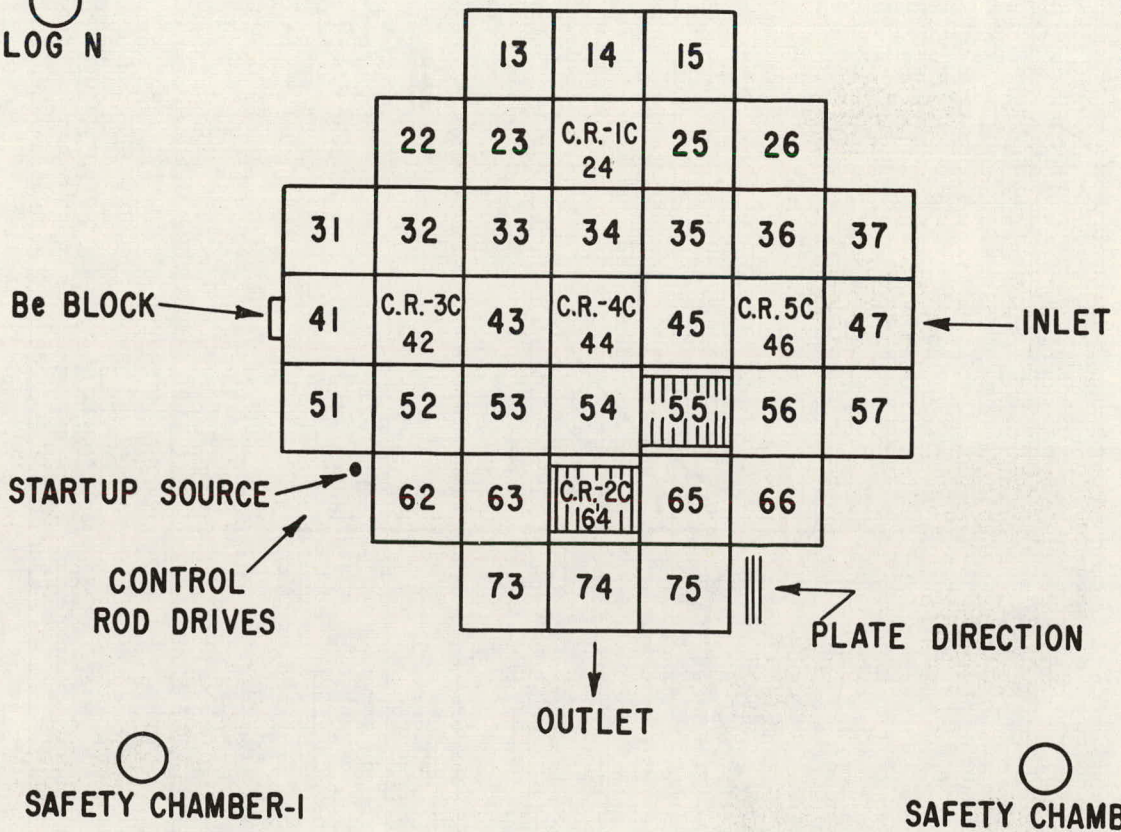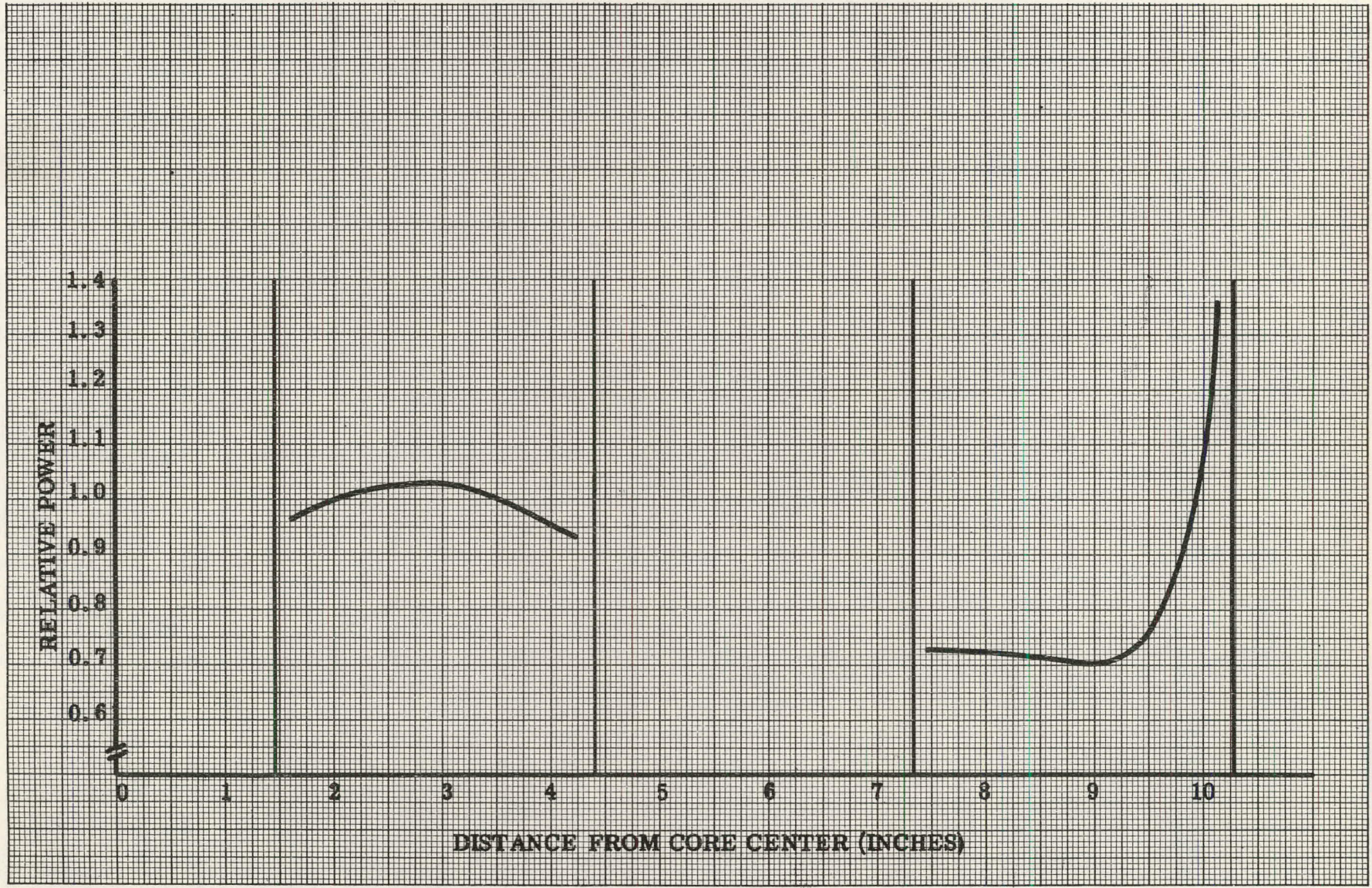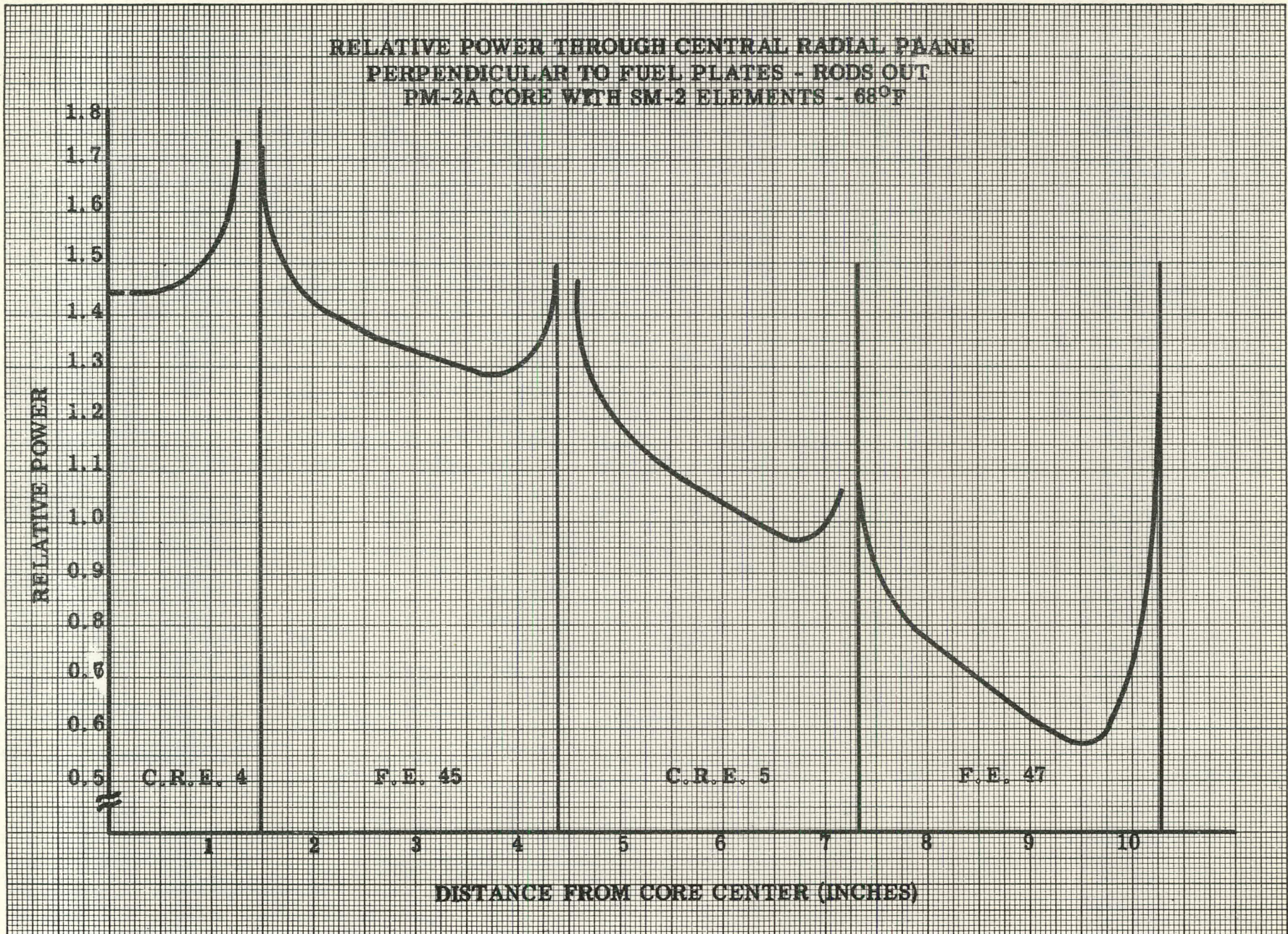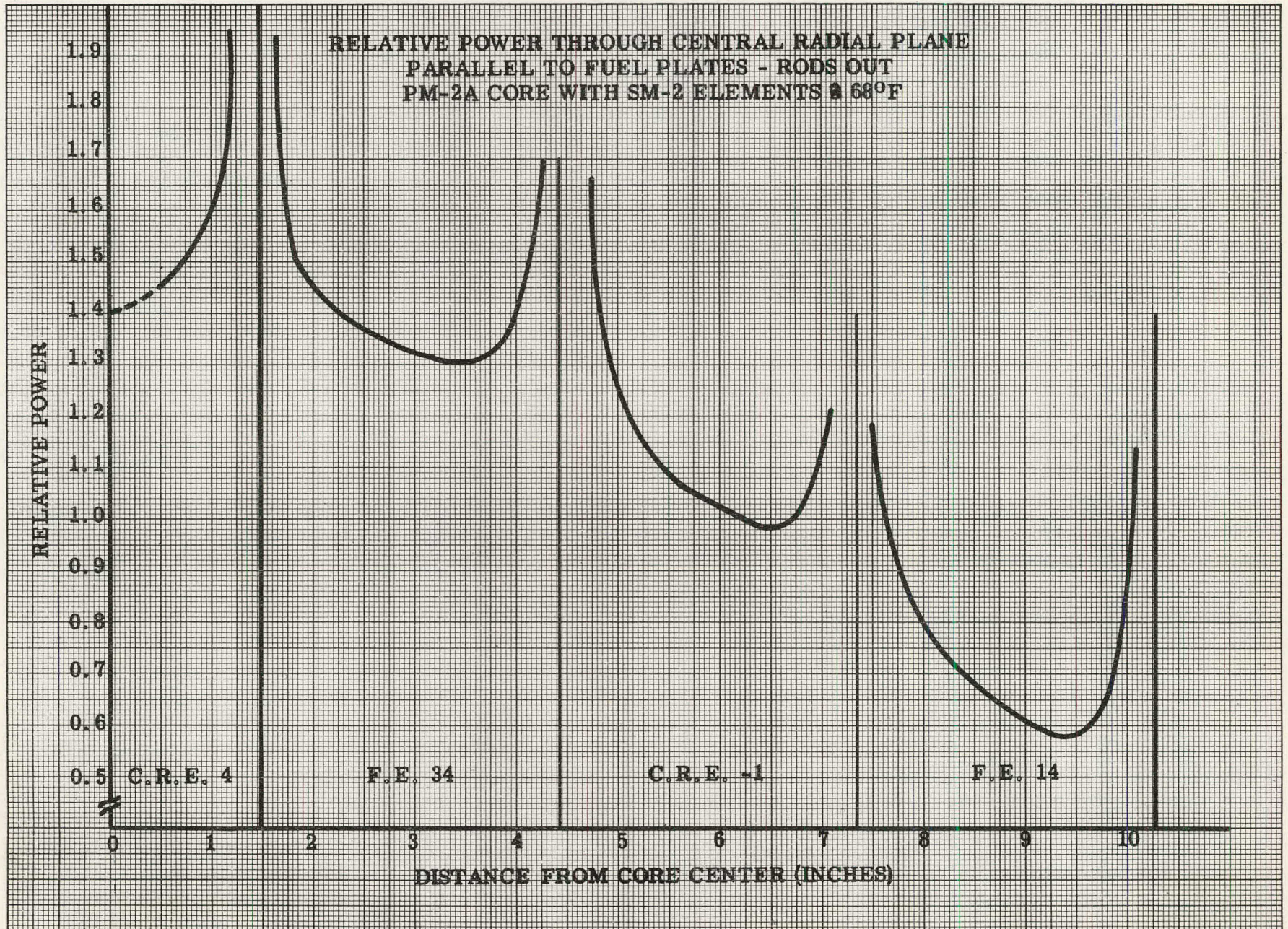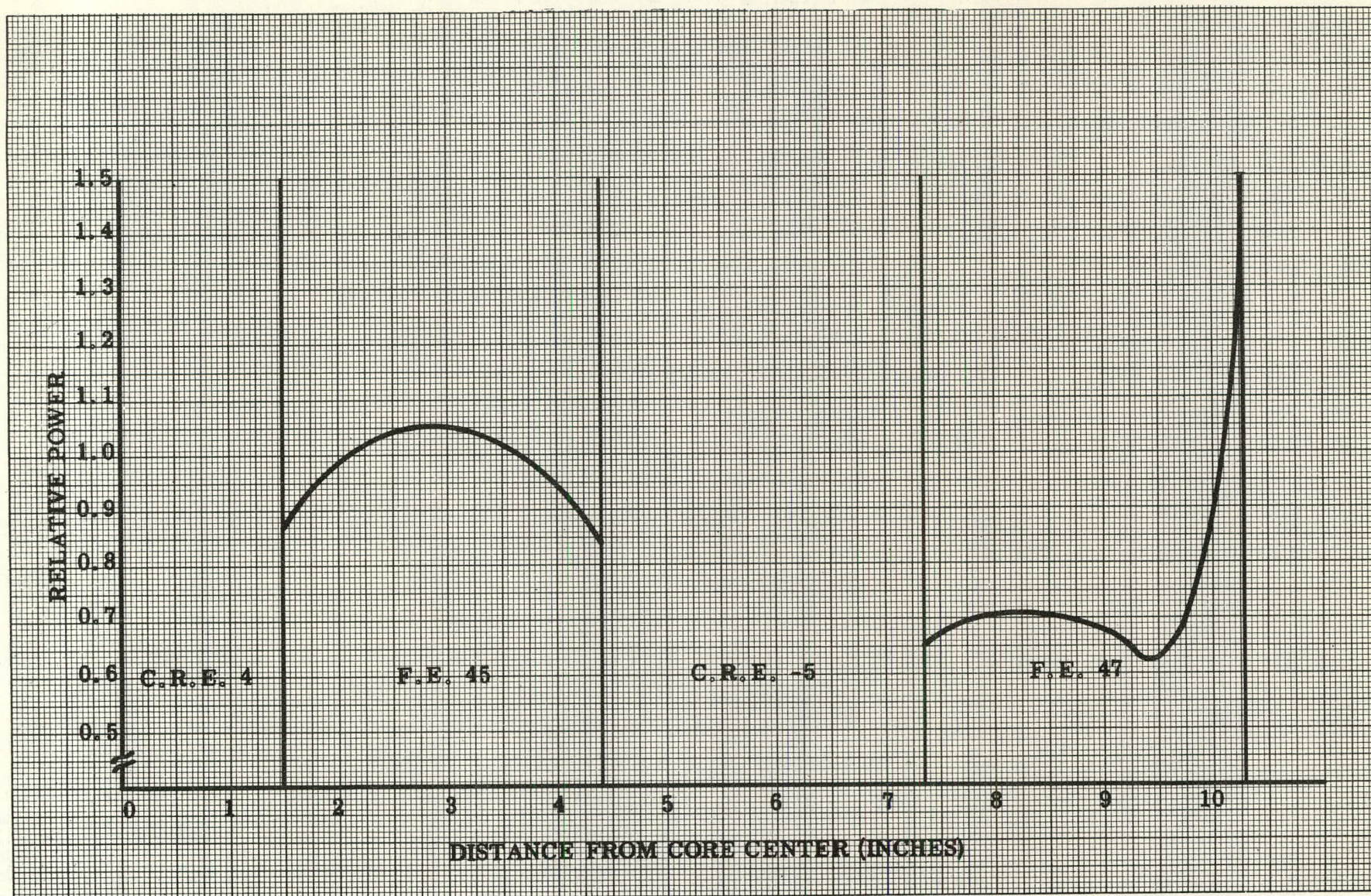Fig. 2.31 -

Fig. 2.32 - Relative Power Through Central Radial Plane
Perpendicular To Fuel Plates - Rods In - PM-2A Core
With SM-2 Elements - 68°F
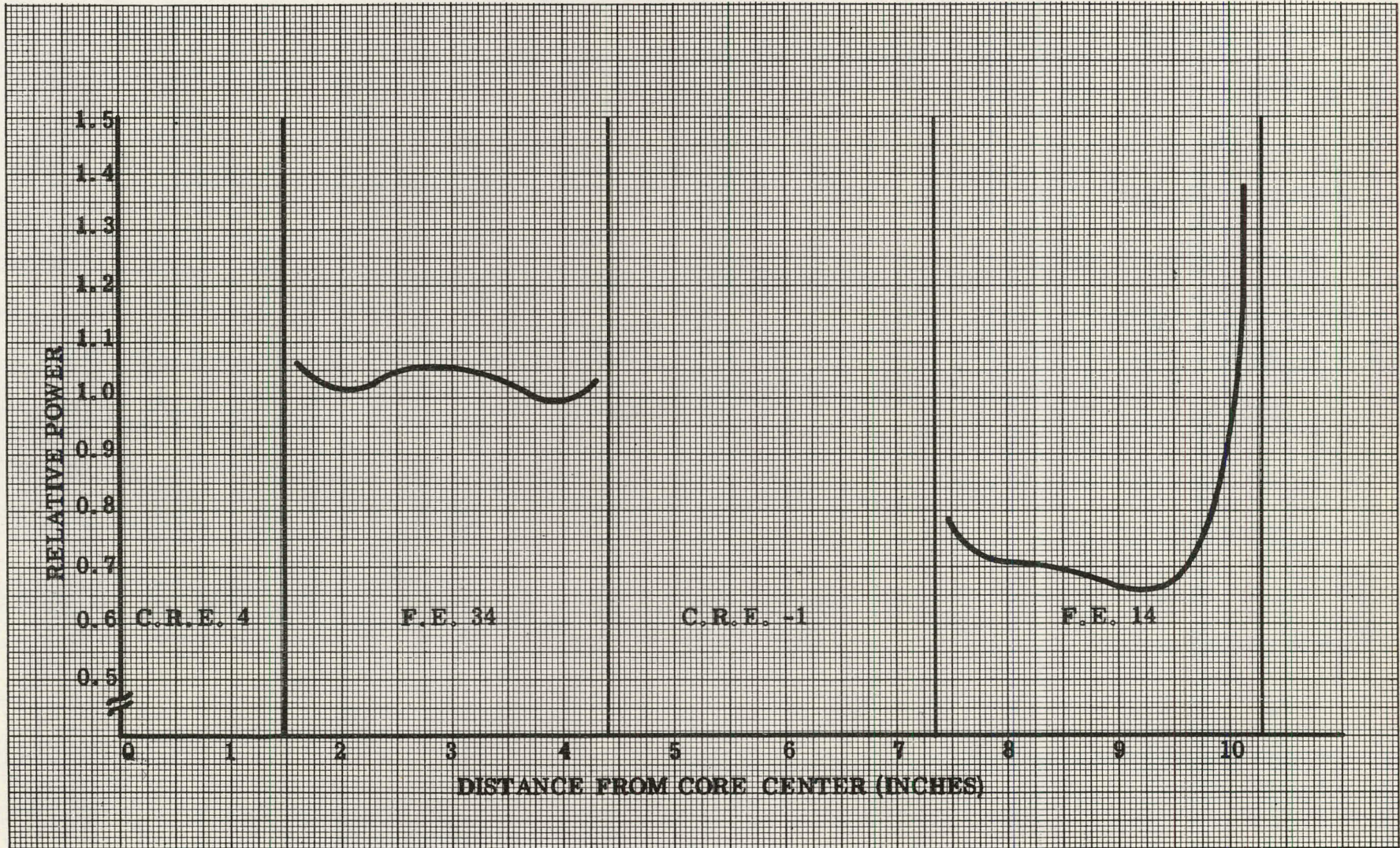
Fig. 2.33 - Relative Power Through Central Radial Plane Parallel
To Fuel Plates - Rods In - PM-2A Core with SM-2
Elements - 68°F
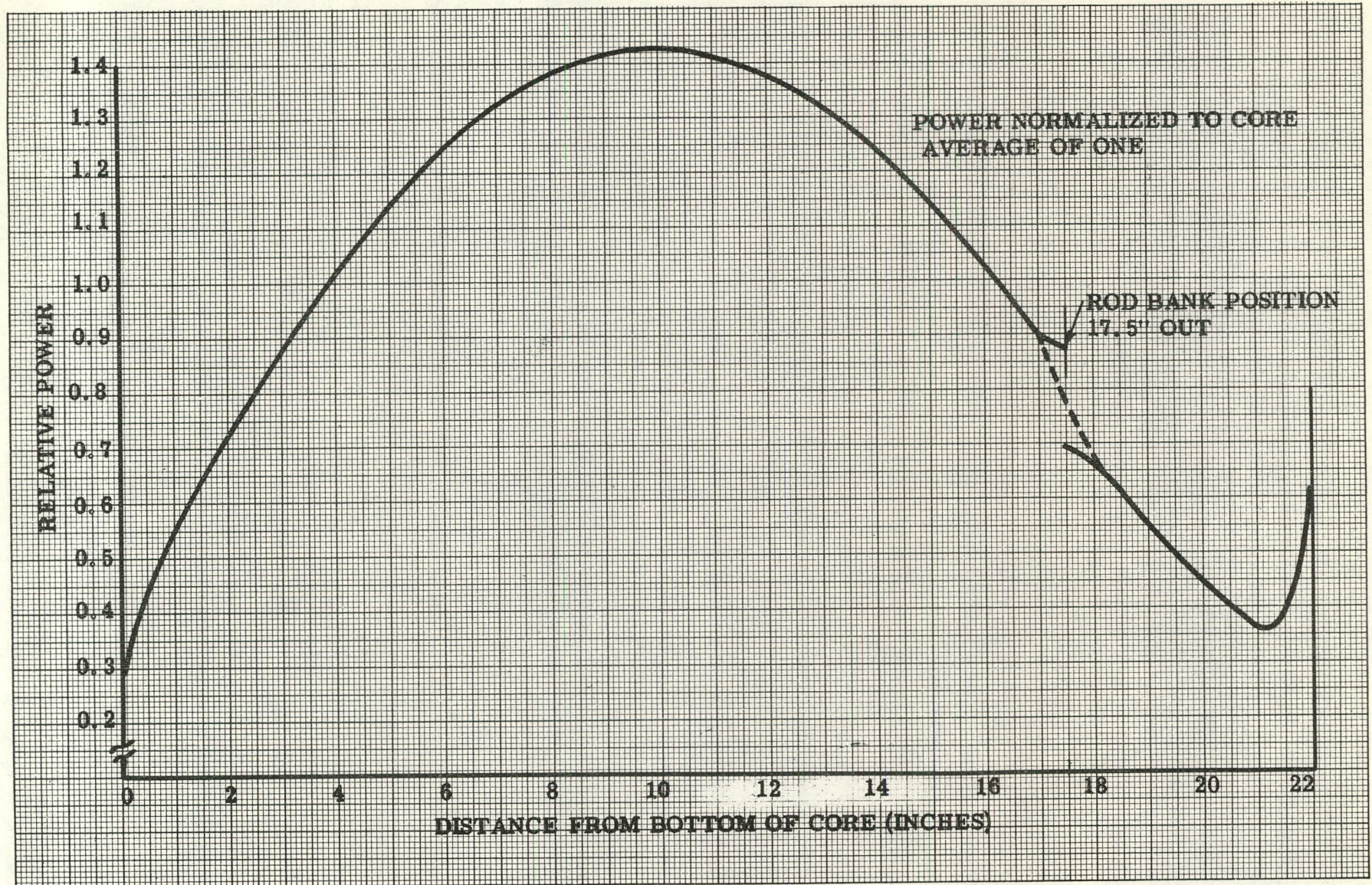
Fig. 2.34 - Relative Axial Power Distribution (Valprod) - PM-2A Core
With SM-2 Elements - 510°F - With Flux Suppressors

2.4 RESULTS

1. Based upon the preliminary analyses, it was found that the overall maximum-to-average power ratios, for the SM-1, SM-1A, and PM-2A with SM-2 fuel elements, are 4.4, 4.7, and 3.2 respectively. These values occur in fuel element locations 41, 67, and 22 respectively. In each case, the maximum power peaking occurs in an outside fuel element, at the core reflector interface. The maximum peaking occurs, in each case at some-time during core life, whereas for the original cores of the SM-1, SM-1A, and PM-2A, the maximum peaking occurs at core startup. This is due to the fact that for the cores employing SM-2 elements, during the first stages of core life, the decrease in radial power peakings is more than offset by the increase in the axial peak due to the rod bank motion.

2. The maximum power in the SM-1 with SM-2 elements may be compared to that calculated, using the same analytical techniques, for the SM-1 Core $I^{(4)}$. For the latter core, ignoring the power spike at the bottom of the active core, the maximum-to-average power ratio was calculated to be 2.8, which occurs at core startup; this may be compared to the value of 4.4 for the SM-1 with SM-2 elements. In the SM-1 Core I, the maximum power peaking occurs in element 44, the central control rod fuel element. Using SM-2 elements with their relatively high fuel and poison loadings, the maximum peaking occurs at the core-reflector interface.

3. In the above analysis, seven rod bank operation was assumed for the SM-1 and SM-1A with SM-2 fuel elements. The axial peak-to-average power ratios were calculated to be 1.91 and 1.81, for the seven and five rod bank, respectively. Even though the axial peaking is more severe for seven rod bank operation, this mode of operation was chosen because of stuck rod considerations. The final mode of rod operation will be studied further and presented in the final report.

4. The maximum reactivity to be controlled for the SM-1, SM-1A and PM-2A with SM-2 fuel elements occurs at about midlife, at 68°F, and no xenon; the calculated values were found to be 15.1% ρ, 15% ρ, and 14.4% ρ, respectively. The total available rod worths were calculated to be about 22% ρ, 22% ρ, and 20% ρ, respectively. Therefore, no control problems are expected.

2.5 CONCLUSIONS

Based upon the preliminary nuclear analysis of power distributions, core reactivities, and total control rod bank worths, no serious problems are expected by using SM-2 fuel elements as replacement cores for the SM-1, SM-1A, and PM-2A.

THIS PAGE

WAS INTENTIONALLY

LEFT BLANK

3.0 CORE THERMAL ANALYSIS

3.1   INTRODUCTION

A preliminary thermal analysis of use of SM-2 elements in SM-1, SM-1A and PM-2A cores was performed to determine whether any serious problems existed.   The limitations of this analysis are:

1. The most adverse power distributions were based on analytical predictions corrected by the use of SM-2 analysis and experimental deviations.

2. Velocity variation within the SM-2 fuel elements in the various cores was only estimated.

3. Loss of pump problem was treated as a quasi-steady state model.

The above limitations will be removed in the final thermal analysis by:

1. Comparison of analytical power distributions and measurements in the critical experiment mockups using SM-2 elements in SM-1, SM-1A and PM-2A configurations.

2. Measurements will be made of the velocity variations within SM-2 fuel plate bundles in SM-1, SM-1A and PM-2A end box and core support configurations.

3. A detailed transient analysis will be performed with the SM-2 elements in the SM-1, SM-1A and PM-2A during loss of flow transients and decay heat removal.

3.2   METHODS OF ANALYSIS

3.2.1 Steady State

The steady state analysis was performed using the STDY-3 code. [11] This code is a one-dimensional steady state code written for pressurized water reactors by WAPD.   The code performs a complete steady-state parallel channel analysis resulting in enthalpy, temperature rise and quality calculations for the nominal channel; and enthalpy, steam quality, plate surface temperature, bulk water temperature, meat centerline temperature, and burnout ratios for the hot channel.   Results are given for each axial channel point based on input properties and two-phase core pressure drop equations where applicable.   If local or bulk boiling exists, the axial position at which the phenomena starts is designated.

The correlations programmed into this code to determine burnout and local boiling are of utmost concern in considering the safe operation of these cores and will be discussed in detail. The remainder of the design equations programmed in the code are described in reference (11).

The burnout correlations used in the code are controlled by the local enthalpy, the channel mass flow rate and the system pressure. The general equation selected for system pressure 1850 psia is given by

$$DNB = BOC \left[\frac{H_j}{1000} \right]^{-2.5} e^{-.0012 \, L/S} \tag{1}$$

where:

DNB = Departure from nucleate boiling

BOC = Burnout constant

H_j = Local enthalpy at a specific axial increment, Btu/lb

L = Channel length, in.

S = Channel spacing, in.

The ratio of DNB to operating heat flux is found by dividing the result from equation (1) by

$$\phi_{avg.} \, F_{\Delta\theta} \, f'(z) \tag{2}$$

where ϕ avg. = Average core heat flux, Btu/hr-ft^2

$F_{\Delta\theta}$ = Local hot channel factor

$f'(z)$ = Axial power generation at a specific axial increment.

$$DNBR = \frac{DNB}{\phi_{avg} \, F_{\Delta\theta} \, f'(z)}$$

The criteria for a channel to be in local boiling based on pressure drop only, is if the film drop calculated from equation (3) below is equal to or greater than the Jens-Lottes temperature drop given in equation (4).

Local boiling exists if $\theta_f \geq \theta_{J\&L}$

$$\theta_f = \frac{\phi_{avg} \, F \Delta T \, f'(z)}{h} \tag{3}$$

where

θ_f = Film temperature drop (Plate surface temperature - bulk water temperature), (^{O}F)

h = Film heat transfer coefficient, $\dfrac{Btu}{hr\text{-}ft^2 \text{-}^OF}$

$$\theta_{J\&L} = T_{sat} + \frac{60 \left(\dfrac{\phi_{avg} \, F \Delta T \, f'(z)}{10^6} \right)^{1/4}}{e^{P/900}} - T_j \tag{4}$$

where $\theta_{J\&L}$ = Difference between the plate surface temperature and the bulk fluid temperature as given by the Jens and Lottes correlation

T_{sat} = Saturation temperature of the fluid, ^{O}F

P = System pressure, psia

T_j = Bulk temperature of fluid at a specific axial increment (j), ^{O}F

Plate surface temperature (T_s) is calculated by adding the film drop to the bulk temperature at any particular axial location (j)

$$T_s = T_j + \theta_f \tag{5}$$

3.2.2 Transients

A pseudo transient analysis was performed for the SM-1, employing SM-2 fuel elements, using the STDY-3 code. This analysis treats a loss of flow accident as a series of steady state points at reduced core flow rates. The primary objective of this analysis was to approximate the variation of burnout heat flux ratio.

The analysis was based on the loss of flow test results as reported in the Final Report for Test 600, [19] performed on the SM-1 at Fort Belvoir. The results of this test at SM-1 for a loss of flow are plotted in Fig. 3.1 from which values of power and flow rates can be obtained for various times after pump failure.

THIS PAGE

WAS INTENTIONALLY

LEFT BLANK

NORMALIZED POWER (P) AND FLOW (q) AS A FUNCTION OF TIME AFTER SM-1 PUMP FAILURE
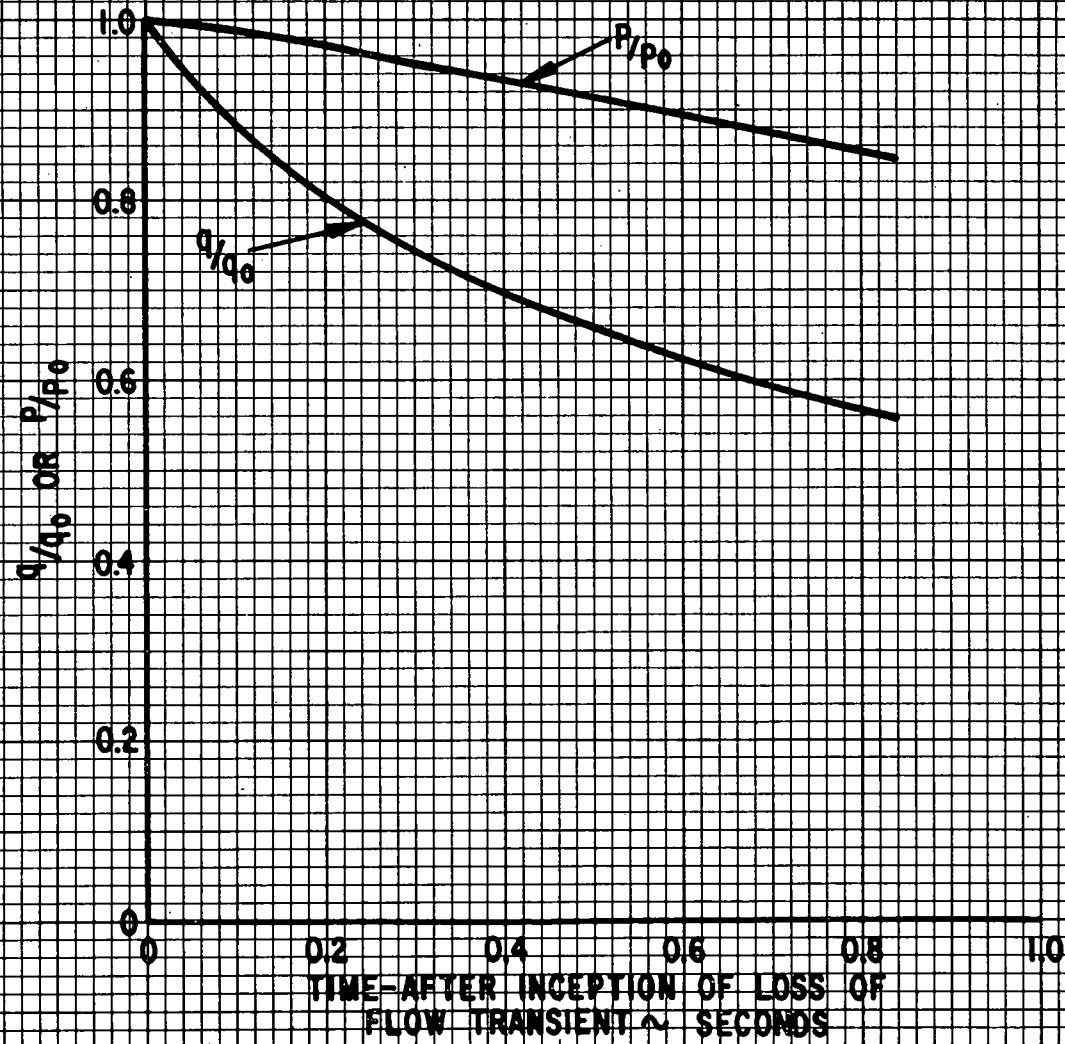
Fig. 3.1 -

THIS PAGE

WAS INTENTIONALLY

LEFT BLANK

3.3 POWER DISTRIBUTION

3.3.1 Maximum Power For Each Reactor

In order to place the analysis of the use of SM-2 elements in the SM-1, SM-1A and PM-2A cores on the most conservative basis, the steady state analysis is performed at the scram power level. This condition might be obtained by operator's error or on a slow rod withdrawal. Scram power level settings are for the SM-1, 13 MW,[12] SM-1A, 24.2 MW,[13] and PM-2A, 12 MW.[14] These power levels and the core heat transfer areas were used to calculate the average core heat flux. The maximum expected core heat fluxes with SM-2 elements are 79, 193 Btu/ft^2 for the SM-1, 142,591 Btu/hr-ft^2 for the SM-1A and 87,268 Btu/hr-ft^2 for the PM-2A.

3.3.2 Axial and Radial Power Distribution

Power distribution and the method for calculation is described in the core analysis section of this report. A description of how the axial and radial factors were used in the thermal analysis follows:

The average and local radial peaking factors were used to select the worst element positions in their respective cores. The element with the highest average and local radial peaking and the lowest available flow rate was selected for each core thermal analysis.

The average and local radial peaking factors were also used to determine hot channel factors for both the nominal and hot channel. Both of these factors are a multiple of the average and local hot channel factor for the nominal and hot channel cases. These are applied as follows:

For the nominal channel:
$$F_{\Delta T_N} = F_N F_\psi \, \overline{Q}_{\Delta T}$$

$$F_{\Delta \theta_N} = F_N F_\psi \, Q_{\Delta \theta}$$

For the hot channel:
$$F_{\Delta T} = F_N F_\psi \, Q_{\Delta T} \, F_{M\Delta T}$$

$$F_{\Delta \theta} = F_N F_{\psi_L} \, Q_{\Delta \theta} \, F_{M\Delta \theta}$$

where

$F_{\Delta T_N}$, $F_{\Delta T}$, $F_{\Delta \theta_N}$, $F_{\Delta \theta}$ = the average and local hot channel factors respectively

F_N, F_{N_L} = nuclear uncertainty factor for average or local condition

F_ψ, F_{ψ_L} = power generation factor for average or local condition

$Q_{\triangle T}$ = average radial peaking factor in the hot channel

$\overline{Q}_{\triangle T}$ = average radial peaking factor in nominal or average channel

$Q_{\triangle \theta}$ = local radial peaking factor

$F_{M_{\triangle T}}$, $F_{M_{\triangle \theta}}$ = mechanical hot channel factor excluding plate spacing factor and plenum maldistribution factor. Average and local respectively.

The relative axial power distribution was averaged over each axial increment. One value of each axial increment for each channel is used in the analysis.

3.4   HOT CHANNEL FACTORS

The mechanical hot channel factors used in this analysis include average and local deviations for meat length, uranium content, and clad thickness. The preceding factors were calculated by methods described in reference (18) and appear in Table 3.1.

Plate spacing and flow maldistribution factors do not appear in the STDY-3 Coade as hot channel factors. Plate spacing appears in the hot and nominal channel description as an average and local dimension. A thermal rippling distortion factor was applied to the hot channel and used as the local dimension of the hot channel. Flow maldistribution is a separate item included as a plenum factor. A 12% maldistribution of flow was used to account for uncertainties in channel-to-flow caused by end box effects and orificing tolerances. An experimental program is presently underway to determine channel-to-channel distribution with SM-2 plates in SM-1, SM-1A and PM-2A stationary and control rod elements. This program will define the value of a mal distribution factor.

TABLE 3.1
COMPOSITE MECHANICAL HOT CHANNEL FACTORS

	Stationary		Control Rod
	$F_{M_{\Delta T}}$	$F_{M_{\Delta \theta}}$	
Meat length	1.0233	1.0233	Same
Uranium content	1.0050	1.0150	Same
Clad thickness	1.0071	1.0119	Same

Composite Mechanical
Factors

$$F_{M_{\Delta T}} = 1.0357$$

$$F_{M_{\Delta \theta}} = 1.0510$$

3.5   ADDITIONAL FACTORS INCLUDED IN THE THERMAL ANALYSIS

In the analysis the following additional factors were used for conservatism
in design:

  a.   Nuclear uncertainty Factor - To allows for uncertainties
       in the calculated power distribution, a nuclear uncertainty factor
       (F_N) of 1.05 was used for the nominal channel and (F_{N_L}) of 1.10
       for the hot channel.

  b.   Core Power Generation - In order to account for the fraction of
       fission heat liberated in the coolant directly $F \psi_L$, a factor of
       0.95 was applied to the power generated in the fuel plates.
       The fraction of power generated in the $(F \psi)$ core is 1.00.

  c.   Instrumentation Tolerances - The worst reactor conditions were
       considered in the thermal analysis and tolerances applied to the
       reactor instrumentation. The following instrumentation tolerances
       were used:

	Instrumentation Tolerance	Value Used In Code
For the SM-1		
Core Power	$\not< 3.5\%$ at Scram Power Level of 13 MW	13.45 MW
Inlet Temp	$\not< 4\%$ At Core Inlet 427.7°F	431.7° F
System Pressure	$\not< 25$ psia At 1200 psia	1175 psia
For the PM-2A		
Core Power	$\not< 3.5\%$ At Scram Power Level of 12.0 MW	12.42 MW
Inlet Temp.	$\not< 4°$ At Core Inlet 500°F	504°F
System Pressure	$\not< 35$ psia at 1750 psia	1715 psia
For the SM-1A		
Core Power	$\not< 3.5\%$ At Scram Power Level of 24.2 MW	25.05 MW
Inlet Temp.	$\not< 4°$ At Core Inlet 423°F	427°F
System Pressure	$\not< 25$ psia at 1200 psia	1175 psia

3.6   CORE FLOW DISTRIBUTION

3.6.1 SM-1 Core with SM-2 Elements

The available flow for each element for the SM-1 core was obtained from full scale flow test measurements.[15] It is expected that the flow distribution within the SM-1 core will be identical with SM-2 elements installed. Flow distribution was based on a primary loop flow rate of 3862 gpm,[12] with 14.7% lattice flow. Figure 3.2 shows the available flow for each element.

3.6.2 SM-1A Core with SM-2 Elements

For the SM-1A, core flow distribution was obtained from a full scale air flow rig, reference (16), in which Figure I gave flow distribution in terms of percent of total flow where internal element flow is 72.9%, internal control rod flow 13.9% and lattice flow 13.2%. Figure 3.3 shows the available core flow distribution for the recommended orifice plate. Since the SM-1A has two pumps having different operating lines, the shaft seal pump which delivers the lower flow of 7400 gpm was used to obtain the flow rates.

(Element Flow Rates in GPM)

12 46.57	13 56.27	14 59.57	15 57.63	16 45.60

21 43.66	22 67.13	23 89.64	24 94.34	25 88.28	26 66.75	27 45.60
31 55.30	32 87.70	33 89.20	34 100.90	35 100.60	36 87.31	37 56.85
41 57.63	42 94.69	43 106.13	44 94.34	45 105.16	46 92.16	47 62.89
51 58.60	52 86.34	53 97.40	54 106.13	55 89.00	56 88.48	57 57.43
61 44.24	62 67.91	63 92.75	64 94.69	65 86.93	66 67.99	67 45.21

72 47.15	73 58.60	74 58.99	75 50.25	76 45.21

Inlet →

Fuel Plate Orientation
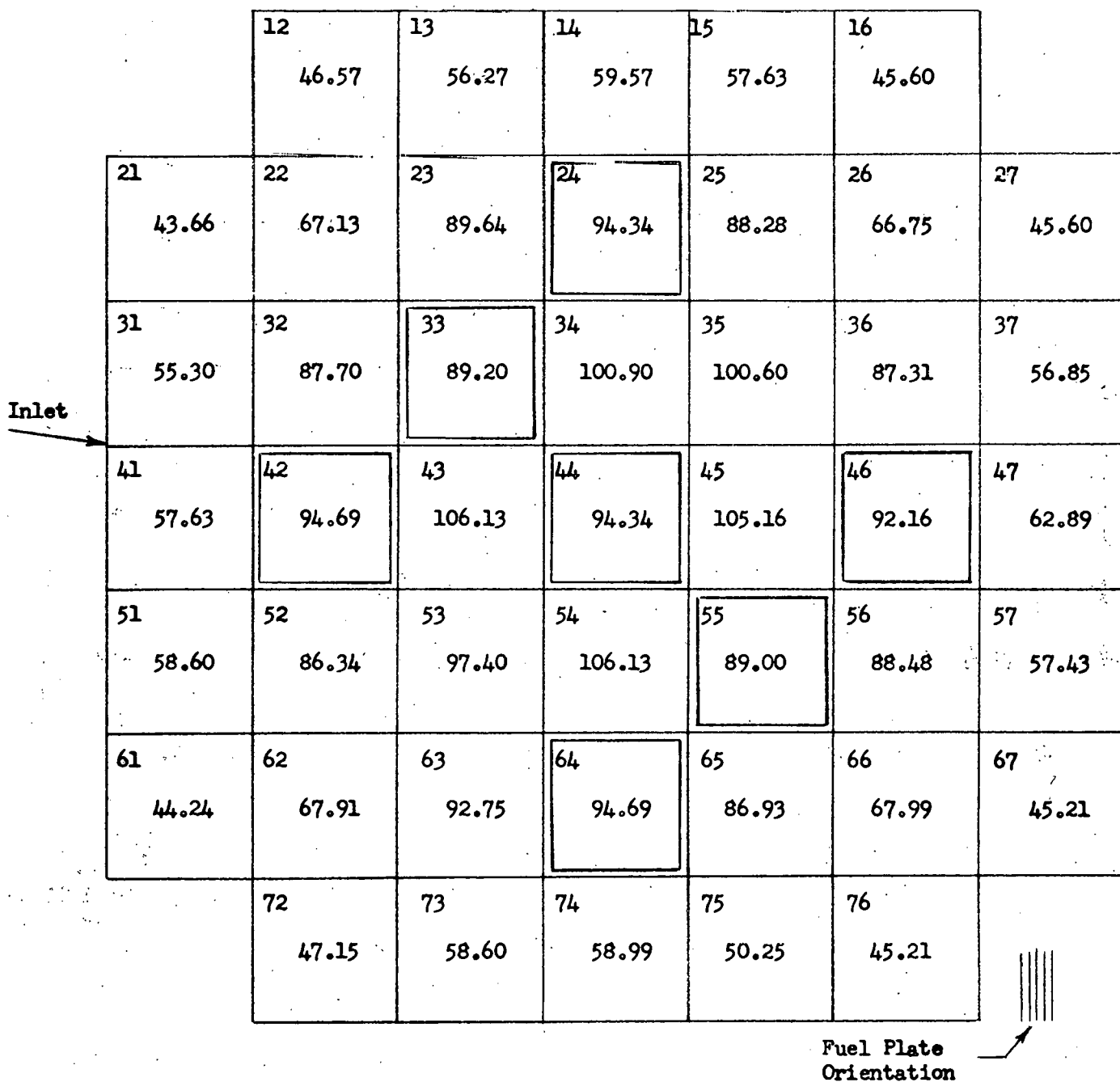
Fig. 3.2 - SM-1 Core Flow Distribution

(Element Flow Rates In GPM)

12 138	13 146	14 148	15 148	16 136	
21 132	22 127	23 142	24 147	25 142	26 131	27 131	Inlet
31 146	32 135	33 147	34 157	35 149	36 135	37 145
41 148	42 147	43 152	44 147	45 155	46 147	47 148
51 146	52 135	53 153	54 155	55 147	56 141	57 155
61 132	62 127	63 136	64 147	65 143	66 129	67 129
	72 134	73 147	74 149	75 149	76 141	Fuel Plate Orientation
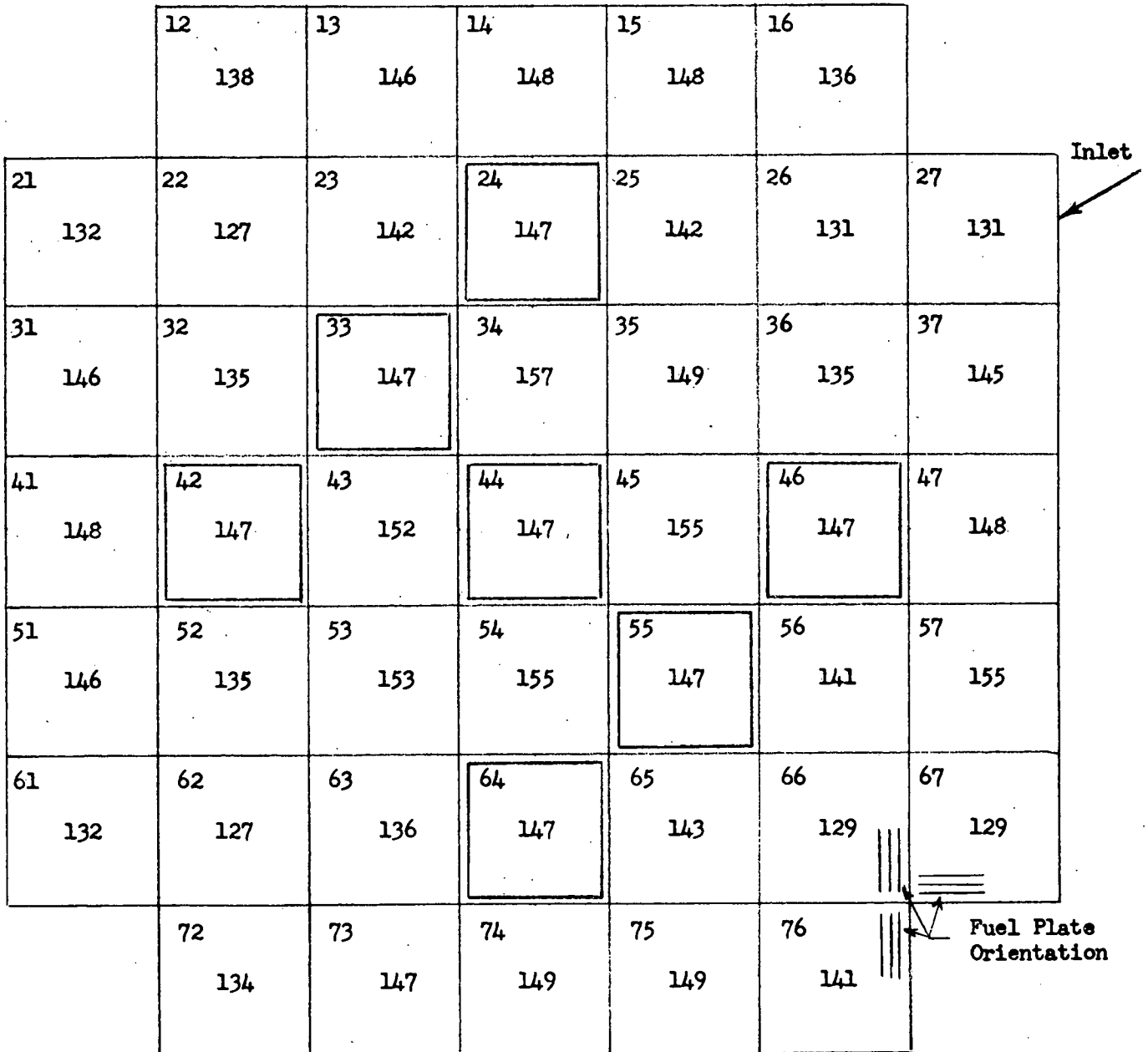
Total Core Flow: 7400 gpm
Lattice Flow: 98 gpm

Fig. 3.3 - SM-1A Core Flow Distribution

72

(Element Flow Rates In GPM)

Inlet

13 115	14 113	15 113

Fuel Plate Orientation

22 113	23 109	24 110	25 113	26 115

31 115	32 114	33 115	34 108	35 115	36 114	37 114

41 115	42 110	43 111	44 110	45 115	46 110	47 117

51 115	52 115	53 114	54 116	55 110	56 113	57 115

62 113	63 113	64 110	65 114	66 114

73 109	74 118	75 115

Total loop flow: 4890 gpm
Lattice flow: 707 gpm

Fig. 3.4 - PM-2A Core Flow Distribution

73

THIS PAGE

WAS INTENTIONALLY

LEFT BLANK

3.6.3 PM-2A Core with SM-2 Elements

Flow distribution was based on a primary loop flow rate of 4890 gpm measured at Camp Century in the PM-2A startup test program.(20)   Internal element flow distribution was taken from Fig. 11 of reference (17) in which the distribution is expressed in percent of total flow where 14.45% of total flow is lattice flow.   This data was developed thru flow measurements of each stationary element and control rod element in a full scale flow rig using air as the test fluid.   Figure 3.4 shows the available flow for each element.

3.7 PERFORMANCE OF SM-2 ELEMENTS IN THE SM-1 REACTOR

3.7.1 Steady State Design Conditions

A steady state thermal analysis was performed on eight element groupings within the SM-1 core.   These groupings are based on radial peaking.   The element in each group with the maximum peak-to-average power generation was selected for analysis.   These elements appear in Table 3.2.
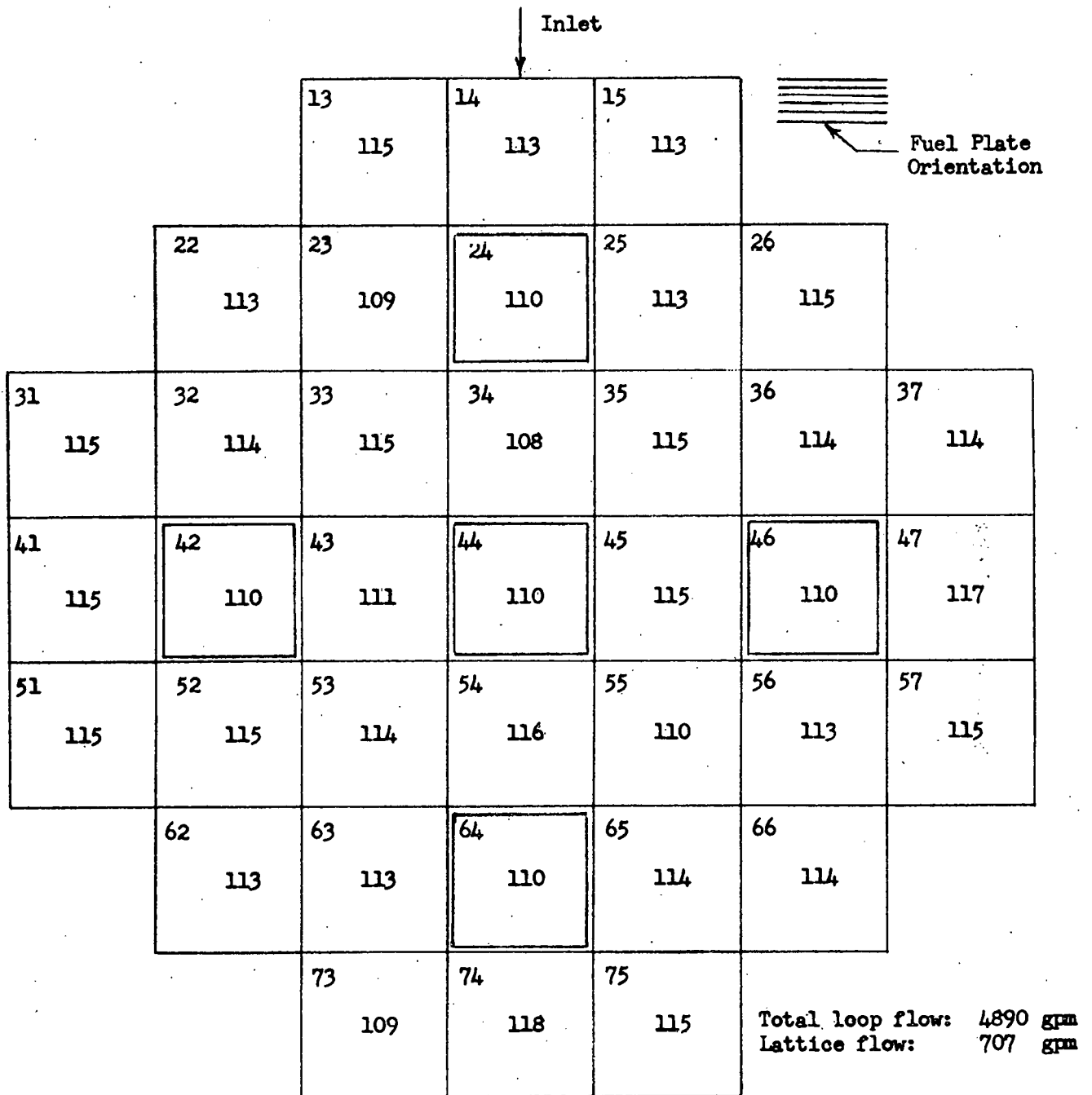
Reactor power was 10 MW with a core heat flux of 63,354 Btu/hr-ft^2 and inlet temperature of 431.7^o.   The hot channel factors used were calculated based on radial peaking factors presented in the core analysis section of this report, and the manufacturing and metallurgical tolerances presented for SM-2 elements in reference (18).   The available flow rates for these elements are shown in Fig. 3.2.   Plate surface temperature, bulk water temperature, departure from nucleate boiling, and quality were calculated for one-inch increments up the 22-in. channel.

The results of this analysis at 10 MW are shown in Table 3.2.

TABLE 3.2
RESULTS OF STEADY STATE THERMAL ANALYSIS,
SM-1 CORE, REACTOR POWER 10 MW

Element Position	Max. Surface Temp. ^{o}F	Max. Bulk Water Temp, ^{o}F	Min. DNBR	Quality
44	558.4	478.7	8.2	0
55	557.4	478.8	8.4	0
34	554.1	475.1	8.7	0
53	547.3	472.0	9.4	0
32	561.0	478.2	9.2	0
66	551.7	474.2	12.2	0
61	576.5	517.7	7.6	0
75	575.2	486.5	9.3	0

The results of this analysis indicate that the SM-1 core with SM-2 elements is safe during steady state 10 MW operation. This is based on DNBR's well above the minimum DNBR of 2.0 and the existence of no local boiling.

3.7.2 Maximum Operating Conditions

A steady state analysis of core positions 61 and 44 was made at the reactor scram power level of 13.0 MW. The selection of these elements was based on the minimum DNBR presented in Table 3.2. Core inlet temperature was reduced to 429°F and core heat flux increased to 79,193 Btu/hr-ft². The results of this analysis at 13.0 MW are shown in Table 3.3.

TABLE 3.3
RESULTS OF STEADY STATE THERMAL ANALYSIS,
SM-1 CORE HOT CHANNEL, REACTOR POWER 13 MW

Element Position	Max. Surface Temp. °F	Max. Bulk Water Temp, °F	Min. DNBR	Quality
61	577.1	535.5	6.0	0
44	577.4	487.6	6.5	0

The results of this analysis indicate that local boiling starts at 5 in. from the bottom of the core for element 61. Figures 3.5 and 3.6 show a plot of plate surface temperature and bulk water temperature in the hot channel of the stationary element 61 and the control rod element 44. A relatively flat surface temperature curve is shown for element 61 for approximately 2/3 of the channel. This flatness is attributed to the increase of the heat transfer coefficient near the nucleate boiling region and is typical with the other cores analyzed.

3.8   PERFORMANCE OF SM-2 ELEMENTS IN THE SM-1A REACTOR

3.8.1 Steady State Design Conditions

A steady state thermal analysis was performed on eight element positions selected from eight element groupings within the SM-1A core. The basis for selection is the same as discussed in section 3.7.1. These elements are listed in Table 3.4.

Fig. 3.5 - SM-2 Elements in SM-1 Core, Hot Channel Plate Surface Temp. & Bulk Water Temp. vs. Length Along Channel From Bottom of Core Element Position 61

78
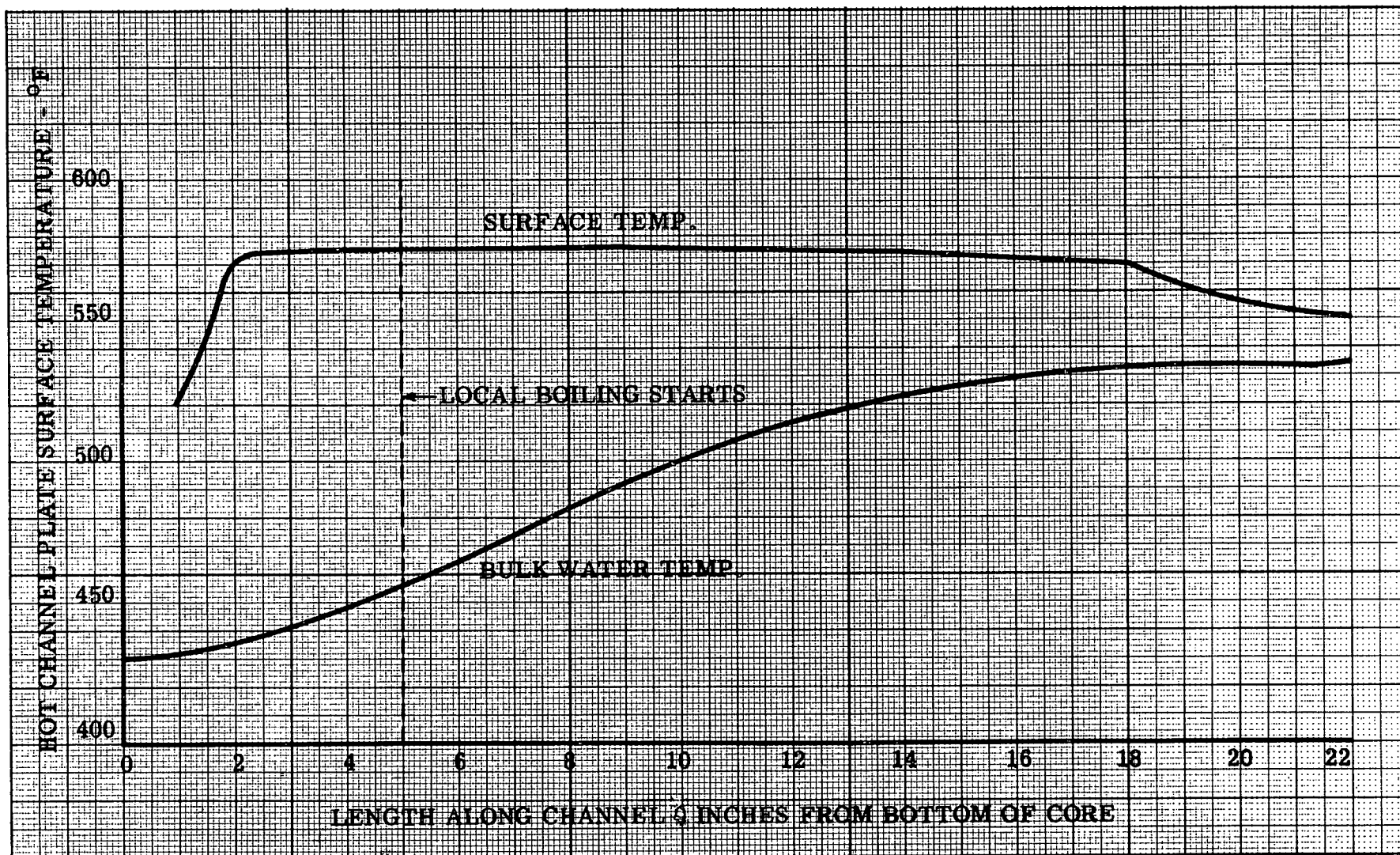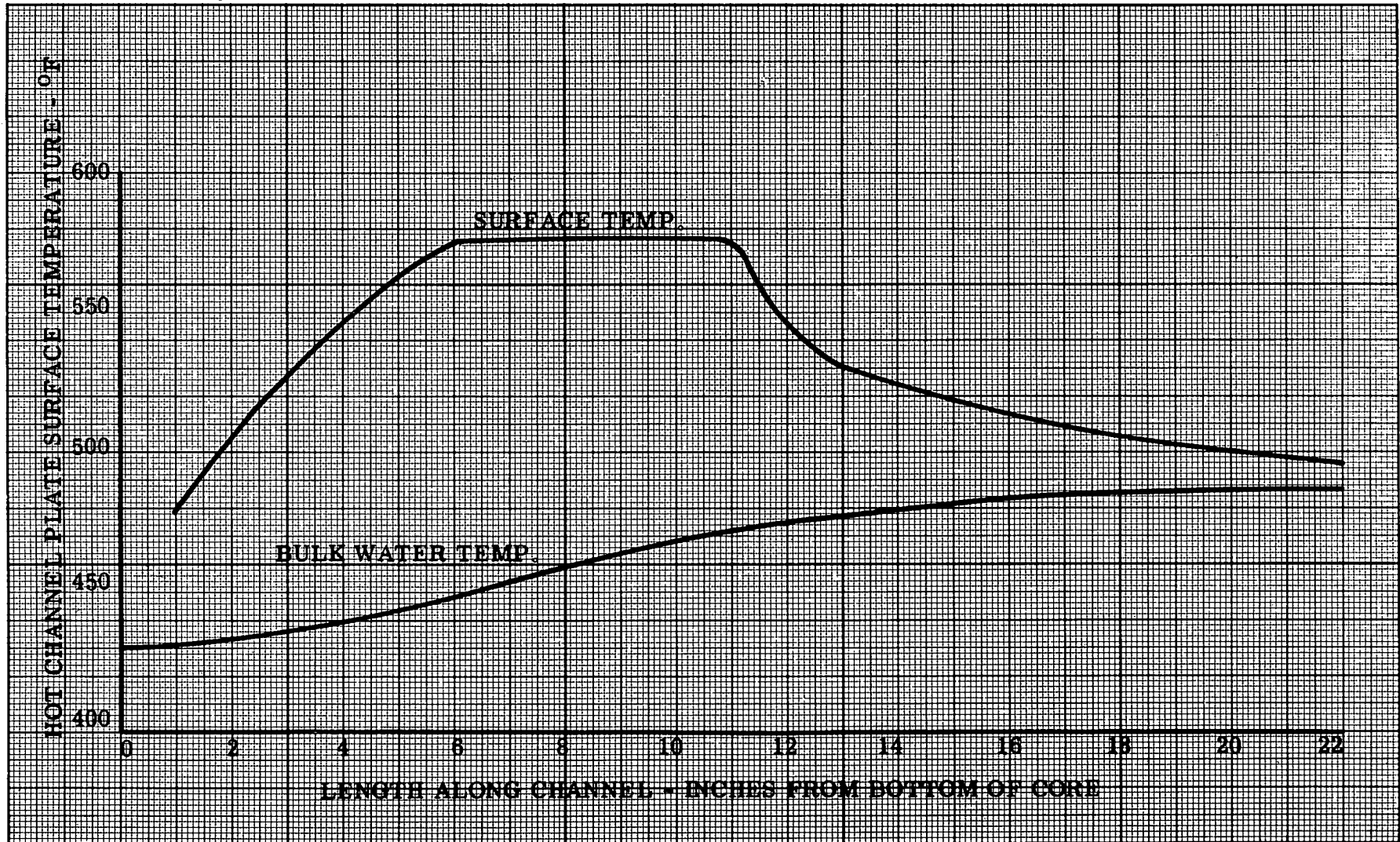
Fig. 3.6 - SM-2 Elements in SM-1 Core, Hot Channel Plate
Surface Temp. and Bulk Water Temp. vs. Length
Along Channel From bottom of Core Element
Position 44

Reactor power was 20.2 MW with a core heat flux of 118,826 Btu/hr-ft^2 and inlet temperature of 427°. The hot channel factors used were based on radial peaking factors presented in the core analysis section of this report, and the manufacturing and metallurgical tolerances presented for SM-2 elements in reference (18). The available flow rates for these elements are shown in Fig. 3.3.

TABLE 3.4
RESULTS OF STEADY STATE THERMAL ANALYSIS,
SM-1A CORE, REACTOR POWER 20.2 MW

Element Position	Max. Surface Temp. ^{O}F	Max. Bulk Water Temp. ^{O}F	Min. DNBR	Quality
67	578.3	488.1	3.9	0
44	578.7	482.5	4.4	0
46	569.1	475.9	5.0	0
43	578.5	482.1	4.6	0
32	578.1	482.2	4.91	0
63	577.9	479.1	5.1	0
36	571.5	474.0	5.7	0
22	560.8	471.3	6.5	0

The results of this analysis indicate that the SM-1A with SM-2 elements is safe during steady state 20.2 MW operation. This is based on DNBR's well above the minimum DNBR of 2.0 and the existence of no local boiling.

3.8.2 Maximum Operating Conditions

A steady state analysis of core positions 67 and 44 was made at the reactor scram power level of 24.2 MW. The selection of these elements was based on the minimum DNBR's presented in Table 3.5. Core inlet temperature was reduced to 422.9^O and the core heat flux increased to 142,591 Btu/hr-ft^2.

TABLE 3.5
RESULTS OF STEADY STATE THERMAL ANALYSIS,
SM-1A CORE, REACTOR POWER 24.2 MW

Element Position	Max. Surface Temp. ^{O}F	Max. Bulk Water Temp. ^{O}F	Min. DNBR	Quality
67	578.9	496.1	3.2	0
44	579.3	489.4	3.6	0

The results of this analysis indicate no local boiling and a minimum DNBR above the design criteria of 2.0. Figures 3.7 and 3.8 show a plot of plate surface temperature and bulk water temperature for stationary element 67 and control rod element 44. On the basis of no local boiling and the DNBR's, the scram power level condition does not affect the safe operation of the SM-1A core.

3.9 PERFORMANCE OF SM-2 ELEMENTS IN THE PM-2A REACTOR

3.9.1 Steady State Design Conditions

A steady state thermal analysis was performed on nine element positions selected from nine element groupings within the PM-2A core. The basis for element selection is the same as discussed in Section 3.7.1. These elements are listed in Table 3.6.

Reactor power was 10.0 MW with a core heat flux of 72,723 Btu/hr ft^2 and inlet temperature of 504°F. The hot channel factors used were based on radial peaking factors presented in the core analysis section of this report, and the manufacturing and metallurgical tolerances presented for SM-2 elements in reference (18). The available flow rates for these elements are shown in Fig. 3.4.

The result of this analysis at 10 MW are shown in Table 3.6.

TABLE 3.6
RESULTS OF STEADY STATE THERMAL ANALYSIS - PM-2A CORE, REACTOR POWER 10.0 MW

Element Position	Max. Surface Temp. ^{O}F	Max. Bulk Water Temp, ^{O}F	Min. DNBR	Quality
44	604.5	549.1	8.5	0
34	601.8	543.8	9.3	0
55	595.1	541.0	9.7	0
23	617.8	550.5	7.9	0
56	586.9	537.4	10.6	0
22	614.9	550.0	7.9	0
37	576.9	534.9	12.2	0
14	562.6	525.5	14.8	0
73	597.4	546.9	10.1	0

Fig. 3.7 - SM-2 Elements in SM-1A Core, Hot Channel Plate
Surface Temp. and Bulk Water Temp. vs. Length
Along Channel From Bottom of Core, Element
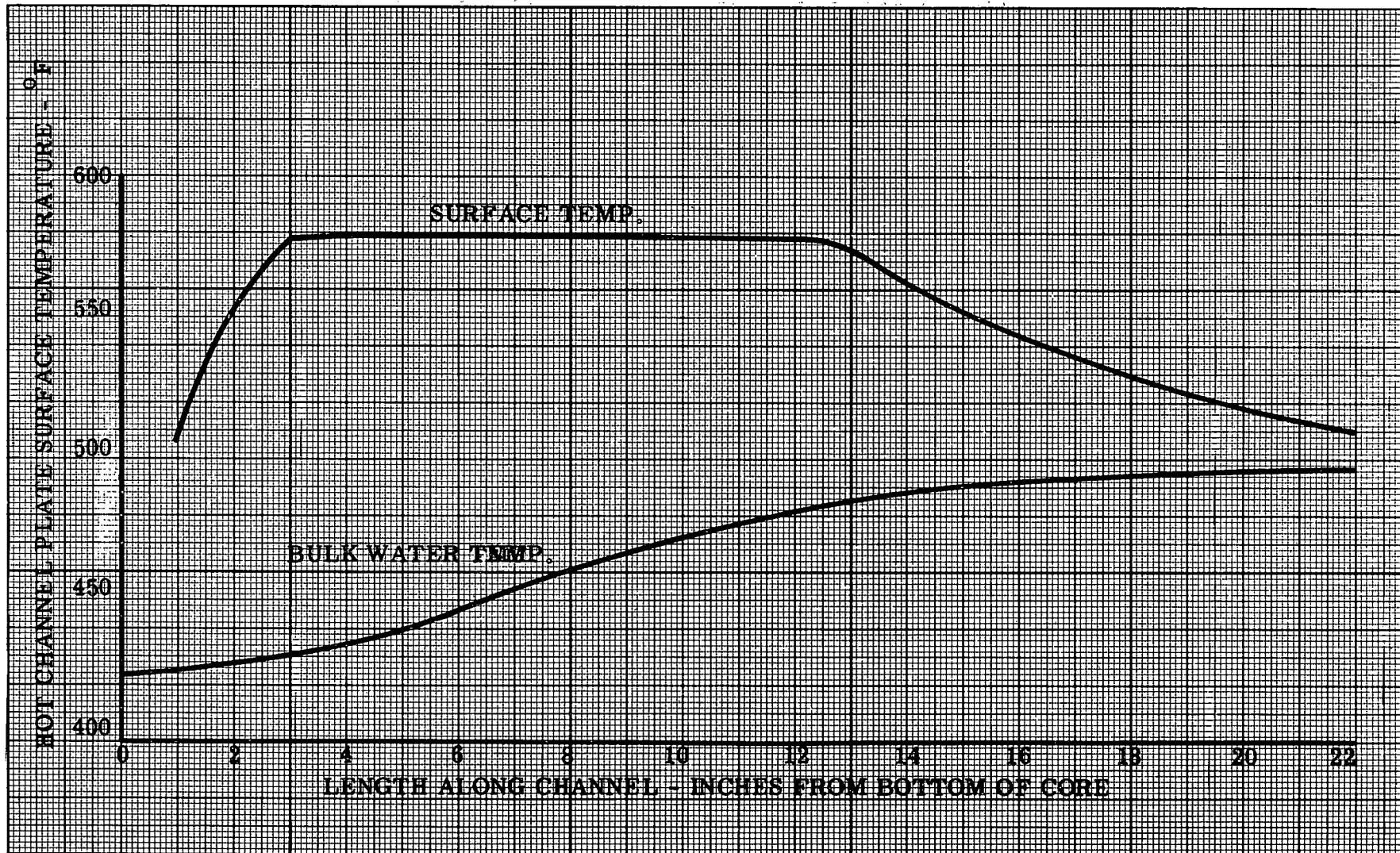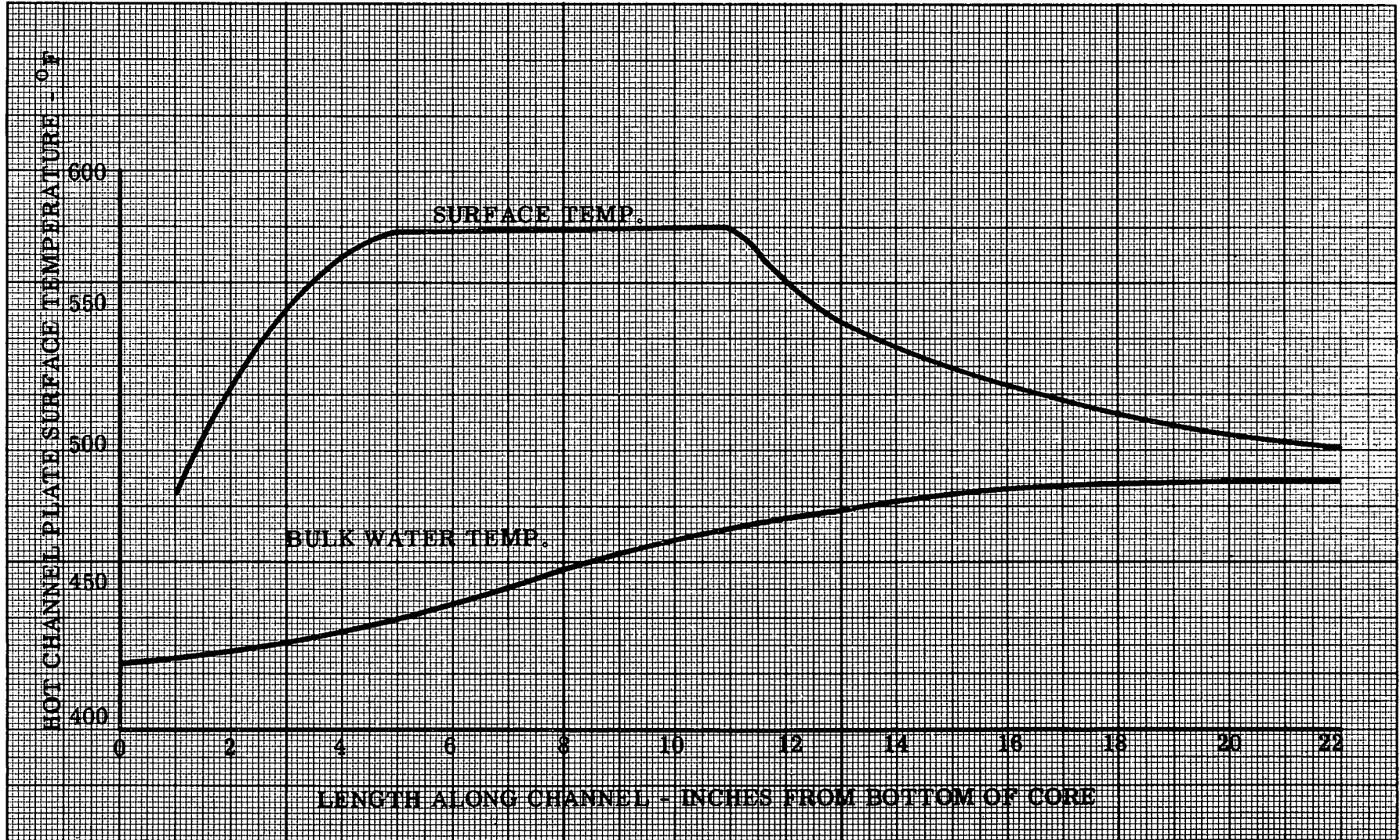Position 67

Fig. 3.8 - SM-2 Elements in SM-1A Core, Hot Channel Plate
Surface Temp. and Bulk Water Temp. vs. Length
Along Channel From Bottom of Core, Element
Position 44

The results of this analysis indicate no local boiling and minimum DNBR's above the thermal design criteria of 2.0. On this basis the PM-2A core will operate safely at 10.0 MW with SM-2 elements installed.

3.9.2 Maximum Operating Conditions

A steady state analysis of core positions 23 and 44 was made at the reactor scram power level of 12.0 MW   The selection of these elements was based on the minimum DNBR's presented in Table 3.6. Core inlet temperature was reduced to 500.4°F and the core heat flux increased to 87,268 Btu/hr-ft^2.

The results of this analysis at 12.0 MW are given in Table 3.7.

TABLE 3.7
RESULTS OF STEADY STATE THERMAL ANALYSIS,
PM-2A CORE, REACTOR POWER 12.0 MW

Element Position	Max. Surface Temp. °F	Max. Bulk Water Temp, °F	Min. DNBR	Quality
23	620.80	556.0°	6.6	0
44	620.83	554.3	7.1	0

Results indicate no local boiling and minimum DNBR's are above 2.0. Figures 3.9 and 3.10 show plots of plate surface temperature and bulk water temperature for stationary element 23 and control rod element 44. The PM-2A core is the safest core(has minimum DNBR's) operating with SM-2 elements installed.

3.10 TRANSIENT OPERATION OF THE SM-1 CORE WITH SM-2 ELEMENT

A transient analysis was performed on element 61 in the SM-1 core for a loss of flow accident. This required the reactor's coastdown information given in Figure 3.1 which was taken from the data of Test Procedure 600,[19] conducted at Fort Belvoir. At time intervals of 0.1, 0.2, 0.3, 0.4 and 0.5 sec after pump failure, flow rates and reactor power were calculated based on a reactor power of 13.45 MW. These were placed in STDY-3 code as a series of steady state runs. The results of this analysis are shown in Fig. 3.11. This analysis indicates that the minimum burnout ratio is far above the thermal design requirements of 1.5 for safe core transient operation and that DNBR increases in this loss of pump accident.

A transient analysis will be included in the final report making use of a transient code for the analysis.

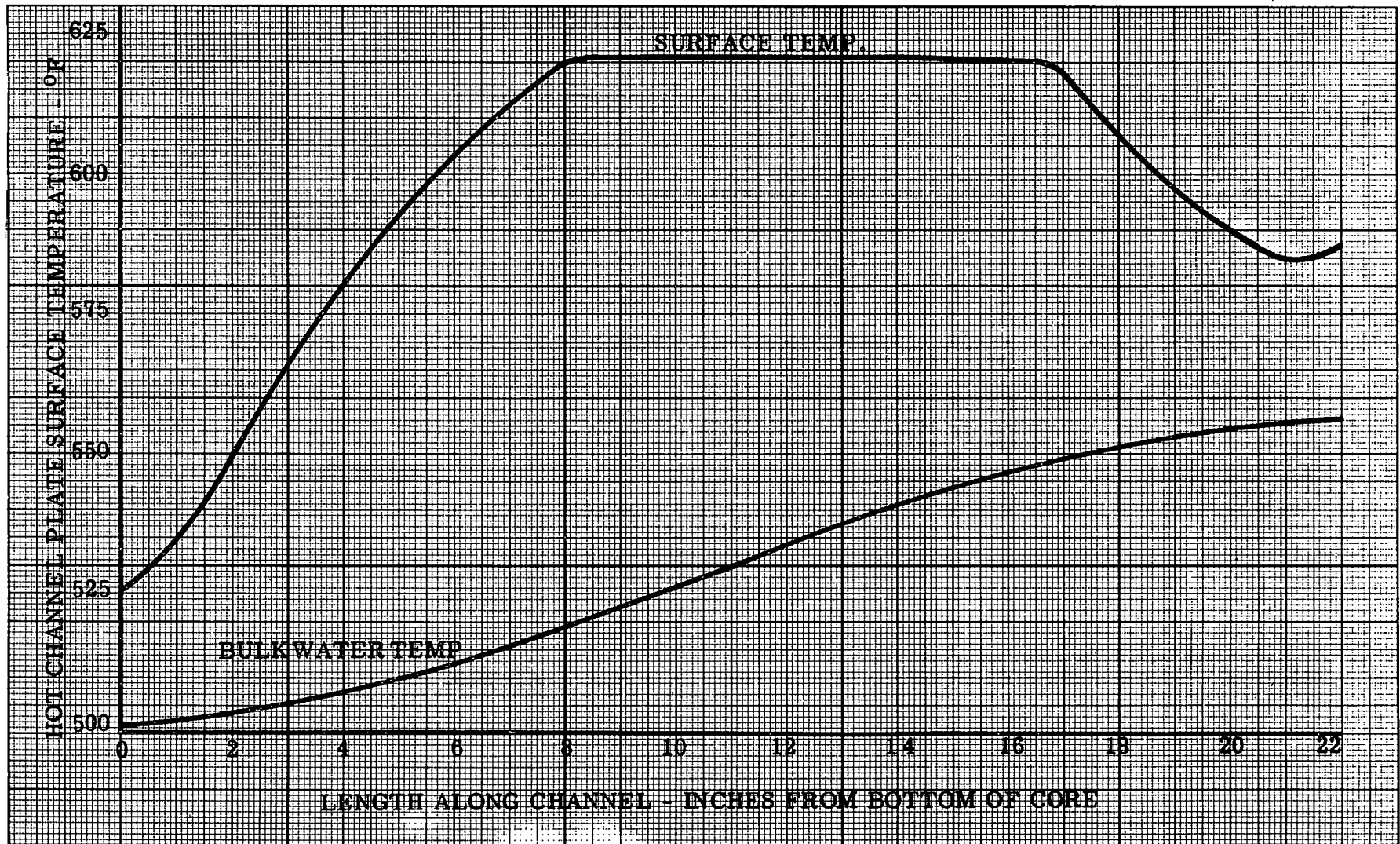THIS PAGE

WAS INTENTIONALLY

LEFT BLANK

Fig. 3.9 - SM-2 Elements in PM-2A Core, Hot Channel Plate
Surface Temp. and Bulk Water Temp. vs. Length
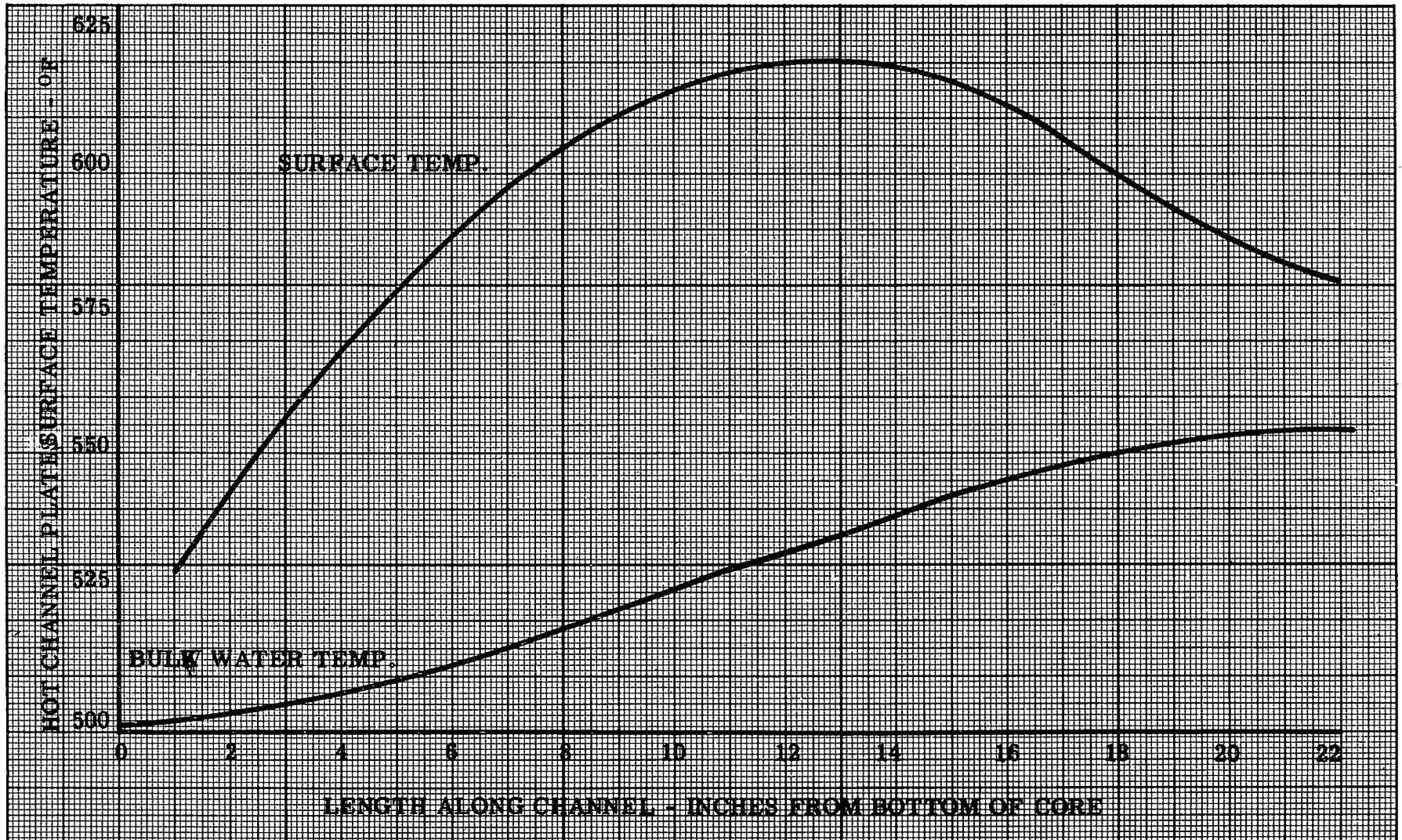Along Channel From Bottom of Core - Element
Position 23

Fig. 3.10 - SM-2 Elements in PM-2A Core, Hot Channel Plate
Surface Temp. and Bulk Water Temp. vs. Length
Along Channel From Bottom of Core, Element
Position 44

MINIMUM BURNOUT RATIO AS A FUNCTION OF
TIME AFTER LOSS OF FLOW

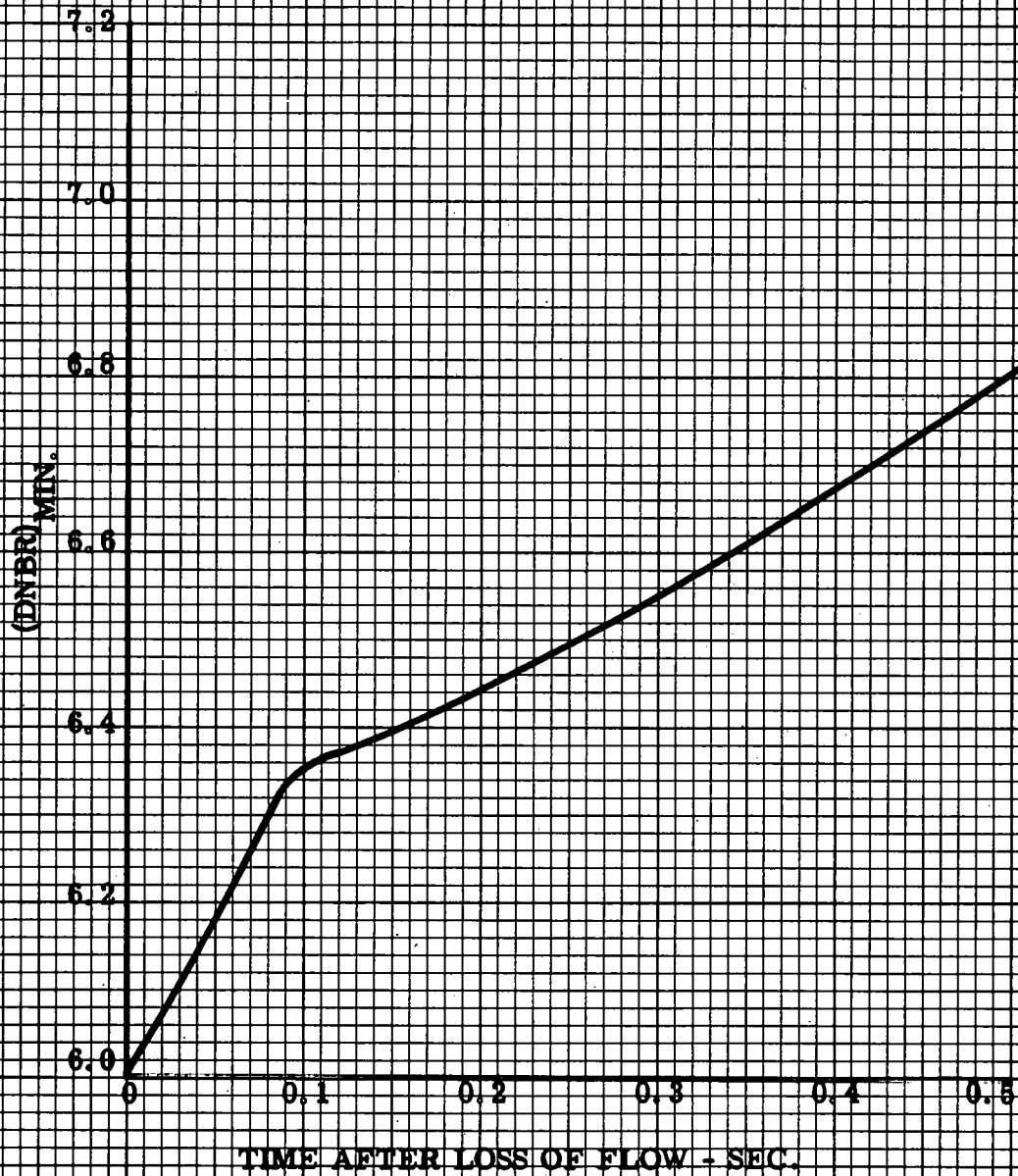SM-1 REACTOR, CORE POSITION 61
AXIAL POSITION, J=8

Fig. 3.11 –

THIS PAGE

WAS INTENTIONALLY

LEFT BLANK

3.11 CONCLUSIONS

1. The preliminary thermal analysis indicates that at design power output the SM-1, SM-1A and PM-2A cores operate safely. There is no evidence of local boiling and DNBR's are above 2.0.

2. The preliminary thermal analysis indicates that at the reactor scram power level setting the SM-1A and PM-2A operate safely with no local boiling evident and DNBR's well above 2.0. In the SM-1, element 61 indicates that local boiling exists for approximately 2/3 of its hot channel. Considering the high DNBR (6.0) and the fact that this is the scram level setting, results indicate that the SM-1 will be safe to operate with SM-2 elements.

3. During a loss of pump transient, the preliminary thermal analysis performed on the SM-1 core indicates no local boiling, with DNBR's above the thermal transient criteria of 1.5.

THIS PAGE

WAS INTENTIONALLY

LEFT BLANK

REFERENCES

1. Bobe, P. E., Editor, "Interim Report of Nuclear Analysis Performed on SM-2 Core and Vessel" APAE No. 65, May 27, 1960.

2. Williamson, T. E., Editor, "Reactor Analysis APPR-1 Core II," APAE No. 32, July 15, 1958.

3. Fried, B. E., Alford, M. R., Oggerino, J. P., "SM-2 Flux and Power Distribution for the Reference and Critical Experiment Cores," APAE Memo No. 286, to be published.

4. Paluszkiewicz, S., "Analysis of Zero Power Experiments on SM-1 Core II and SM-1A Core I," APAE No. 71, October 5, 1960.

5. Fried, E. E., Oggerino, J. P., Alford, M. R., "Analysis of Reactivity, Burnup, and Lifetime for the SM-1 and SM-2 Cores Using the CANDLE-2 Code," APAE Memo No. 285, to be published.

6. Geisler, H. W., Editor, "Results and Analysis of the APPR-1 Zero Power Experiments, Part 1," APAE Memo No. 61, November 7, 1956.

7. Hoover, H. L., Project Engineer, "SM-2 Core and Vessel Design Analysis," APAE No. 69, Vol III, March 8, 1961

8. Byrne, B. J., "Power Distribution for APPR-Type Cores," APAE Memo No. 195, July 25, 1959.

9. Paluszkiewicz, S., Byrne, B. J., "Analysis of Zero Power Experiments on the PM-2A Core I," APAE Memo No. 277, January 17, 1961.

10. Paluszkiewicz, S., "Nuclear Analysis of Various SPERT-III Critical Experiments," APAE Memo No. 279, April 27, 1961.

11. Pyle, R. S., "STDY-3 - A Program for the Thermal Analysis of a Pressurized Water Nuclear Reactor During Steady State Operation," WAPD-TM-213, June, 1960.

12. Rosen, S. S., "Hazards Summary Report for the Army Package Power Reactor SM-1," APAE 2, Revision 1, May,1960.

13. Gallagher, J. G., "Hazards Summary Report for SM-1A," APAE No. 13,Supplement 2,Rev. 1, October 7, 1960.

REFERENCES (CONT'D)

14. "Hazards Summary Report for a Prepackaged Nuclear Power Plant for an Ice Cap Location (PM-2A)," APAE No. 49, Alco Products, Inc., July 1, 1959.

15. Ingeneri, S. M., "Coolant Flow Tailoring Program of the APPR-1 Core Employing a Full Scale Model of the Reactor Vessel," APAE Memo No. 108, November, 1957.

16. Matthews, F. T., "Revised Thermal Analysis of the SM-1A Core," AP Note 307, Alco Products, Inc., December 8, 1960.

17. Matthews, F. T., "Results of the Experimental Flow Distribution Program for the PM-2A Reactor - Summary Report, " AP Note 266, Alco Products, Inc., May 31, 1960.

18. Hoover, H. L., Project Engineer, "SM-2 Core and Vessel Design Analysis," APAE No. 69 Volume I, Section 2 - Core Thermal Analysis, March 8, 1961.

19. Morrison J. H., Lee, D. H., "Evaluation of Loss of Flow Accident in the SM-1," Final Test Report 600, Alco Products, Inc., April 22, 1960.

20. Richards, W. M. S., "Primary System Thermal and Hydraulic Performance During Heat-Up of the PM-2A Reactor Plant, Test No. C-603," AP Note 323, Alco Products, Inc., February 15, 1961.